

Direct real photons in relativistic heavy ion collisions

Gabor David
Stony Brook University

Abstract. Direct real photons are arguably the most versatile tools to study relativistic heavy ion collisions. They are produced, by various mechanisms, during the entire space-time history of the strongly interacting system. Also, being colorless, most the time they escape without further interaction, *i.e.* they are penetrating probes. This makes them rich in information, but hard to decypher and interpret. This review presents the experimental and theoretical developments related to direct real photons since the 1970s, with a special emphasis on the recently emerged “direct photon puzzle”, the simultaneous presence of large yields and strong azimuthal asymmetries of photons in heavy ion collisions, an observation that so far eluded full and coherent explanation.

CONTENTS

| | |
|--|----|
| I. Introduction | 3 |
| II. Sources of photons | 4 |
| A. Terminology | 4 |
| B. The fundamental processes to produce direct photons | 5 |
| 1. Partonic processes in hadron-hadron collisions | 5 |
| 2. Radiation from the QGP | 7 |
| 3. Radiation from the hadron gas | 8 |
| C. Who outshines whom? From pre-equilibrium to QGP to hadron gas | 10 |
| III. Experimental techniques | 11 |
| A. Real photons (calorimetry) | 11 |
| B. External and internal conversion | 12 |
| C. Other tools and techniques | 14 |
| D. Ways to present direct photon data | 15 |
| IV. The high p_T region. | 17 |
| A. Hard photons in pp and $p\bar{p}$ collisions | 17 |
| 1. Spectra | 17 |
| 2. Photon-jet, photon-hadron and photon-photon correlations | 19 |
| B. Hard photons in heavy ion collisions | 20 |
| 1. Invariant yields | 21 |
| 2. Nuclear modification factor | 22 |
| 3. Collision centrality – photons as the standard candle | 24 |
| 4. Expected deviations of the photon R_{AA} from unity | 26 |
| 5. Photon - hadron/jet correlations: energy loss in the medium | 27 |
| 6. Nuclear PDFs and fragmentation function modification | 28 |
| 7. A collateral benefit: photon-photon scattering | 29 |
| V. “Thermal” radiation (low p_T region) | 30 |
| A. SPS, FNAL and AGS | 30 |
| B. RHIC and LHC | 32 |
| 1. “Thermal” photon yields and effective temperatures | 32 |
| 2. Scaling of direct photon yields with $dN_{ch}/d\eta$ | 39 |
| VI. Direct photon flow – the era of the “direct photon puzzle” | 41 |
| A. First results on v_2 and v_3 | 41 |
| B. The Devil’s advocate | 43 |
| C. Methodology: v_n with respect to what and how? | 46 |
| 1. Event plane method | 46 |
| 2. Scalar product method | 47 |
| D. Attempts to resolve the direct photon puzzle | 48 |

| | |
|---|----|
| 1. Hydrodynamical models | 48 |
| 2. Initial state, (fast) thermalization | 50 |
| 3. Transport calculations | 50 |
| 4. Other ideas | 52 |
| VII. Concluding remarks | 54 |
| VIII. Acknowledgements | 55 |
| References | 56 |

I. INTRODUCTION

The centuries old quest to reveal the “ultimate” constituents of matter and the laws of Nature governing them, and the realization from quantum mechanics that mapping smaller and smaller objects requires ever larger energy probes, made high energy physics one of the dominant scientific disciplines of the XXth century. At first we took advantage of the Universe as an “accelerator” providing high energy probes (cloud chamber and emulsion experiments), but soon we started to build our own accelerators, constantly increasing their energy and luminosity. The most spectacular and best known results came in elementary particle physics, but astrophysics and nuclear physics were a close second, benefiting enormously from the progress in experimental and theoretical tools.

The central question in particle physics was the substructure of hadrons and the nature of confinement, while high energy nuclear physics’ foremost concern was the behavior of high density nuclear matter, including its collectivity and possible phase transition into partonic matter, which in turn evoked the early stages of the Universe. Albeit particle and nuclear physics came with different perspectives, both were concerned with the strong interaction and its underlying theory, quantum chromodynamics (QCD), so the birth of a new discipline at their intersection, relativistic heavy ion physics, was almost inevitable. From Princeton and Berkeley to Dubna the race for larger and larger ions, energies and luminosities was on. Hadrons and nuclear fragments were studied extensively, and the applicability of thermo- and hydrodynamics gradually recognized. An excellent review of these first facilities and early developments – both experimental and theoretical – can be found in [1] by Goldhaber, while a (literally) insightful account of the genesis and achievements of RHIC and LHC was given by Baym in [2].

Although lepton and photon production in hadronic and nuclear collisions was studied almost since the birth of quantum mechanics and quantum electrodynamics [3–6], the golden era started in the early 1970s when ISR and Fermilab became operational. The available large energies allowed almost from the beginning to explore both fundamental facets of direct photons: at high transverse momentum (p_T) they are probes of QCD hard scattering, while at low p_T they help to shed light on multiparticle production. The high p_T aspect was first pointed out by Escobar [7], Farrar and Frautschi [8] in 1975. At low p_T , the first one to emphasize their importance in the context of multiparticle production was Feinberg [9] in 1976, famously stating that “the thermodynamical approach naturally leads to direct γ ’s and dilepton production. ... If the multihadron production process contains an intermediate stage of a thermodynamical hadronic matter, then this kind of γ and dilepton production *inevitably* exists. The question is only on its intensity and on the detailed behaviour of the spectra.”¹ A few years later Shuryak [10] already estimated the lepton and photon production from the “Quark-Gluon Plasma” (along with the hadronic production). The idea that photons can test the most diverse manifestations of the strong interaction took hold. The rapid growth of the field has been documented in several reviews in the past (see for instance [11–17]). By now, photon physics became mature, but by no means a closed chapter – just the opposite.

This review was written with the following goals in mind. It is trying to be *accessible* even for physicists outside our field, but providing plenty of references for those who want to learn the details. It intends to show the *historic context and evolution of ideas*, in the firm belief that nothing is more instructive and promotes creativity and progress better, than understanding not only *what* do we know now, but also the process *how* did we acquire this current knowledge. It is aiming to be as *up-to-date* as possible, by including even very recent preliminary results (as of early 2019). Also, it is meant to be *realistic* in its claims on which issues are really settled and which ones are not. If in doubt, we would rather err on the side of under-, than overconfidence.

Photons taught us a lot already, but in the process new questions emerged, and a fully self-consistent description of direct photons in heavy ion collisions is not available yet, not the least because important measurements are still missing or not sufficiently precise to discriminate between theories. The field is very much open and if this review helps to raise fresh interest and generate new efforts, it achieved more than we ever dared to hope for.

In this review first we introduce the basic theory concepts (Sec. II) and experimental techniques (Sec. III), then we discuss the results from past decades, concentrating on the direct photon spectra in hadron-hadron and heavy ion collisions. As mentioned above, the relevant physics (and even the experimental techniques) of high and low p_T photon production are quite different, so we describe them in separate sections, in their own historic context. On the other hand observations in heavy ion collisions can not be understood without the corresponding “baseline” in pp . Therefore, we group together all high p_T photon results in pp and A+A and their impact on jet physics, collision centrality determination, nuclear PDFs and other issues in Sec. IV, whereas the low p_T (or “thermal”) production in all colliding systems will be discussed in Sec. V. Finally, we

¹ Feinberg in [9] even provided an estimate (based on Landau theory) of the N_γ photon yield w.r.t. the N_π pion yield, with the expression

$$N_\gamma = 6.4Ae^2 N_\pi^{4/3} \left(1 - \frac{1}{N_\pi^{1/3}} + 0.21 \ln N_\pi \right)$$

which gives N_γ/N_π in the 0.1-0.15 range for realistic pion multiplicities; remarkably close to today’s measurements!

review the challenging developments of the past few years, starting with the 2011 observation of elliptic flow of “thermal” photons and resulting in the so-called “direct photon puzzle”, its consequences, the attempts to resolve the “puzzle” and the questions that are still open in Sec. VI.

The blessing and curse of direct photons.

Photons play a special role in the study of high-energy hadronic and nuclear interactions, because they are *penetrating probes*. Being color neutral, their mean free path is rather large not only in very dense hadronic matter, but also in a medium of deconfined quarks and gluons, the quark-gluon plasma, or QGP (see Sec. IV B). This ensures that if they are created at any time, they will escape the interaction region (mostly) unaltered and will be detectable. This is true even if they have to cross the hot, dense medium of QGP. On the other hand, to our current best knowledge at every stage (or at the very least at *most* stages) of the collision there are physics mechanisms to produce photons, providing direct information both on the process itself and the environment (*e.g.* the initial state including geometry, the expansion of the plasma or the hadron gas, and so on). In this sense photons are the perfect “historians” of the evolution of the system.

Unfortunately, all that information on instantaneous rates and expansion dynamics is convolved (integrated in space-time) leaving us with just a few high level experimental observables: the all-inclusive spectrum, possible azimuthal asymmetries, energy deposit or lack thereof around the photons (isolation), rapidity distribution, correlations, and so on. Therefore, disentangling the contributions from the various processes is nearly impossible without relying on models. Finally, the number of photons created in the collision, before the final chemical and kinematic freeze-out of the system (*direct photons*) is usually small compared to the photons coming from the decay of final state hadrons, like π^0 , η . While these decay photons are highly interesting in hadron physics, they pose a serious background problem for direct photon measurements.

II. SOURCES OF PHOTONS

A. Terminology

The prevalent (although not completely unique) terminology of real photons in heavy ion physics, referring to their sources, is shown in Fig. 1. The two main categories are *direct* and *decay* photons. Decay photons come from electromagnetic decays of long lifetime final state hadrons² and as such are extremely valuable – sufficient to say that π^0 ’s reconstructed from $\pi^0 \rightarrow \gamma\gamma$ provided the first strong hint that QGP has been formed in relativistic heavy ion collisions [18]. However, when measuring *direct* photons, *i.e.* those that are produced any time during the collision proper, before the final products completely decouple, the decay photons are a large background and often the principal source of systematic uncertainties of the direct photon measurement.

The subcategory *prompt* as a rule includes photons from initial hard parton-parton scattering (see for instance [19]). Usually other conjectured early sources, like photons from the “hot glue”, created before local thermalization [20] or the Glasma [21, 22], photons from the strong initial magnetic field [23, 24], synchrotron radiation [25], are also included here as *pre-equilibrium*.

The subcategory *thermal* is widely used but problematic, even theoretically, since thermalization is local at best, and the instantaneous rates calculated with evolving temperature are in addition subject to blue-shift due to medium expansion, so the inverse slope parameter of p_T spectra does not directly represent any “temperature” [26–28]. Depending on their origin (partonic or hadronic processes, see Sec. II B) they are called photons from the *QGP* or the *hadron gas* [29]. To complicate things, several other sources (like Bremsstrahlung) emit photons in the thermal range, which are indistinguishable from truly “thermal” photons. Therefore, in experimental papers “thermal” is usually just a shorthand for photons in the few hundred MeV – few GeV p_T range, and we will put the word in quotation marks whenever experimental results are discussed.

Other sources include photons from *jet fragmentation* in vacuum, well known and measured in pp [19, 30–33]. They should be distinguished from *jet Bremsstrahlung* which occurs while the parton is still traversing the (QGP) medium and losing energy in it [19]. *Jet-medium* or *jet-photon conversion*, *jet-thermal* photons [34, 35] are a special case of the ultimate parton energy loss where a high p_T quark collides with a thermal parton and

² Long lifetime means that it significantly exceeds 10-100 fm/c after which the colliding system is completely decoupled.

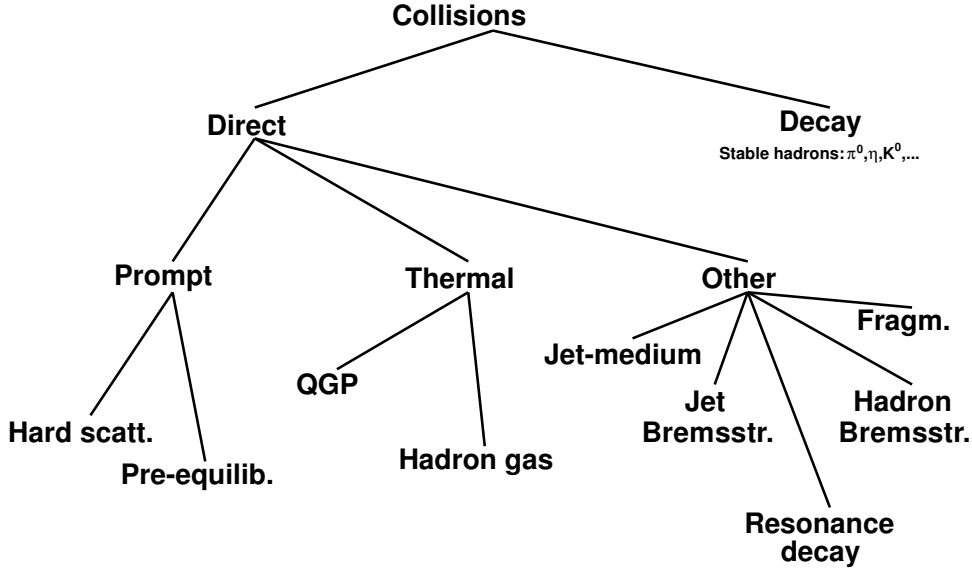


FIG. 1. Prevalent terminology, referring to the sources of real photons in heavy ion physics

transfers all its momentum to a photon flying out in the same direction (see IV B). *Hadron Bremsstrahlung* happening in the hadron gas is yet another source of photons [36, 37]).

Words of caution.

There are many sources of direct photons that are hard or impossible to disentangle experimentally. This often leads to some misunderstanding when comparing data to model calculations. For instance, in the high p_T region (above 4-5 GeV/c), dominated by hard scattering, experiments often publish results on *isolated* photons even in A+A collisions [38], using well-defined isolation criteria. These results are then compared to perturbative QCD (pQCD) calculations, but the comparison is only valid if the same isolation criteria are applied as in the data. In case of pp this is relatively straightforward but in A+A the underlying event has to be properly simulated, too – a very non-trivial task. Also, in A+A “jet-conversion” photons (from the interaction of a hard-scattered fast parton with the medium) are an additional source of isolated photons in the experiment, but seldom included in theory calculations.

Even the distinction between direct and decay photons can become problematic. Short-lived *resonances*, like ω , ϕ , A_1 are sources of decay photons [39], but rarely if ever are actually subtracted by the experiments from the inclusive photon yields (not the least because the parent distributions are usually not or poorly known. Typically only π^0 and η decays are considered and the effect of all other hadron decays included in the systematic uncertainties). While raising this issue may sound somewhat pedantic, we should point out that at some point for instance the A_1 has been predicted to be a major source of photons [40].

B. The fundamental processes to produce direct photons

In this section we review the fundamental sources that were believed for a long time to be the main sources of photons in relativistic heavy ion collisions. More “exotic” mechanisms will be described in the context of the “direct photon puzzle” (see Sec. VI).

1. Partonic processes in hadron-hadron collisions

To leading order there are two types of partonic processes that produce photons: quark-gluon Compton-scattering and quark-antiquark annihilation (see Fig. 2).

For massive quarks and using the Mandelstam variables $s = (p_g + p_q)^2$, $t = (p_g - p_\gamma)^2$ and $u = (p_q - p_\gamma)^2$ the cross section for the $gq \rightarrow \gamma q$ Compton process is [41]

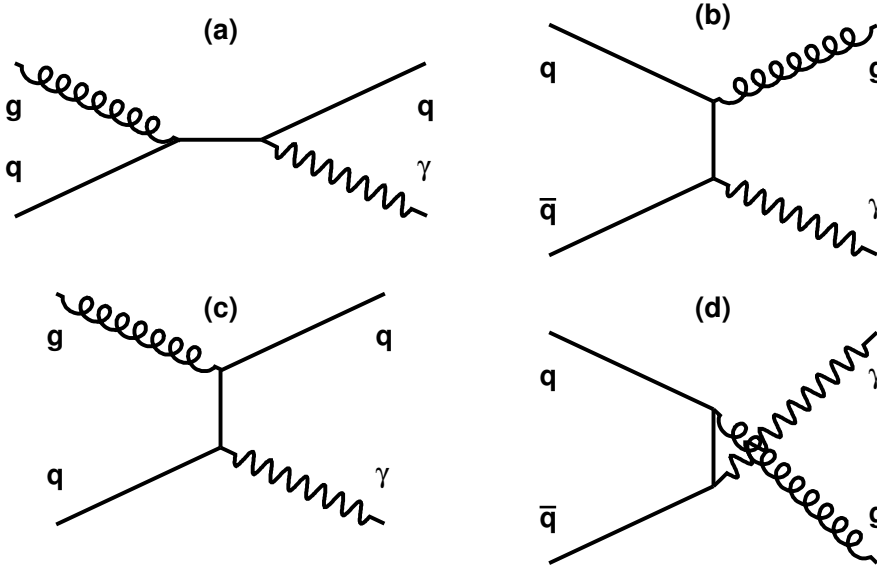


FIG. 2. Leading order Feynman diagrams contributing to direct photon production. (a) and (c): s and u channel quark-gluon Compton scattering. (b) and (d): t and u channel quark-antiquark annihilation.

$$\frac{d\sigma}{dt}(gq \rightarrow \gamma q) = \left(\frac{e_q}{e}\right)^2 \frac{8\pi\alpha_s\alpha_{em}}{(s-m^2)^2} \left\{ \left(\frac{m^2}{s-m^2} + \frac{m^2}{u-m^2}\right)^2 + \left(\frac{m^2}{s-m^2} + \frac{m^2}{u-m^2}\right) - \frac{1}{4} \left(\frac{s-m^2}{u-m^2} + \frac{u-m^2}{s-m^2}\right) \right\} \quad (1)$$

and with $s = (p_q + p_{\bar{q}})^2$, $t = (p_q - p_\gamma)^2$ and $u = (p_{\bar{q}} - p_\gamma)^2$ the cross section for the $q\bar{q} \rightarrow \gamma g$ annihilation process is

$$\frac{d\sigma}{dt}(q\bar{q} \rightarrow \gamma g) = \left(\frac{e_q}{e}\right)^2 \frac{8\pi\alpha_s\alpha_{em}}{s(s-4m^2)} \left\{ \left(\frac{m^2}{t-m^2} + \frac{m^2}{u-m^2}\right)^2 + \left(\frac{m^2}{t-m^2} + \frac{m^2}{u-m^2}\right) - \frac{1}{4} \left(\frac{t-m^2}{u-m^2} + \frac{u-m^2}{t-m^2}\right) \right\} \quad (2)$$

These are the cross-sections of the lowest order photon-producing partonic $2 \rightarrow 2$ processes (for higher order corrections in hadron-hadron collisions see for instance [32]). In order to calculate the photon rates the initial parton distribution functions (PDF) have to be known. At higher order the fragmentation functions (FF) of the outgoing partons into photons are also needed [30–33]. The FFs are defined as $D_{q,g}^\gamma(z, Q^2)$ providing the probability that a quark or gluon fragments into a photon carrying the fraction z of the original parton momentum. (For a recent review see [42].)

For high momentum transfer Q^2 (hard scattering) *factorization* holds [19, 43, 44], meaning that the cross-section of an $AB \rightarrow \gamma A$ process is the incoherent sum of the cross-sections $\sigma_{ij \rightarrow kl}$ of all contributing constituent scattering processes, each convolved in the available phase-space with the respective initial parton distributions (PDFs), and, if relevant, with the final state parton fragmentation functions (FFs). Schematically, for an inclusive hadron production in pp

$$\sigma^{pp \rightarrow hX} = \hat{\sigma} \otimes PDF \otimes PDF \otimes FF$$

The PDFs and FFs cannot be calculated using perturbation theory, but they are *universal* and can be obtained from data for various types of well-controlled (*e.g.* e^+e^-) hard processes [19]. The cross-sections $\sigma_{ij \rightarrow kl}$ can be calculated in pQCD.

For instance, the single inclusive photon cross-section in hadron-hadron collisions ($h_1 h_2 \rightarrow \gamma X$) to lowest order will have the form [45]

$$\frac{d\sigma}{dy d^2p_T} = \sum_{i,j} \frac{1}{\pi} \int dx_1 F_{h_1,i}(x_1, Q_s^2) dx_2 F_{h_2,j}(x_2, Q_s^2) \times \frac{1}{\hat{s}} \left(\frac{1}{v} \frac{d\sigma_{i,j}}{dv}(\hat{s}v) \delta(1-w) + \text{corr.} \right)$$

with $v = 1 - x_2(p_T/\sqrt{\hat{s}}e^{-y})$, $w = (1/ux_1(p_T/\sqrt{\hat{s}}e^y)$, the indices i, j run over the quarks, antiquarks and gluons of the initial hadrons, and $F_{h_1,i}, F_{h_2,j}$ are the respective parton distribution functions, while the next-to-leading order corrections are omitted. For fragmentation photons (an outgoing parton k emits a photon) an

additional convolution is necessary with the photon fragmentation function $D_{k,\gamma}$

$$\frac{d\sigma}{dyd^2p_T} = \sum_{i,j,k} \frac{1}{\pi} \int dx_1 F_{h_1,i}(x_1, Q_s^2) dx_s F_{h_s,j}(x_2, Q_s^2) \times \frac{dx_3}{x_3} D_{k,\gamma}(x_3, Q_d^2) \times \frac{1}{\hat{s}} \frac{1}{v} \frac{d\sigma_{i,j}}{dv}(\hat{s}v) \delta(1-w)$$

In lowest order only the Compton ($qg \rightarrow q\gamma$) and annihilation ($q\bar{q} \rightarrow q\gamma$) processes contribute to prompt photon production, the latter being suppressed in pp due to the lack of valence antiquarks. This provides (at least in principle) a way to disentangle the two processes by measuring the cross-section differences $\sigma(p\bar{p} \rightarrow \gamma X) - \sigma(pp \rightarrow \gamma X)$ which provides direct access to the valence-quark and gluon PDFs [46].

Some higher order processes – like Bremsstrahlung or fragmentation – can contribute to the partonic rates at a strength comparable to the fundamental Compton-scattering and annihilation. The calculations are quite complex, and usually implemented in Monte Carlo programs, like JETPHOX [47], but they are reasonably well understood and are consistent with the available data [32].

2. Radiation from the QGP

When the QGP, a medium of deconfined quarks and gluons is formed in a heavy ion collision, it will also radiate photons. The basic partonic interactions producing photons are still the same as discussed above, but the role of the traditional PDFs (obtained for partons *confined* in hadrons in vacuum and fixed long time before the collision) is taken over by the dynamically evolving distribution of *deconfined*, interacting partons, mostly produced in the collision itself, and collectively forming the “medium”. Under these circumstances there are two complementary ways to handle the problem of having parton distributions that now strongly depend (including their number!) on space-time, and keep changing as the medium evolves. The first is to prepare the initial state of the partons then follow their paths and interactions one-by-one (*microscopic transport*), circumventing the concept of the medium. The second is to model the medium as a statistical ensemble, describe its properties and evolution, like that of a gas or fluid (thermo- or hydrodynamical system)³.

The very first attempt to predict radiation from the QGP [10] starts with an ensemble of quarks and gluons assumed to be already in local thermal equilibrium with initial temperature T_i “at which the thermodynamical description becomes reasonable”, and continues up to the final temperature T_f “where the system breaks into secondaries”. The production cross-section of a (penetrating) particle “a” is then given by the integral over the space-time plasma region

$$\sigma_a = \sigma_{in} \int_{T_i}^{T_f} W_a(T) \Phi(T) dT$$

where σ_{in} is the inelastic cross-section, W_a the production rate per unit volume of the plasma, $\Phi(T)$ is a temperature-dependent weighting factor, estimated as $\Phi(T) = A(s)T^{-7}$ for various expansion (Feynman scaling and Landau hydrodynamics) scenarios. Note that $\Phi(T)$ strongly favors small T , *i.e.* production in the later stages. In specific, the author [10] finds for the p_T distribution of direct leptons from the elementary $gq(\bar{q}) \rightarrow \gamma q(\bar{q})$ and $q\bar{q} \rightarrow \gamma g$ processes

$$d\sigma/dp_T^2 = (\alpha^2 \sigma_{in} A(s) / \sqrt{2\pi} 18 p_T^4) \Gamma(7/2, M/T_i)$$

where σ_{in} is the inelastic cross-section, $A(s)$ is a slowly varying function of the c.m.s. energy (like $\ln s$ or \sqrt{s}). The direct photon yield is a factor of $20\alpha_s \ln(p_T/m_0)/3\alpha \sim 600$ higher [10]. In addition to its historic value, it is interesting to note that this early calculation claims that photons of quite high p_T (3-5 GeV/c) are produced predominantly not by hard scattering but in the plasma, and late (at lower T).

A more formal treatment is based on the imaginary part of the photon self-energy $\Pi_{\mu\nu}$ in the medium which is related to the escape rate of photons from the medium [49–51]. For small thermal systems (compared to the photon mean free path) the emission rate R of photons, valid to all orders in α_s and first order in α_{em} is [29]

$$E \frac{dR}{d^3p} = \frac{-2}{(2\pi)^3} \text{Im} \Pi_{\mu}^{R,\mu} \frac{1}{e^{E/T} - 1}$$

³ There are also hybrid techniques like *coarse graining* introduced in [48].

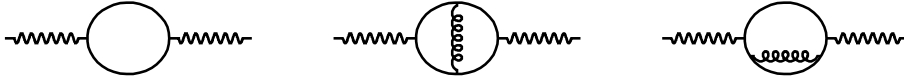


FIG. 3. One- and two-loop contributions to the photon self-energy in QCD

The one- and two-loop contributions to $\Pi_{\mu,\nu}$ are shown in Fig. 3, and $\text{Im}\Pi_{\mu,\nu}$ obtained by cutting the two-loop diagrams⁴, which then reproduces the basic graphs in Fig. 2. For vanishing quark masses the differential cross-sections go to infinity as $t \rightarrow 0$ and/or $u \rightarrow 0$ (see Eqs. 1,2). This infrared divergence can be regulated using the resummation technique of Braaten and Pisarski [52]. Assuming a thermalized QGP the first compact formula for photon radiation at $E \gg T$ was given in [29] as

$$E \frac{dR}{d^3p} = \frac{5}{9} \frac{\alpha\alpha_s}{2\pi^2} T^2 e^{-E/T} \ln\left(\frac{2.912}{g^2} \frac{E}{T}\right) \quad (3)$$

In the following decade, in part inspired by the availability of new data from the SPS, the calculations were extended to include Bremsstrahlung in the plasma [53], the effect of soft gluons [54], and the Landau-Pomeranchuk-Migdal effect [55]. A comprehensive set of rates contributing in leading order to photon emission from the QGP were given in [56]; those “AMY rates” are often used even today in hydro codes (see for instance [57, 58]). It should be noted, however, that the AMY rates (and most other explicit calculations) assume a weakly coupled ultrarelativistic plasma [56], calculating photon emission one by one for various leading order processes (diagrammatic approach). Note that these are only the *rates*, which then have to be convolved with some description of the space-time evolution of the QGP. The first attempt to describe the QGP evolution by longitudinal (1+1D) hydrodynamics was made by Bjorken [59], who in turn relied heavily on Landau’s seminal work on the hydrodynamic theory of multiple particle production [60], largely inspired by Fermi [61]. Deep are the roots... We will discuss some more recent models in Sec. VI.

3. Radiation from the hadron gas

Radiation from the hadron gas can be calculated in similar ways as the radiation from the QGP – from kinetic theory or by loop expansion of the photon self-energy – but the processes are different. Some basic diagrams are shown in Fig. 4. The first estimate of the photon emission rate from hot hadronic gas at a fixed temperature T was made in [29] calculating processes (a)-(f) in Fig. 4 (all except the A_1 channel [40]), and the authors concluded that *at the same temperature* the QGP and the hadron gas radiate photons in the 1-3 GeV/c p_T range at the same rate, summarized in the oft-quoted sentence: “The hadron gas shines just as brightly as the quark-gluon plasma.” It was assumed that the phase transition is first order and the system will spend a long time at the transition temperature T_c *i.e.* the thermal photon spectrum would allow to measure T_c .

The concept of *quark-hadron duality* [62], inspired by dilepton production at the SPS (CERES and NA50) and rooted in *chiral symmetry restoration* initially led to similar conclusions⁵. Ironically, this has cast early on some doubts on the usefulness of “thermal” photons to diagnose the QGP [15]. However, initially the expansion of the hot matter (QGP or hadronic) was often not taken into account, despite the pioneering work by Bjorken in 1983 [59] pointing out the applicability of hydrodynamics to the temporal evolution of the hadronic matter in highly relativistic nucleus-nucleus collisions⁶. In [63] the temperature-dependent emission rates for “thermal” photons from hadronic matter are described using an effective chiral Lagrangian ($\pi\rho \rightarrow \pi\gamma$, $\pi\pi \rightarrow \rho\gamma$, and $\rho \rightarrow \pi\pi\gamma$, allowing intermediate A_1 states). Substantial enhancement of the rates in case of finite pion chemical potential has been pointed out in [64]. Calculations in the Hadron String

⁴ Cutting the one-loop diagram leads to $q\bar{q} \rightarrow \gamma$ prohibited for a photon on mass shell.

⁵ In its original form duality meant that the hadronic and quark-gluon degrees of freedom are equally well describing the emissivity of strongly interacting matter if the temperature is the same.

⁶ And even in [59] only longitudinal flow was discussed, the transverse motion of the fluid, which became an all-important issue in understanding “thermal” photon production, was not addressed.

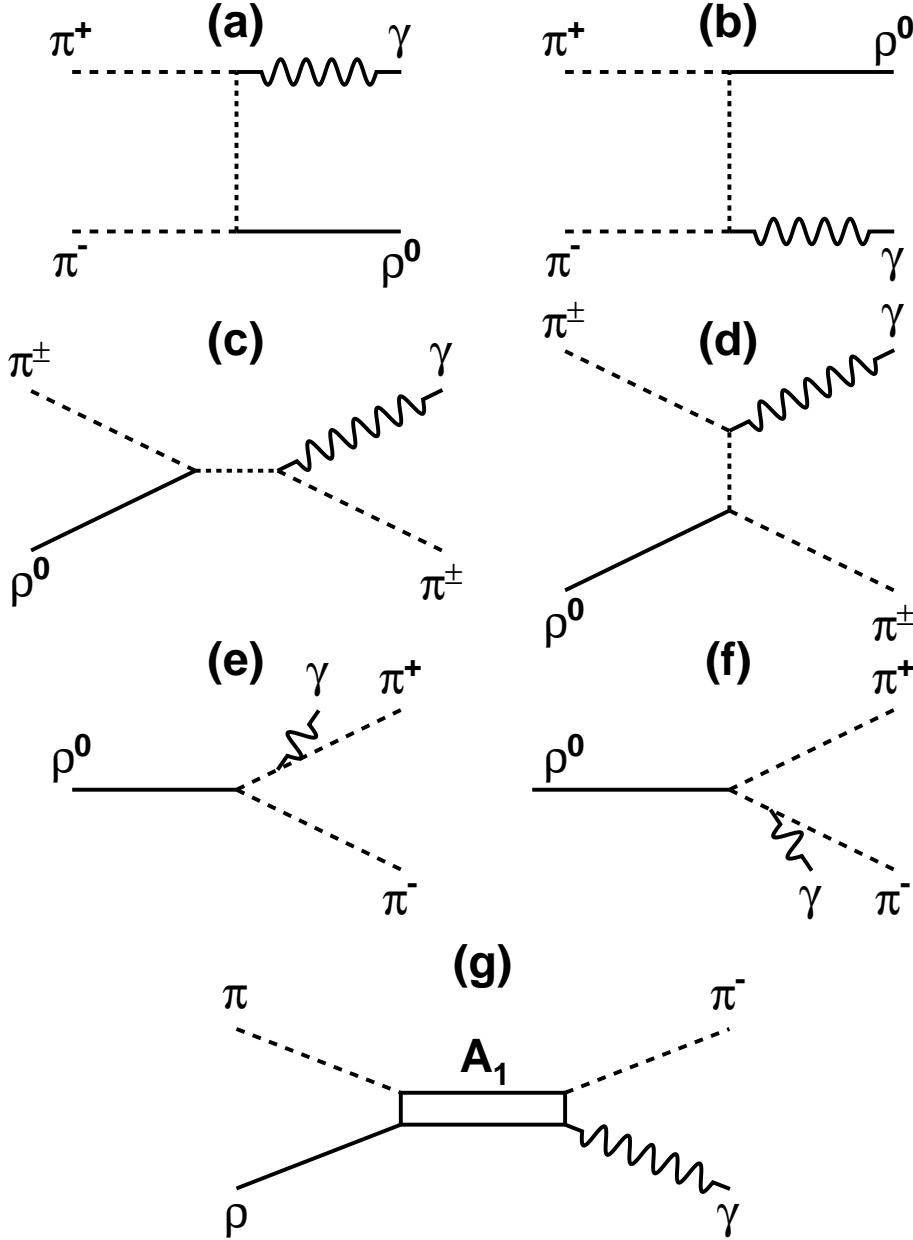


FIG. 4. Panels (a)-(f): some photon producing hadronic reactions arising from the imaginary part of the photon self-energy involving charged pions and neutral ρ mesons. Above $E_\gamma > 0.7\text{GeV}$ the dominant process is (c) [29]. Panel (g): contribution from the A_1 resonance that according to [40] “outshines” process (c).

Dynamics framework (see also Sec. VI) have been presented in [13]. Results with another microscopic transport model (uRQMD) are shown in [65].

The role of radial expansion (v_0) in modifying the photon spectra was first emphasized in the attempts to explain the WA80/WA98 data [66, 67] and the effective temperature T_{eff} was first considered in [68] where $v_0 = 0.3$ described the low end of the available WA98 data [69] well. A major update of thermal photon production in a radially expanding fireball [70] introduced strangeness-bearing channels but found the $\pi\rho a_1$ less important than earlier thought. A year later this work was followed by a calculation of the high p_T π^0 and direct photons [71] simultaneously⁷, and, in parallel, first predictions of azimuthal asymmetries (v_2 , or *elliptic* flow) of direct photons have been made [72, 73], including *negative* v_2 for high p_T photons.

⁷ It is very important that the π^0 and photon production will be accounted for in the same theoretical framework – unfortunately few publications satisfy this requirement. A good early example from 1995 is the three-fluid model in [66].

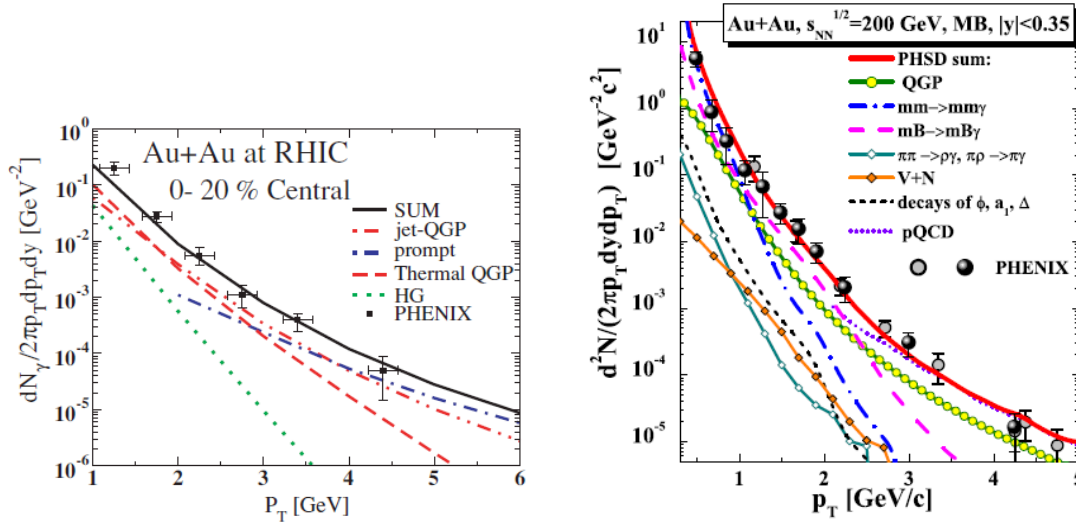


FIG. 5. (Left panel) Contributions from different sources and total yield of photons in central Au+Au collisions at RHIC, according to a 2008 hydrodynamic calculation. (Figure taken from [73].) (Right panel) Contributions from the QGP and various hadronic sources and the total yield of photons in Au+Au collisions at RHIC, according to a 2015 PHSD calculation. (Figure taken from [74].)

Unlike Eq. 3 there is no simple “pocket formula” for the radiation from the hadron gas. Schematically the total cross section for a particular process like $\pi\pi \rightarrow \rho\gamma$ reads [17]

$$\sigma_{\pi\pi \rightarrow \rho\gamma}(s, \rho_N) = \int_{M_{min}}^{M_{max}} dM dM \sigma_{\pi\pi \rightarrow \rho\gamma}^0(s, M) A(M, \rho_N) P(s) \quad (4)$$

i.e. folding the vacuum cross section $\sigma_{\pi\pi \rightarrow \rho\gamma}^0(s, M)$ with the in-medium spectral function $A(M, \rho_N)$ and $P(s)$ accounts for the fraction of the available part of the full ρ spectral function available in the phase space limited by \sqrt{s} . Similar schemes apply for other hadronic processes, but while the ρ spectral function is relatively well known, others, like a_1 are not. Calculations of the meson-meson and meson-baryon Bremsstrahlung are equally involved [37]. The complexity of calculating the direct photon yield, particularly the hadronic part is well illustrated in Fig. 5, where the contributions from different sources are shown from a 2008 hydrodynamic and a 2015 microscopic transport calculation.

C. Who outshines whom? From pre-equilibrium to QGP to hadron gas

Like with any new phenomenon, the hunt for the QGP started with theorizing about the decisive signal, whose presence (or disappearance) would unambiguously prove that this new state of matter has been formed. Historically the earliest suggestions were strangeness enhancement⁸, radiation from the QGP [10], and J/Ψ suppression [76].

First estimates of direct photon radiation from relativistic heavy ion collisions [10, 77, 78] assumed that the dominant source will be a thermally equilibrated QGP, and the shape of the p_T spectrum would reflect its properties. Then in 1991 a very influential paper [29] came to the conclusion that “the hadron gas shines just as brightly as the quark-gluon plasma”. The primacy of QGP radiation has been questioned. Note that in this calculation the space-time evolution of the system was not yet considered. Due to technical and conceptual difficulties it took some time before the dynamical expansion of the radiating system became standard part of photon yield calculations.

Around 2000, based on Pb+Pb direct photon results from WA98 [69], quark-hadron duality and the space-time evolution of the fireball modeled in Bjorken hydrodynamics [59] the calculations became more sophisticated and the predictions more differential (in p_T). For instance, in [79] it has been predicted that at RHIC and LHC the QGP will “outshine” the hot hadron gas above p_T of 3.2 and 2.5 GeV/c , respectively, while below that (and at the SPS in the entire spectrum) radiation from the hadron gas will dominate. The

⁸ See a lively historic review in [75].

complexity of the problem⁹ is illustrated by the fact that right before the appearance of the Pb+Pb data the dominance of the partonic phase was claimed [80] (“photons from quark matter could easily outshine those from the hadronic matter”), but within less than a year, in light of the new data, which, if anything, should be richer in QGP, the same author(s) reach the conclusion [81] that “the photon yield... gets a dominant contribution from the radiations in hadronic matter”. As we pointed out repeatedly, direct photon yields are a convolution of many terms that are hard to “factorize” experimentally.

With the observation of an unexpectedly large direct photon flow v_2 [82] (essentially the same magnitude as hadron v_2) the situation became even more complicated: models had to simultaneously explain large yields and v_2 . Large yields are usually easier to get early (at higher temperatures, *i.e.* from the QGP phase), but large v_2 usually indicates late production (hadronic phase). However, this is not the only possibility: in the past few years some mechanisms producing photons with large asymmetries very early, pre-equilibrium have also been proposed. We will discuss the current models in Sec. VI, but it is safe to say that for the time being we are not sure which stage of the evolution dominates the emission of low p_T photons, but most likely it is not the QGP.

III. EXPERIMENTAL TECHNIQUES

Direct photon measurements are “notoriously difficult” due to a combination of low rates, large physics background (photons from hadron decays), occasional instrumental background (photons from secondary interactions with detector components) and issues with photon identification (contamination from misidentified hadrons at low p_T and hadron decay photon pairs merged and misidentified as a single photon at high p_T).

There are two fundamentally different techniques to measure real photons: *electromagnetic calorimetry* where the energy of the photon itself is measured directly, and *conversion*, where the photon converts into an e^\pm pair¹⁰; the original photon direction and energy are then reconstructed from the measured e^\pm pair momenta.

A. Real photons (calorimetry)

Electromagnetic calorimeters are detectors in which the impinging photons and electrons lose (ideally) all their energy, part of which is converted into some detectable signal. The energy loss mechanism is the production of secondary particles in an alternating sequence of pair creation ($\gamma \rightarrow e^+e^-$) and Bremsstrahlung ($e^\pm \rightarrow e^\pm\gamma$), until the energy of the secondaries fall below the critical energy [83]. The set of all secondaries is the (electromagnetic) *shower*, a statistical object. The average depth of the shower is proportional to $\ln(E)$, and is usually measured in units of *radiation length* X_0 (related to the mean free path of the shower particles in the material), while the transverse size is characterized by the *Moliere-radius* ρ_M (about 95% of the electromagnetic shower is contained laterally in a cylinder with radius $2\rho_M$ [83]). Part of the deposited energy is converted into some detectable signal, like Cerenkov or scintillation light, captured by some photosensitive device, or the number of electrons at various depths, typically measured by silicon detectors. The transverse size of the detector modules read out individually (*granularity*) is of the order of ρ_M , optimizing the contradictory requirements of energy and position resolution¹¹. To prevent *shower leakage* at the far end the depth of the modules should be at least $18\text{--}20X_0$.

Calorimeters can be *homogeneous*, like scintillating crystals or strong Cerenkov emitters; in these transparent detectors the entire volume is *active*, because light is produced everywhere and most of it can be collected and observed. In *sampling calorimeters* highly absorbing *passive* regions (usually high Z material) absorb most of the energy without producing detectable signals. These alternate with regions of active material, where the remaining energy of the shower produces observable light or charge (“visible energy”). The ratio of visible to total energy is called the *sampling fraction*. Due to the statistical nature of shower development the resolution of sampling calorimeters is inferior to homogenous ones, but they can be much more compact and cost-effective. For good calorimeters the resolution is dominated by the *statistical term* $\sigma_E/E \propto A/\sqrt{E(\text{GeV})}$, with A in the few percent range for homogenous and $\approx 8\text{--}15\%$ for sampling calorimeters. Excellent reviews of calorimeter technologies, performance, applications (and pitfalls!) can be found in [84–86].

Photon reconstruction in electromagnetic calorimeters involves identifying showers (clusters in the raw data) that are likely coming from photons, rejecting hadrons, reconstructing the photon energy and its

⁹ Not the least due to the incomplete knowledge of the equation of state, governing the space-time-temperature evolution of the system.

¹⁰ Preferably, but not necessarily at a known place in the detector.

¹¹ In heavy ion physics calorimeters are usually designed such that a shower from a single impinging particle deposits energy in several neighboring modules (“cluster”). Energy measurement is usually better, if the cluster consists of fewer modules, but impact position measurement improves with the number of modules.

impact point on the calorimeter surface. An additional, extremely important step is at higher energies to determine whether a single, photon-like cluster comes indeed from a single photon, or two nearby photons, *e.g.* from a π^0 decay (merging). Hadron rejection is sometimes aided by a thin, charge-sensitive device in front of the calorimeter (charge veto), while the position measurement and the resolution of two nearby photons can be enhanced by a high granularity “pre-shower” detector. The principal tool for photon identification is the analysis of the shower shape (size, compactness, dispersion, ellipticity, comparison to the predictions of a shower model *etc.*), where the different characteristics are often combined stochastically [87]. – Yet another way to distinguish between single photons and merged decay photons of the same total energy is to use a longitudinally segmented calorimeter (see for instance the UA1 detector at CERN [88]): the penetration of the two smaller energy photons is shallower, so the ratio of energy deposit in the first and second segment discriminates between a single high energy and two lower energy, but merged photons.

As mentioned before, the direct photon signal has a large background from hadron decay photons. In a low multiplicity environment, like pp collisions, such decay photons can be *tagged* in each event with a reasonable efficiency by checking if it has an invariant mass $m_{\gamma\gamma}$ consistent with π^0 if combined with *any* other photon in the event. In high multiplicity events, like A+A, such tagging isn’t possible, because the *combinatorial background* – two, in reality uncorrelated, photons having by accident $m_{\gamma\gamma}$ consistent with the π^0 mass – is too large. In A+A the direct photon yield is usually obtained *statistically*, by subtracting the *estimated* decay photon yield from the observed *inclusive* yield. The decay kinematics is known, but it is hard to overemphasize how much in these type of measurements the accuracy of the final direct photon result depends on the knowledge of hadron yields, particularly those of π^0 and η . Ideally those are measured in the same experiment, with the same setup, to minimize systematic uncertainties from acceptance, absolute calibration, and so on. Note that the photon contribution from other meson decays is usually small compared to other uncertainties of the measurement.

Once the π^0 and η spectra are known, their decay photon contribution in the detector has to be simulated (including the acceptance and analysis cuts), then this simulated decay spectrum is subtracted from the inclusive photon spectrum. Finally, the difference (inclusive - decay), *i.e.* the direct photon spectrum has to be unfolded for detector resolution and other effects [87].

B. External and internal conversion

In high multiplicity heavy ion collisions calorimetry is not ideal for photon measurements in the low p_T (less than 3-4 GeV/c) range¹². Instead, photons that converted into an e^+e^- pair in some (external) detector material are reconstructed from the invariant mass $m_{e^+e^-}$ of dielectrons. Momentum resolution in tracking is usually much superior to energy resolution in calorimeters, so the photon energy is measured more precisely and the direction of the photon is reconstructed, too. The method is described for the case where the conversion point (radius) is assumed in [89], or explicitly known from secondary vertex reconstruction in [90]. Hadron contamination is typically very small (less than 1-5% of the sample); the main background is due to dielectrons from π^0 Dalitz-decay. The drawback is small statistics, since detectors, for obvious reasons, tend to put as little material as possible in the region where high precision tracking is done, so the probability for real photons to convert on such material is small. This limits the high p_T reach of the measurement typically to a few GeV/c. –

Recently, another technique has been introduced that does not require *a priori* knowledge of the conversion point (radius) [91]. It relies on the fact that if a pair of well-identified e^+e^- tracks cross at a certain point, which is at macroscopic distance from the vertex with some detector material nearby *and* the opening angle of the tracks at this point is zero, it is virtually certain that they come from a converted photon (see Fig. 6).

Yet another method (“internal conversion”) takes advantage of the fact that any process emitting real photons can also produce off-shell virtual photons (γ^*), which then emerge as low invariant mass e^+e^- pairs. The relation between real photon production dN_γ/dp_T and associated e^+e^- production can be written as [92–94]

$$\frac{d^2 N_{ee}}{dm_{ee} dp_T} = \frac{2\alpha}{3\pi} \frac{1}{m_{ee}} \sqrt{1 - \frac{4m_e^2}{m_{ee}^2}} \left(1 + \frac{2m_e^2}{m_{ee}^2}\right) S(m_{ee}, p_T) \frac{dN_\gamma}{dp_T} \quad (5)$$

¹² The principal reasons are rapidly deteriorating resolution ($\propto 1/\sqrt{E_\gamma}$), increasing contamination from hadrons, including neutral ones like n, \bar{n} , and lack of direction which hinders rejection of instrumental background photons.

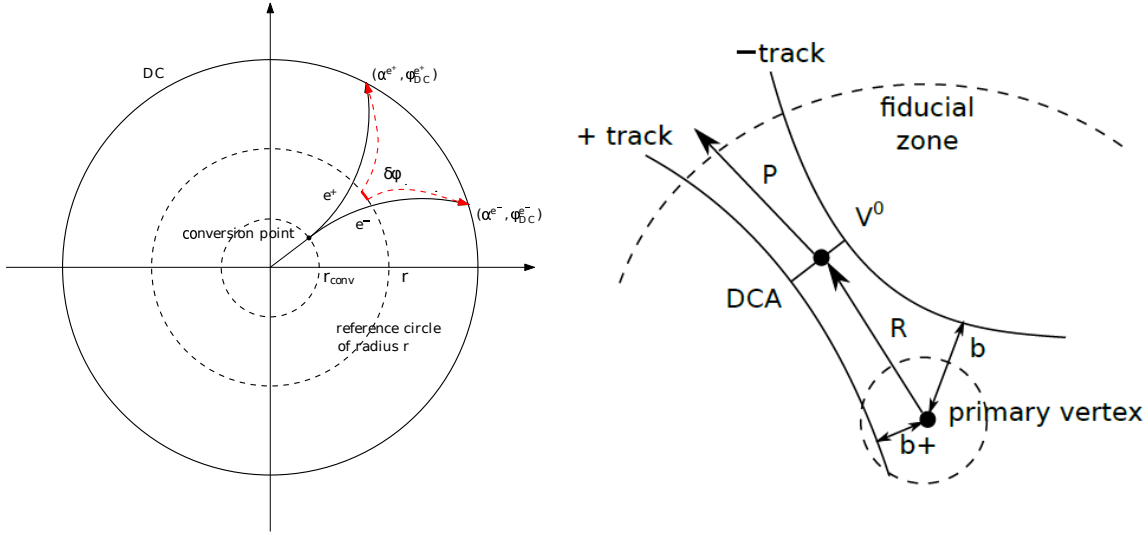


FIG. 6. (Left) e^+e^- conversion pair reconstruction in PHENIX, based on the fact that the tracks cross at a point with known detector material and at that point their opening angle is zero. Electrons are identified via Cherenkov-radiation, energy deposit pattern and E/p ratio in the calorimeter. (Figure courtesy of Wenqing Fan.) (Right) Conversion pair reconstruction in ALICE based on the distance of closest approach (DCA) far from the collision vertex. Electrons are identified via dE/dx in the TPC. (Figure courtesy of Friederike Bock.)

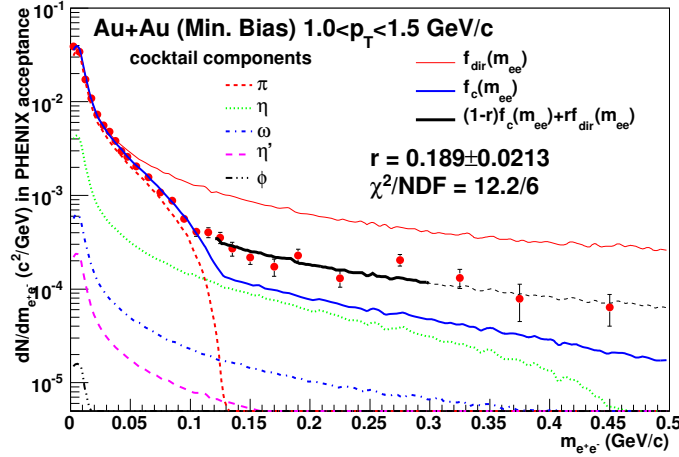


FIG. 7. Electron pair mass distribution for minimum bias Au+Au collisions, $1.0 < p_T < 1.5 \text{ GeV}/c$. The red curve shows the expected shape from direct (virtual) photons ($f_{dir}(m)$), the blue curve is the expected shape from the hadron cocktail ($f_c(m)$), r is the direct photon fraction of the total dielectron yield, the free parameter of the two-component fit (black curve). (Figure taken from [92].)

where α is the fine structure constant, m_e is the electron mass, m_{ee} the mass of the dielectron pair, $S(m_{ee}, p_T)$ is a process-dependent factor encoding the differences between real and virtual photon production. The terms containing m_e^2/m_{ee}^2 go to unity for $m_{ee} \gg m_e$. The factor $S(m_{ee}, p_T)$ is *assumed*¹³ to become unity as $m_{ee} \rightarrow 0$ or $m_{ee}/p_T \rightarrow 0$, i.e. at sufficiently high p_T [92, 96, 97]. This way Eq. 5 simplifies to

$$\frac{d^2 N_{ee}}{dm_{ee} dp_T} \approx \frac{2\alpha}{3\pi} \frac{1}{m_{ee}} \frac{dN_\gamma}{dp_T} \quad (6)$$

The measurement then proceeds as illustrated in Fig. 7, providing the direct photon excess ratio r . At any given p_T the $m_{e^+e^-}$ distribution is fitted with a two-component function

$$f(m_{ee}, r) = (1 - r)f_c(m_{ee}) + rf_{dir}(m_{ee})$$

¹³ There are some arguments about the validity of this assumption, for instance in [95].

where $f_c(m_{ee})$ is the expected shape of the background (“cocktail”) mass distribution, $f_{dir}(m_{ee})$ is the expected shape of the virtual direct photon internal conversion mass distribution, both separately normalized to the data for $m_{ee} < 30 \text{ MeV}/c^2$. The direct photon excess ratio r is the only free parameter. If the inclusive photon yield is known, the direct photon yield can be calculated as $dN_\gamma^{dir}(p_T) = r \times dN_\gamma^{incl}(p_T)$.

C. Other tools and techniques

Pre-shower / photon multiplicity detectors

In a high multiplicity environment electromagnetic calorimeters often cannot measure individual photons (and their energy) due to the inherent limitation given by the transverse size of the electromagnetic showers¹⁴. However, sometimes the sheer number of photons – irrespective of their energy – can be an important observable (see Sec. V A). Photon multiplicity detectors are simple devices, with a thin ($2\text{--}3X_0$) converter followed by a high granularity sensitive layer, like small scintillator pads [98, 99], read out separately. Most hadrons crossing the scintillator deposit only minimum ionization energy, so counting the pads with energy above this threshold is a good proxy of the number of photons. The readout device can be as simple as a CCD camera [100]. – *Pre-shower detectors* are usually installed in front of electromagnetic calorimeters meant to solve the problem of resolving single photons from two close-by photons from the decay of a high momentum π^0 and to provide a very precise measurement of the impact point. They usually consist of layers of thin ($0.5\text{--}1 X_0$) converters and high granularity, position sensitive detectors, like fine pitched Si pads or wire chambers [101]. The electromagnetic showers start *before* entering the calorimeter proper, their transverse size is still very small, so even close-by particles can be well distinguished. A variation on the idea is the *shower maximum detector*, a similar, charge-sensitive, high granularity device placed at $5\text{--}6X_0$ depth in the calorimeter, where the showers are already well developed [102].

Isolation cuts

Isolated high p_T prompt photons are a precious tool to investigate pQCD, the gluon distribution functions [46, 103, 104] and, in back-to-back correlation measurements, setting the parton energy scale (γ -jet) and measuring fragmentation functions of partons into final state hadrons (γ -hadron)¹⁵. Here *isolated* means little or no activity – at least no *correlated* activity – in the vicinity of the photon. Isolation cuts are not uniquely defined, they vary depending on the experiment, colliding system and energy, but typically they impose an upper limit on the energy observed in a certain radius around the photon, derived from the average “underlying event”. As an example, for $\sqrt{s_{NN}} = 2.76 \text{ TeV}$ Pb+Pb collisions and photons of 20 GeV energy or higher CMS requires less than 5 GeV energy in an isolation cone of the size $\Delta R = \sqrt{(\Delta\eta)^2 + (\Delta\varphi)^2} < 0.4$ around the photon [105]. For $\sqrt{s} = 200 \text{ GeV}$ pp collisions PHENIX requires that the sum of the momenta of charged tracks in a cone $\Delta R < 0.3$ should be less than 10% of the photon energy [106]. Lack of a single, unique definition makes the comparison of isolated photon data from different experiments difficult, and of course theory calculations should always try to implement the same cuts as the experiment they are compared to.

Hanbury Brown – Twiss correlations.

Hanbury Brown – Twiss (HBT) interferometry [108] has been extensively used for hadrons [109] earlier to explore the space-time extent of the emitting source at kinetic freeze-out. Applying it for momentum differences of photon pairs from heavy ion collisions sounds eminently plausible: after all, the method has been first introduced to measure the size of distant stars using two-photon correlations. For a chaotic source and photons of similar momenta ($p_1 \approx p_2$) the correlation of the invariant relative momenta $Q_{inv} = \sqrt{-(p_1 - p_2)^2}$ is Gaussian and it characterizes both the source size and its relative strength with respect to other sources [110]. The ΔQ_{inv} region where the correlation is enhanced (width of the Gaussian) is inversely proportional to the source size R ($\Delta Q_{inv} \sim \hbar/R$). That means that HBT at very low ΔQ_{inv} can in principle differentiate between photons from the collision itself (length scale is fm, $\Delta Q_{inv} \sim \hbar/fm \sim 100 \text{ MeV}$) and final state hadron decay (length scale is nm, $\Delta Q_{inv} \sim \hbar/fm \sim 100 \text{ eV}$)¹⁶. Furthermore, if f is the fraction of photons from a particular source, the λ strength parameter of the respective correlation is proportional

¹⁴ They still can measure total neutral energy in a solid angle, a quantity relevant for instance in jet physics.

¹⁵ In Sec. II we discussed fragmentation of a quark or gluon into a photon, *i.e.* the photon is non-isolated, part of a jet, carrying a fraction of the original parton energy. Here we discuss back-to-back correlation of an isolated photon, that emerges unchanged from the hard scattering, and a jet on the opposite side. The isolated photon has the same energy as the quark or gluon originating the opposing jet, setting the scale to the fragmentation function of the original parton into the final state hadrons observed in the jet.

¹⁶ In [111] it has been suggested that HBT of photons at $k_T = 2 \text{ GeV}/c$ could be used to measure the system size at the time of hard scattering, *before* thermalization. Even more detailed information on quark-gluon dynamics using high p_T photon HBT

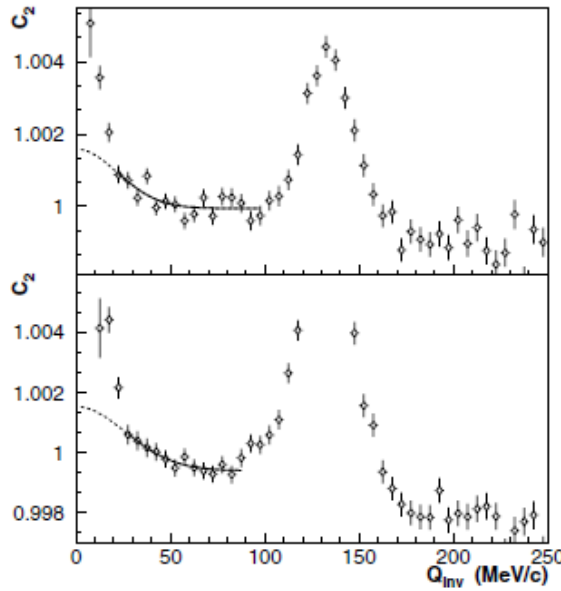


FIG. 8. Two-photon correlation function for average photon momenta $100 < p_T < 200$ MeV (top) and $200 < p_T < 300$ MeV (bottom). The dotted line is the extrapolation to low Q_{inv} assuming chaotic (Gaussian) distribution to get the correlation strength λ . (Figure taken from [107].)

to f^2 [110]. So if one can measure the inclusive yield of photons at momentum p and the correlation strengths of photon pairs with the same average momentum and $\Delta Q_{inv} \sim 10\text{-}100$ MeV, one can assert the direct photon yield at p . As seen in Fig. 8 the method is quite delicate: around $Q_{inv} \sim 0$ the background is overwhelming, and the Gaussian has to be reconstructed and extrapolated to $Q_{inv} = 0$ in a narrow Q_{inv} window. Furthermore, to measure small differences of large momenta with high precision is a task ill-suited for the average calorimeters. Conversion techniques with their superior energy resolution are more promising, but due to their low rate still very challenging and never tried so far. A very clear and pedagogical description of the method is given in [15].

D. Ways to present direct photon data

There are several ways to present the direct photon data. The most transparent one is the cross section (for pp) or *invariant yield* (for A+A)

$$\sigma(p) = E \frac{d^3\sigma}{dp^3} \quad \text{and} \quad N_{inv}(p_T) = \frac{1}{2\pi p_T} \frac{1}{N_{evt}} \frac{dN}{dp_T dy}$$

where y is the rapidity (equivalent to pseudorapidity η for photons). This quantity is easy to compare to pQCD or other calculations (see Fig. 9, left panel). However, the uncertainties are usually quite large¹⁷. Another useful observable is the *excess photon ratio*

$$R_\gamma(p_T) = \frac{\gamma^{inclusive}(p_T)}{\gamma^{decay}(p_T)}$$

where $\gamma^{decay}(p_T)$ is the (calculated) number of hadron decay photons in the total inclusive photon spectrum. While information on the absolute yield is lost, in R_γ systematic uncertainties related to particle identification and energy scale are substantially reduced (see Fig. 9, right panel). On the other hand it is not a good quantity to make comparisons between different colliding systems, energies or centralities, because it depends on the yield of neutral mesons, too. If the direct photon yields are unchanged, but some reason mesons are suppressed or enhanced, R_γ becomes artificially high or low.

R_γ is not to be confused with the ratio of direct over inclusive photons

$$r_\gamma(p_T) = \frac{\gamma^{direct}(p_T)}{\gamma^{inclusive}(p_T)}$$

¹⁷ There are many issues, among them the irreducible problem that the direct photon spectrum is the *small* difference of two large numbers: the inclusive minus the hadron decay photons. Uncertainty of the absolute energy scale is another issue: 1% error on E_γ translates to $\sim 6\text{-}11\%$ error on the yield, depending on $\sqrt{s_{NN}}$.

also called “direct photon fraction” and preferred in internal conversion photon analyses [96, 97] (also see the left panel in Fig. 19).

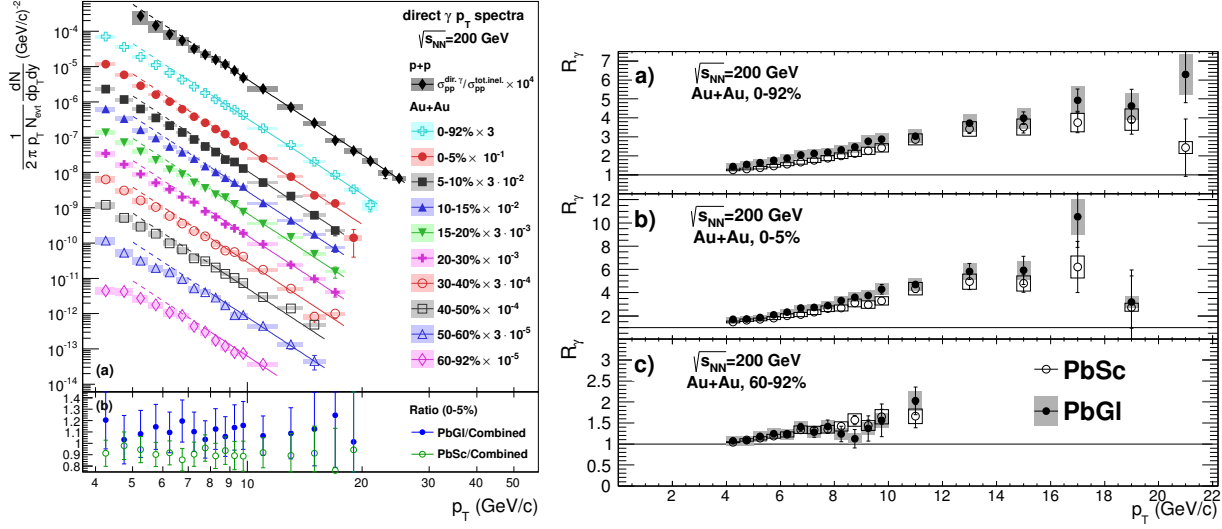


FIG. 9. Different ways to present direct photon data. Left: direct photon invariant yields in $\sqrt{s_{NN}} = 200$ GeV Au+Au collisions at different centralities (figure taken from [87]). Right: direct photon excess ratio, *i.e.* the inclusive/decay photon ratio R_γ for select centralities in $\sqrt{s_{NN}} = 200$ GeV Au+Au collisions (figure taken from [87]). See text for details.

A third way to present the results is the γ/π^0 ratio. Unfortunately it is used two different ways, and it is not always immediately clear which definition is meant in a particular instance. In one case its precise definition is $N_\gamma^{dir}(p_T)/N_{\pi^0}(p_T)$, the ratio of direct photon and π^0 yields at the same p_T . This ratio was very popular since the earliest days of perturbative QCD calculations, many quantitative predictions have been made for γ/π^0 in hadron-hadron collisions (see for instance [7, 8, 11]). The high p_T direct photons come primarily from quark-gluon Compton scattering, and preserve their original p_T , while the π^0 comes from the fragmentation of the scattered parton and carries only a fraction of the original parton p_T . This way the ratio $N_\gamma^{dir}(p_T)/N_{\pi^0}(p_T)$ at the same p_T can become quite large. If the fragmentation functions are known the process provides information on the gluon PDF in the colliding hadron [46, 113]. Experimentally, finding high p_T (isolated) photons in hadron-hadron collisions is moderately difficult (the multiplicity is low).

The second definition of γ/π^0 is the ratio $N_\gamma^{inc}(p_T)/N_{\pi^0}(p_T)$ of the *inclusive* photon and π^0 yields taken at the same p_T . This is a very robust quantity, since inclusive (but not necessarily direct) photons can be measured even in very high multiplicity environments. On the other hand, it carries only limited information content (see Fig. 10, left panel). It can indicate the presence of direct photons in addition to the numerous decay photons, but is rarely used to extract actual yields or cross-sections. Its usefulness is rooted in Sternheimer’s formula [114] stating that at sufficiently high energies ($E > 500$ MeV) the energy spectrum of decay photons is related to the π^0 spectrum (in the same solid angle) as

$$N_\gamma(E_\gamma) = \int_{E_\gamma}^{\infty} \frac{2}{E_{\pi^0}} N_{\pi^0}(E_{\pi^0}) dE_{\pi^0}$$

At mid-rapidity and high energies E_γ and E_{π^0} can be replaced by the respective p_T . Since high p_T particle spectra are power-law ($\sim p_T^{-n}$), the decay photon spectra are related to the π^0 spectra as $N_\gamma(p_T) = (2/n)N_{\pi^0}(p_T)$, and the γ/π^0 ratio converges to a constant $2/n$ at higher p_T , if and only if the sole source of photons is π^0 decay. It was frequently used in the early days of photon physics, and even today it is an important sanity check in any photon analysis. It also inspired the introduction of the *double ratio* of the measured inclusive γ/π^0 and the simulated, purely decay γ/π^0

$$R(p_T) = \frac{\gamma_{meas}^{inc}(p_T)/\pi_{meas}^0(p_T)}{\gamma_{sim}^{dec}(p_T)/\pi_{sim}^0(p_T)}$$

a quantity very similar, but not identical to R_γ discussed above (see Fig. 10, middle panel). Finally, we should mention the N_γ/N_{ch} ratio of photons to charged particles (see Fig. 10, right panel), frequently used in the early days of direct photon physics, because it didn’t require reconstruction of the π^0 spectrum (see Sec. V A).

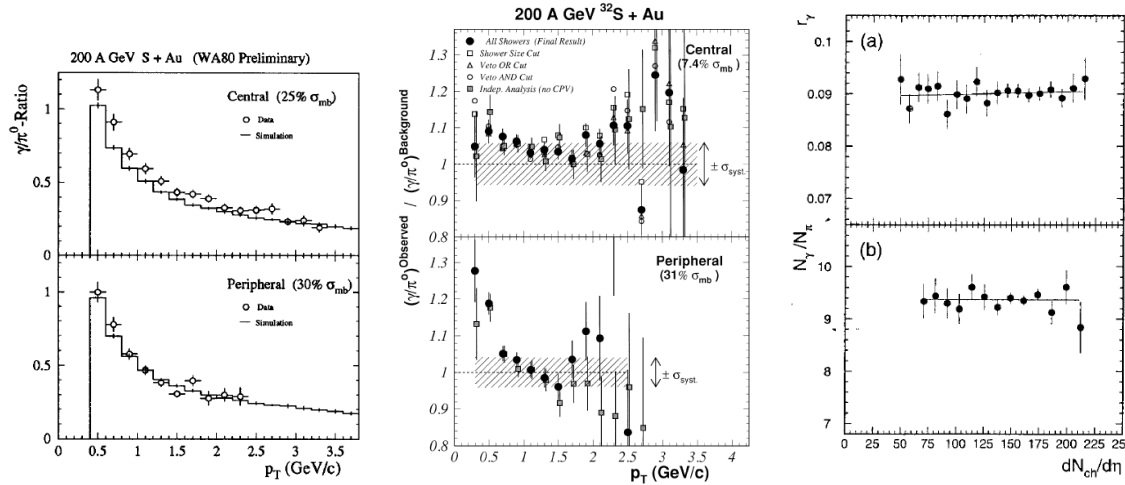


FIG. 10. Different ways to present direct photon data. Left: γ/π^0 ratio [115]. Middle: double ratio [116] of the measured γ/π^0 and the one simulated purely from hadron decays. Right: N_γ/N_{ch} from [117], not requiring reconstruction of π^0 . See text for details.

IV. THE HIGH P_T REGION.

A. Hard photons in pp and $p\bar{p}$ collisions

While the actual transverse momentum above which direct photons are considered “high p_T ” is ill-defined, the term usually refers to photons originating from scattering of hard (large x) partons and calculable with pQCD, with the dominant process being quark-gluon Compton scattering ($qg \rightarrow q\gamma$). Typically p_T larger than 3-5 GeV/ c is considered high p_T (depending on \sqrt{s}), and photon measurements are relatively easy there. Below that the uncertainties on calculations are large (reaching an order of magnitude [118]), not the least because the fraction of fragmentation photons increases, but the actual values are poorly known. As we will see later, at low p_T the experimentally observed yields are usually very small [96] or just upper limits [118], so there is little input to meaningfully test the calculations.

1. Spectra

High p_T direct photons in pp collisions in the $30 < \sqrt{s} < 62$ GeV range have first been studied at the CERN ISR¹⁸ up to $p_T = 7$ GeV/ c [119], by measuring the ratio of single photons to π^0 at the same p_T (γ/π^0) for $\sqrt{s} = 31, 53$ and 63 GeV. For photons coming from π^0 decays this ratio is easy to calculate (see Sternheimer’s formula, Sec. III D); in presence of direct photons the ratio will increase. Within uncertainties γ/π^0 was consistent with no direct photons at $p_T = 3$ GeV/ c (all measured photons were accounted for from hadron decays), then started to rise slowly, reaching about 20% excess above 5 GeV/ c . Remarkably, γ/π^0 didn’t seem to depend on \sqrt{s} . Using the same setup and measuring the differences in same-side and away-side charged multiplicity in events triggered by π^0 and single photons R807 found evidence that the dominant process might indeed be $qg \rightarrow q\gamma$ [120]¹⁹. One interesting consequence is that direct photons offer access to gluon PDFs, another one is that if those “isolated” photons are back-to-back to a jet, they provide a very good estimate of the jet (*i.e.* the original parton) energy.

By 1982 inclusive cross-sections for single- γ and π^0 up to $p_T = 12$ GeV/ c in $30 < \sqrt{s} < 63$ GeV pp collisions were published [121]. The last important attempt at the ISR was the comparison of γ/π^0 in pp and $p\bar{p}$ by the AFS collaboration [122]. This was promising, because due to the presence of large x antiquarks in $p\bar{p}$ collisions the $q\bar{q} \rightarrow g\gamma$ annihilation process was expected to contribute to the high p_T direct photon production, as predicted by QCD, and its amplitude could in principle be determined when photon production in pp and $p\bar{p}$ is compared. Unfortunately, due to the short running time AFS didn’t find a statistically significant difference between the γ/π^0 in pp and $p\bar{p}$.

Shortly thereafter the situation changed when at the CERN $Spp\bar{S}$ the available energy in $p\bar{p}$ collisions increased an order of magnitude, up to $\sqrt{s} = 630$ GeV. Thanks to improvements in detector technology and

¹⁸ For a review of the early experiments at CERN ISR and Fermilab see [11]

¹⁹ A photon produced by this process has no additional multiplicity associated with it.

analysis techniques *isolated* direct photons could be measured²⁰ up to 100 GeV/c at mid-rapidity [88, 123]. Due to the presence of valence antiquarks $p\bar{p}$ collisions made it possible to study for the first time the $q\bar{q} \rightarrow \gamma\gamma$ process²¹, by observing back-to-back, isolated, high p_T “double photons” [88]. This rare process in principle provides information on the intrinsic k_T of the partons, by the transverse momentum imbalance of the two photons²², although perturbative corrections may destroy the significance [124]. Somewhat later, using an internal hydrogen gas jet target, pp and $p\bar{p}$ data were also taken at $\sqrt{s}=24.3$ GeV by UA6 and the difference $\sigma(p\bar{p} \rightarrow \gamma X) - \sigma(pp \rightarrow \gamma X)$ was measured for the first time [125, 126]. The difference isolates the leading order $q\bar{q}$ annihilation term and with the quark distributions known from deep inelastic scattering, this way one could determine the gluon distributions from the other leading order process, the $qg \rightarrow \gamma q$ Compton scattering, and even α_s can be measured [127].

In the early 1990s Fermilab experiments CDF and D0 measured prompt photon cross sections in $\sqrt{s}=1.8$ TeV $p\bar{p}$ collisions up to $p_T=120$ GeV/c. CDF measured at central rapidities [128], while D0 also published results for forward rapidities [129], providing constraints on the low- x gluon distributions. All these data provided input for incremental improvement of NLO, then NNLO calculations [130–132] without any major surprises. However, one particular fixed target experiment (FNAL E706 [133, 134]) strongly disagreed with the calculations, triggering speculations that the effect of intrinsic k_T is much larger than previously assumed, and, to lesser extent, the results from WA70 [135] also deviated from the general trend, shown below. Due to this discrepancy, photon data in pp and $p\bar{p}$ were omitted from global-fit analyses of proton PDFs for about a decade [103].

The relatively wide \sqrt{s} gap between the CERN and FNAL fixed target and collider data has been filled by RHIC when PHENIX published direct photon cross-sections in pp at $\sqrt{s}=200$ GeV [136, 137] and STAR in [138]. Although pp data have been taken at $\sqrt{s}=510$ GeV as well, direct photon spectra have not been published yet. The impact of the FNAL and RHIC data on the gluon distribution in the proton is discussed in [103]. At central rapidities various PDF parametrizations provide cross sections within 15%, while at $y=4$ (low x) the differences are within 30%. The uncertainties are largest at low E_T^γ which has some impact on the “thermal” photon measurements in heavy ion collisions, too.

Beyond FNAL energies at the LHC both ATLAS and CMS measured isolated prompt photon cross-sections at $\sqrt{s}=7$ TeV [139, 140], CMS and ALICE provided data at 2.76 TeV [105, 118], ATLAS and ALICE published results for 8 [118, 141] and ATLAS for 13 TeV, too [142] (see Table I).

A convenient and physics driven way to compare pp photon data taken at very different \sqrt{s} and covering orders of magnitude both in p_T and cross-section is to present them as a function of the *scaling* variable $x_T=2p_T/\sqrt{s}$. For the hard scattering region [143]

$$E \frac{d^3\sigma}{dp^3} = \frac{1}{\sqrt{s}^{n(x_T, \sqrt{s})}} G(x_T)$$

where $n(x_T, \sqrt{s})=4$ for leading order QCD without evolution of α_s , and all effects from the structure function and the fragmentation function into photons are encoded in $G(x_T)$. Higher order effects usually increase the value of $n(x_T, \sqrt{s})$.

An excellent compilation of the data on prompt photon production in hadron-hadron interactions, available until 1997, and comparisons in terms of x_T to contemporary NLO calculations can be found in [144]. The comparisons were moderately successful, meaning that in addition to differences in absolute magnitude often the *shapes* of the spectra in data and theory differed significantly. This can be explained in part by lack of proper tools to implement the precise experimental cuts (like isolation cuts) in the calculations.

A decade later a landmark survey of photon production in hadronic collisions [32], using NLO pQCD calculations implemented in the JETPHOX Monte Carlo code, found much better agreement between data and theory (see Fig. 11, left panel). Apart of two (controversial) datasets from Fermilab E706 [134] and to some lesser extent the D0 results [145] the data are well described from $\sqrt{s_{NN}}=23$ GeV to 1.96 TeV, covering 9 orders of magnitude in cross section.

In Fig. 11, right panel, the pp and $p\bar{p}$ direct photon data available in 2012 are shown. The cross sections are multiplied by $(\sqrt{s})^{4.5}$ and plotted vs x_T . The data covering the range of 19.4 - 7000 GeV in \sqrt{s} line up on a single curve, and the effective exponent $n_{eff}=4.5$ indicates that the role of scaling violations from PDF and running of α_s is small [157]. The fact that hard photon production in pp is well understood is crucial when interpreting certain observations in heavy ion collisions, at least down to $x_T=10^{-2.3}$. Direct photon cross-section measurements in pp are summarized in Table I.

²⁰ In fact, being isolated, *i.e.* a single large neutral energy deposit with no other activity around it became the main identification criterion of direct photons, to distinguish them from two very close decay photons from a π^0 , which in turn was expected to be part of a jet, with plenty of activity near the photon [123].

²¹ A real *tour de force* with altogether 6 events found.

²² For more detailed discussion see Sec. IV A 2.

²³ Recent measurements by ALICE [118] extended the x_T range down to 10^{-4} , although often providing only upper limits. The new data don't line up with the trend seen previously at higher x_T (see Bock [158]).

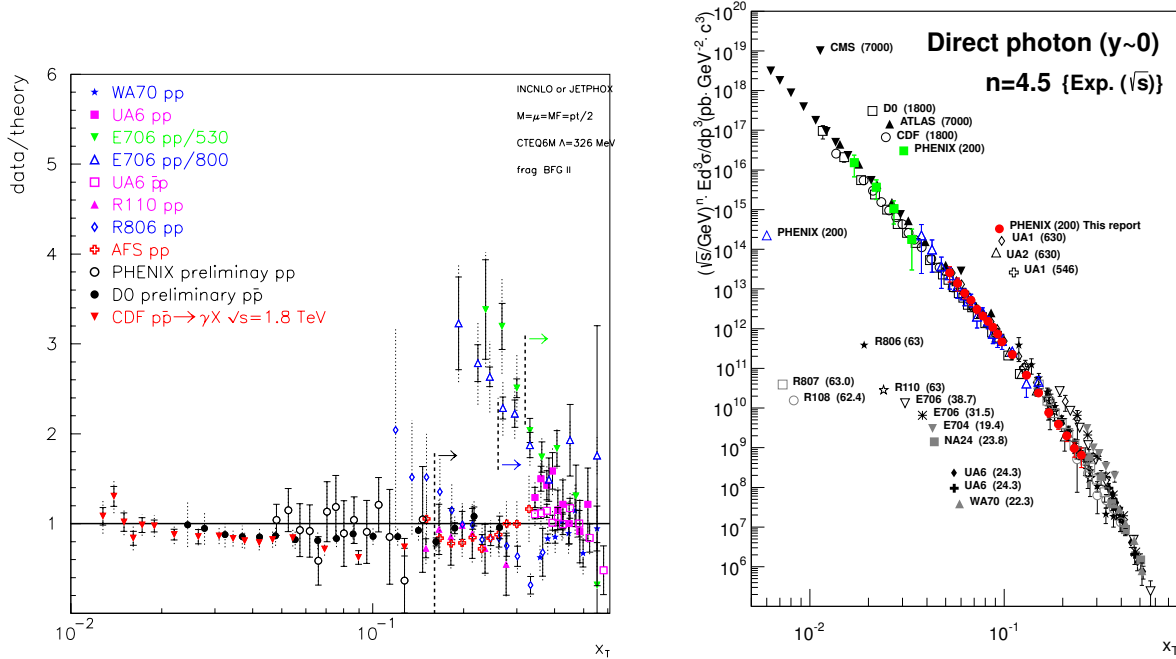


FIG. 11. Left: direct photon data compared to NLO calculations for select pp and $p\bar{p}$ results as of 2006 (figure courtesy of P. Aurenche and M. Werlen, see also [32]). Sources of data: WA70 [135], UA6 [126], E706 [134], R110 [146], R806 [121], AFS [147], D0 [145], CDF [148, 149]. Right: x_T -scaling of the world data on direct photons in pp and $p\bar{p}$ as of 2012 (figure taken from [137]). Sources of additional data included here: CMS [140], ATLAS [150], D0 [151], CDF [128, 152], PHENIX [92, 136, 137], UA1 [88], UA2 [153], R807 [147], R108 [154], E704 [155], NA24 [156], UA6 [125].

2. Photon-jet, photon-hadron and photon-photon correlations

With the caveat mentioned earlier (see also [124]), high p_T isolated photons back-to-back in azimuth with a high p_T hadron or jet can set the energy scale of the original hard scattered parton²⁴. It has been pointed out already in 1980 [113, 167, 168] that back-to-back isolated photon-jet correlation measurements in pp can provide direct information about the gluon distribution (PDF) in the proton, furthermore, if there is good particle identification on the jet side, also provide information on the parton fragmentation into hadrons, primarily of u quarks²⁵.

These measurements are more complicated than the inclusive photon technique by UA6 discussed above, but they are also richer in information [169]. PHENIX estimated the average parton transverse momentum k_T at RHIC energies in pp [106], and measured the ratio $z_T = p_T^h/p_T^\gamma$, a proxy for the fragmentation function [170]. A similar measurement has been published by STAR in [171]. Various proton PDF sets have been tested for instance by back-to-back isolated photon-jet measurements in pp at $\sqrt{s}=7$ TeV by ATLAS [172]. Also, the distribution of the rapidity difference Δy between the photon and the jet reveals that t -channel quark exchange (Compton-scattering) is the dominant source of photons, rather than gluon exchange (fragmentation) [172]. A recently published analysis of the 13 TeV data reaches similar conclusions [173]. The measurements are quite precise tests of pQCD – the experimental uncertainties are smaller than those of the theory calculations. Triple differential cross sections $d^3\sigma/(dp_T^\gamma d\eta^\gamma d\eta^{jet})$ in pp at 7 TeV have been published by CMS and compared to LO (SHERPA) and NLO (JETPHOX) predictions: the LO calculation underpredicts the data by about 10-15%, while NLO describes the data within uncertainties. Recently Pb+Pb γ -jet results at 5.02 TeV have also been published by CMS [174].

While the most important properties of the free proton are encoded in the PDFs, its multi-dimensional structure has long been conjectured (see for instance [43, 175]), and a breakdown of QCD factorization has been predicted when the nonperturbative transverse momentum of partons are explicitly considered (transverse momentum dependent, or TMD framework). Factorization breaking can be studied comparing

²⁴ This is particularly important in heavy ion collisions where the partons lose energy while traversing the QGP.

²⁵ The dominance of u -quarks in back-to-back correlations is demonstrated by the observed charge asymmetry of hadrons opposite to the photon [106, 146].

| Experiment | \sqrt{s} | method | η | p_T | Publications | Comment |
|-------------------------|-------------------------|------------|---------------------|---------------------|----------------------|-----------------------------|
| R412 / CERN ISR | pp 45, 53 GeV | calor. | $ \eta \sim 0$ | 1.6-3.8 GeV/ c | [159] (1976) | γ/π^0 |
| R107 / CERN ISR | pp 53 GeV | calor. | $ \eta \sim 0$ | 2.3-3.7 GeV/ c | [160] (1978) | γ/π^0 |
| AFS / CERN ISR | pp 31, 53, 63 GeV | calor. | $ \eta \sim 0$ | 3 - 7(9) GeV/ c | [119, 120] (1979/80) | γ/π^0 |
| CCOR / CERN ISR | pp 62.4 GeV | calor. | $ \eta < 1.1$ | 5 - 13 GeV/ c | [154] (1980) | |
| AFS / CERN ISR | pp 31, 45, 53, 63 GeV | calor. | $ \eta < \sim 0$ | 3 - 12 GeV/ c | [121] (1982) | |
| AFS R807 / CERN ISR | pp 63 GeV | calor. | $2.0 < \eta < 2.75$ | 1.5-4.25 GeV/ c | [161] (1983) | γ/π^0 |
| AFS R808 / CERN ISR | $pp, p\bar{p}$ 53 GeV | calor. | $ \eta < 0.4$ | 2-6 GeV/ c | [122] (1985) | γ/π^0 |
| UA2 / CERN $Spp\bar{S}$ | $p\bar{p}$ 630 GeV | calor. | $ \eta < 1.8$ | 15-43 GeV/ c | [123] (1986) | |
| NA24 / CERN SPS | pp 23.7 GeV | calor. | $ \eta < 0.8$ | 3-6 GeV/ c | [156] (1987) | fixed tgt |
| WA70 / CERN SPS | pp 22.3 GeV | calor. | | 4-6.5 GeV/ c | [135] (1988) | fixed tgt |
| UA1 / CERN $Spp\bar{S}$ | $p\bar{p}$ 546, 630 GeV | calor. | $ \eta < 3.0$ | 16-100 GeV/ c | [88] (1988) | |
| CMOR / CERN ISR | pp 63 GeV | calor. | $ \eta < 1.1$ | 4.5 - 10 GeV/ c | [146] (1989) | |
| AFS / CERN ISR | pp 63 GeV | calor. | $ \eta < 1$ | 4.5 - 11 GeV/ c | [147] (1990) | |
| CDF / FNAL | $p\bar{p}$ 1.8TeV | calor,conv | $ \eta < 0.9$ | 10-60 GeV/ c | [162] (1993) | iso. |
| UA6 / CERN $Spp\bar{S}$ | $pp, p\bar{p}$ 24.3 GeV | calor. | $-0.2 < \eta < 1$ | 4.1 - 5.7 GeV/ c | [125] (1993) | fixed tgt |
| E704 / FNAL | pp 19.4 GeV | calor. | $ \eta < 0.15$ | 2.5-3.8 GeV/ c | [155] (1995) | fixed tgt |
| UA6 / CERN $Spp\bar{S}$ | $pp, p\bar{p}$ 24.3 GeV | calor. | $-0.1 < \eta < 0.9$ | 4.1 - 7.7 GeV/ c | [126] (1998) | fixed tgt |
| D0 / FNAL | $p\bar{p}$ 1.8TeV | calor. | $ \eta < 2.5$ | 10-110 GeV/ c | [163] (2000) | iso. |
| D0 / FNAL | $p\bar{p}$ 0.63 TeV | calor. | $ \eta < 2.5$ | 10-30 GeV/ c | [145] (2001) | iso. |
| CDF / FNAL | $p\bar{p}$ 0.63, 1.8TeV | calor. | $ \eta < 0.9$ | 10-30(110) GeV/ c | [148] (2002) | iso. |
| CDF / FNAL | $p\bar{p}$ 1.8TeV | conv. | $ \eta < 0.9$ | 10-60 GeV/ c | [149] (2004) | iso. |
| E706 / FNAL | pp 31.8, 38.7 GeV | calor. | $ \eta < 0.75$ | 3.5 - 12 GeV/ c | [134] (2004) | fixed tgt |
| PHENIX / BNL RHIC | pp 200 GeV | calor. | $ \eta < 0.35$ | 5.5-7 GeV/ c | [164] (2005) | |
| PHENIX / BNL RHIC | pp 200 GeV | calor. | $ \eta < 0.35$ | 3-16 GeV/ c | [136] (2007) | iso. |
| PHENIX / BNL RHIC | pp 200 GeV | int. conv. | $ \eta < 0.35$ | 1-4.5 GeV/ c | [92, 96] (2010) | |
| STAR / BNL RHIC | pp 200 GeV | calor. | $ \eta < 1$ | 6-14 GeV/ c | [138] (2010) | |
| CMS / CERN LHC | pp 7 TeV | calor. | $ \eta < 1.45$ | 21-300 GeV | [140] (2011) | iso. |
| ATLAS / CERN LHC | pp 7 TeV | calor. | $ \eta < 1.81$ | 15-100 GeV | [139] (2011) | iso. |
| ATLAS / CERN LHC | pp 7 TeV | calor. | $ \eta < 2.37$ | 45-400 GeV | [150] (2011) | iso. |
| PHENIX / BNL RHIC | pp 200 GeV | calor. | $ \eta < 0.35$ | 5.5-25 GeV/ c | [137] (2012) | iso. |
| CMS / CERN LHC | pp 2.76 TeV | calor. | $ \eta < 1.44$ | 20-80 GeV | [105] (2012) | iso. |
| ATLAS / CERN LHC | pp 7 TeV | calor. | $ \eta < 2.37$ | 100-1000 GeV | [165] (2014) | iso. |
| ATLAS / CERN LHC | pp 8 TeV | calor. | $ \eta < 2.37$ | 25-1500 GeV | [141] (2016) | iso. |
| ATLAS / CERN LHC | pp 13 TeV | calor. | $ \eta < 2.37$ | 125-1000 GeV | [142] (2017) | iso. |
| ALICE / CERN LHC | pp 2.76 and 8 TeV | comb. | $ \eta < 0.9$ | 0.3-16 GeV | [118] (2018) | iso. |
| ATLAS / CERN LHC | pp 13 and 8 TeV | calor. | $ \eta < 2.37$ | 125-1500 GeV | [166] (2019) | iso. σ_{13}/σ_8 |

TABLE I. Summary of pp and $p\bar{p}$ direct photon data (spectra, cross-sections).

the acoplanarity [176] in back-to-back dihadron (dijet) and photon-hadron (photon-jet) angular correlation and its dependence on the hard scale (*i.e.* the trigger p_T). Measurements of π^0 -h and γ -h correlations in pp at $\sqrt{s}=200$ and 510 GeV [177, 178] have so far not confirmed factorization breaking in these processes.

As mentioned earlier, the $q\bar{q} \rightarrow \gamma\gamma$ and the $gg \rightarrow \gamma\gamma$ channels give access to the primordial (or intrinsic) k_T of partons, the driving factor behind the Cronin-effect [179]. In order to get high p_T photons valence antiquarks are needed. The WA70 experiment at CERN studied the $\pi^-p \rightarrow \gamma\gamma$ process at 280 GeV/ c beam momentum looking for two high p_T photons (>2.75 GeV/ c) and estimated the effective intrinsic k_T using three different observables ($\Delta\Phi, p_{out}$ and p_T ($\gamma\gamma$)), which all provided consistent $\langle k_T \rangle$ values in the 0.91-0.98 GeV/ c range [180]. At FNAL the CDF experiment measured isolated prompt diphoton $\langle k_T \rangle$ and cross-section in $p\bar{p}$ ($\sqrt{s}=1.8$ TeV) collisions [181] primarily with the goal to estimate a possible background to the Higgs-search in the $\gamma\gamma$ channel. Similar studies of diphoton angular and momentum correlations have been done at the LHC (see for instance [182]), not only to facilitate the Higgs search, but also because they are potent probes of QCD in some kinematic regions.

B. Hard photons in heavy ion collisions

As mentioned before, the definition of “hard” (high p_T) photons is somewhat arbitrary, but at RHIC and LHC energies usually photons above 3-5 GeV/ c are considered hard. The key issue is their origin: most hard photons come from low-order scattering of incoming partons with relatively high x momentum fraction, and are calculable in pQCD using the free hadronic or nuclear PDFs. This is to be contrasted with “soft” photons, that come from non-perturbative sources, ranging from “thermal” production to hadron Bremsstrahlung. Also note, that – somewhat misleadingly – hard photons are sometimes called “prompt” (first interaction)

photons, although not all prompt photons are necessarily high p_T and not all high p_T photons are prompt (*e.g.* fragmentation or jet-photon conversion photons).

Contrary to high p_T hadrons, invariant yields of hard photons in relativistic heavy ion collisions so far didn't provide major surprises, drastically new physics insights. Paradoxically, *this is the most favorable outcome possible*. High p_T photons are indeed penetrating probes, as advertised, well calculable in pQCD²⁶, unmodified by the QGP, thus they are important reference and solid calibration tools for hadronic processes, even if a medium is formed in A+A with a complicated space-time evolution.

1. Invariant yields

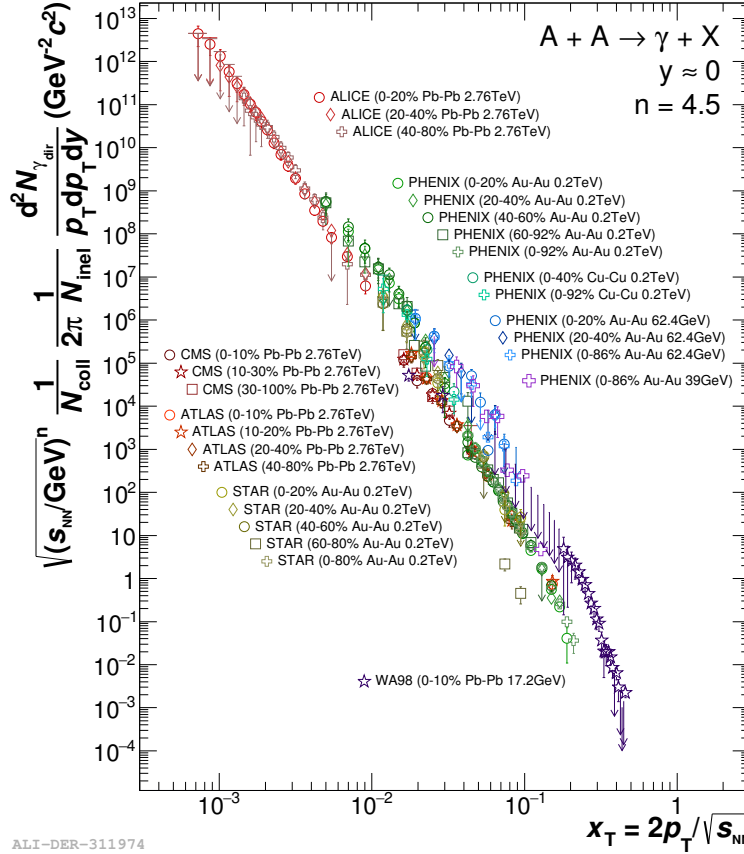


FIG. 12. x_T scaling of direct photon invariant yields at mid-rapidity in A+A collisions at different $\sqrt{s_{NN}}$ and centralities. (Figure courtesy of Friederike Bock.)

The first measurement of direct photon production at moderately high p_T ²⁷ in collisions involving nuclei (p +Be at 19.4 and 23.8 GeV) was published by Fermilab E95 in 1979 [183] and used calorimetry to establish the (inclusive) γ/π^0 ratio. The authors found an excess of single photons above that was expected from π^0 and η decays. The excess was consistent with the predictions in [184], and the signal increased both with increasing p_T and x_F . The next two decades were dominated by the CERN SPS program, with some activity at Fermilab and BNL AGS, and restricted mostly to fixed target pA collisions.

The first ion-on-ion results, published 1996 by WA80 [116] and NA45/CERES [117] still provided only upper limits on direct photon production in $S + Au$ collisions (5% and 14% of the inclusive photon yield, respectively, reproduced on two panels of Fig. 10). The first significant direct photon signal in A+A collisions ($Pb + Pb$ at 17.4 GeV) was published by WA98 [69] in 2000²⁸, and served as one of the strong evidences when CERN announced February 9, 2000 the “*creation of a new state of matter ...[exhibiting] features which cannot be understood in terms of conventional hadronic interactions*”.

²⁶ This means that the contribution of hard, but non-prompt photons to the total yield is relatively small.

²⁷ For a summary of the published invariant yield measurements see Table II.

²⁸ Photons were measured up to 4 GeV/c which can be considered high p_T at that $\sqrt{s_{NN}}$.

The first measurement of direct photon production at truly high p_T in collisions involving nuclei ($p+Be$ at 530 and 800 GeV/c) was published by FNAL E706 [133, 134] and has shown a large discrepancy between the data and the NLO pQCD calculations, irrespective of the scales applied. A similar discrepancy has been observed in π^0 production, too, leading the authors to suggest adding a supplemental Gaussian transverse momentum smearing to the incoming partons with $\langle k_T \rangle$ in the 1-1.7 GeV/c range to describe the data. Although never officially withdrawn, the validity of these data has been questioned [32].

| Experiment | $\sqrt{s_{NN}}$ | method | η | p_T | Publications | Comment |
|-------------------|----------------------------|------------|-----------------------|----------------|-----------------|-----------------|
| E95 / FNAL | $p + Be$ 19.4, 23.8 GeV | calor. | $-1.74 < \eta < 0$ | 1.5-4 GeV/c | [183] (1979) | γ/π^0 |
| E629 / FNAL | $p + C$ 19.4 GeV | calor. | $-0.75 < \eta < 0.2$ | 2.1-5 GeV/c | [185] (1983) | γ/π^0 |
| NA3 / CERN SPS | $p + C$ 19.4 GeV | calor. | $-0.4 < \eta < 1.2$ | 3-5 GeV/c | [186] (1986) | spectrum |
| NA34 / CERN SPS | $p + Be, p + Al$ 29 GeV | calor. | $-0.1 < \eta < 2.9$ | 0.0-0.1 GeV/c | [187] (1989) | spectrum |
| WA80 / CERN SPS | $(p, O)^+, (C, Au)$ 19 GeV | calor. | $1.5 < \eta < 2.1$ | 0.4-2.8 GeV/c | [188] (1991) | γ/π^0 |
| WA80 / CERN SPS | $S + Au$ 19 GeV | calor. | $2.1 < \eta < 2.9$ | 0.5-2.5 GeV/c | [116] (1996) | upp. lim. |
| NA45 / CERN SPS | $S + Au$ 19 GeV | conv. | $2.1 < \eta < 2.65$ | 0.4-2 GeV/c | [117] (1996) | upp. lim. |
| E855 / BNL AGS | $p + Be, W$ 18 GeV | calor. | $-2.4 < \eta < 0.5$ | 0.0-1 GeV/c | [189] (1996) | had. Brems. |
| E706 / FNAL | $p + Be$ 31.8, 38.7 GeV | calor. | $ \eta < 0.75$ | 3.5 - 12 GeV/c | [133] (1998) | spectra |
| WA98 / CERN SPS | $Pb + Pb$ 17.4 GeV | calor. | $2.35 < \eta < 2.95$ | 0.5-4 GeV/c | [69] (2000) | spectra |
| STAR / BNL RHIC | $Au + Au$ 130 GeV | conv. | $ \eta < 0.5$ | 1.65-2.4 GeV/c | [190] (2004) | R_γ^{-1} |
| E706 / FNAL | $p + Be$ 31.8, 38.7 GeV | calor. | $ \eta < 0.75$ | 3.5 - 12 GeV/c | [134] (2004) | spectra |
| WA98 / CERN SPS | $Pb + Pb$ 17.4 GeV | calor. | $2.35 < \eta < 2.95$ | 0.1-0.3 GeV/c | [107] (2004) | γ HBT |
| PHENIX / BNL RHIC | $Au + Au$ 200 GeV | calor. | $ \eta < 0.35$ | 1-14 GeV/c | [191] (2005) | spectra |
| PHENIX / BNL RHIC | $Au + Au$ 200 GeV | int. conv. | $ \eta < 0.35$ | 1-4.5 GeV/c | [92, 96] (2010) | spectra |
| STAR / BNL RHIC | $d + Au$ 200 GeV | calor. | $ \eta < 1$ | 6-14 GeV/c | [138] (2010) | |
| CMS / CERN LHC | $Pb + Pb$ 2.76 TeV | calor. | $ \eta < 1.44$ | 20-80 GeV | [105] (2012) | iso. |
| PHENIX / BNL RHIC | $d + Au$ 200 GeV | mixed | $ \eta < 0.35$ | 1-17 GeV/c | [192] (2013) | |
| WA98 / CERN SPS | $p + (C, Pb)$ 17.4 GeV | calor. | $2.3 < \eta < 3.0$ | 0.7-3 GeV/c | [193] (2013) | upp. lim. |
| PHENIX / BNL RHIC | $Au + Au$ 200 GeV | conv. | $ \eta < 0.35$ | 0.6-4 GeV/c | [89] (2015) | |
| ALICE / CERN LHC | $Pb + Pb$ 2.76 TeV | mixed | $ \eta < 0.9$ | 1-14 GeV/c | [90] (2016) | |
| ATLAS / CERN LHC | $Pb + Pb$ 2.76 TeV | calor. | $ \eta < 2.37$ | 22-280 GeV/c | [38] (2016) | |
| STAR / BNL RHIC | $Au + Au$ 200 GeV | int. conv. | $ \eta < 1$ | 1-10 GeV/c | [97] (2017) | |
| ATLAS / CERN LHC | $p + Pb$ 8.16 TeV | calor. | $-2.83 < \eta < 1.91$ | 25-500 GeV/c | [194] (2017) | iso. |
| PHENIX / BNL RHIC | $Cu + Cu$ 200 GeV | int. conv. | $ \eta < 0.35$ | 1-4 GeV/c | [195] (2018) | |

TABLE II. Summary of pA and AA, AB direct photon data (invariant yields).

RHIC enabled for the first time the study of photon production with heavy ions at p_T that is unquestionably in the pQCD range. PHENIX measured direct photons in 200 GeV Au+Au up to 14 GeV/c [191], followed by a $d+Au$ measurement by STAR [138]. Apart of the “isospin effect” (see Sec. IV B 4) the results were consistent with NLO pQCD calculations [131] scaled by the expected number of binary nucleon-nucleon collisions (see also Sec. IV B 2). The calculation used the CTEQ6 [196] set of parton distribution functions and the GRV [30] set of fragmentation functions. With the start of the LHC heavy ion program both $\sqrt{s_{NN}}$ and the p_T range increased considerably, but the measurements at CMS [105] (Pb+Pb at 2.76 TeV up to 80 GeV/c p_T), ALICE [90] (up to 14 GeV/c) and ATLAS [38] (up to 280 GeV/c) also agreed well with the respective NLO pQCD calculations, properly scaled, at least at central rapidity. These observations are strong evidence that the dominant sources of high p_T photons are the same in A+A as in pp , namely hard scattering, and those photons are unaffected by any later state or evolution of the colliding system. The nuclear modification factor of high p_T photons is about unity.²⁹

2. Nuclear modification factor

When nuclei A and B collide, the nuclear modification factor R_{AB} quantifies those effects on particle production in hard scattering processes that arise because entire nuclei collided rather than individual hadrons (like pp). Such effects can be the formation of the QGP, in which the hard scattered parton loses energy (final state or FS effects), but also the modification of the parton distribution functions in the nuclei with respect to those of free hadrons (nPDF, an initial state or IS effect). For an observable a (like jets, hadrons, photons) the yield measured in A+B is compared to the yield expected from the properly scaled number of independent nucleon-nucleon collisions. The scaling factor is the *nuclear overlap function* T_{AB} , originated

²⁹ Some small deviations are expected and well understood – see Sec. IV B 4.

in [197], or, more often, its equivalent $\langle N_{\text{coll}} \rangle$, the number of binary pp collisions, where the two quantities are connected by the total inelastic cross section

$$\langle T_{AB} \rangle = \langle N_{\text{coll}} \rangle / \sigma_{pp}^{\text{inel}}$$

N_{coll} can be derived for instance from a Monte-Carlo implementation of the Glauber model [198–200]. The nuclear modification factor is then defined as

$$R_{AB}^a(p_T) = \frac{(1/N_{AB}^{\text{evt}}) d^2 N_{AB}^a / dp_T dy}{(\langle N_{\text{coll}} \rangle / \sigma_{pp}^{\text{inel}}) d^2 \sigma_{pp}^a / dp_T dy}$$

where $d^2 \sigma_{pp}^a / dp_T dy$ is the measured pp cross section for observable a (jets, leading hadrons, photons) and $\sigma_{pp}^{\text{inel}}$ is the total inelastic pp cross section. If the yield of an observable a in A+A collisions is unaffected by the environment, *i.e.* it is a simple incoherent superposition of the yields from N_{coll} elementary pp collisions, R_{AA} would be unity³⁰. This is exactly the case for high p_T photons.

Contrary to that, already from the very first data taken at RHIC it was found that R_{AA} is much smaller than unity for high p_T π^0 – their production at any given p_T is *suppressed* in central Au+Au collisions as compared to the N_{coll} -scaled pp expectation [18]. The phenomenon, dubbed as “jet quenching”, and confirmed by numerous other measurements of hadrons and jets at RHIC and LHC, became a crucial evidence of QGP formation in heavy ion collisions. The interpretation was that while in A+A collisions high p_T partons are still produced at the expected rate (N_{coll} -scaled pp), they suffer radiative and collisional energy loss when moving through the colored QGP medium formed around them, and fragment into final state particles as a smaller energy parton would in a pp collision.³¹

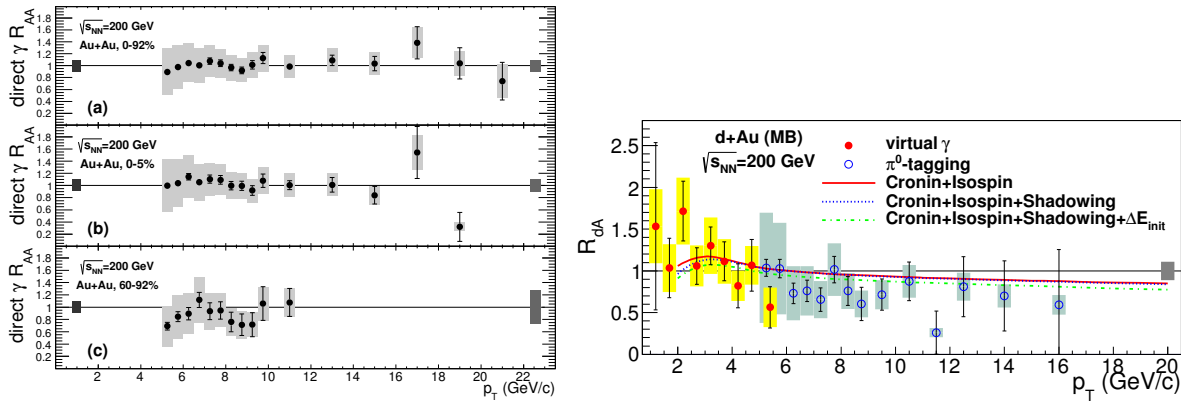


FIG. 13. Left: Direct photon nuclear modification factor R_{AA} for three different centrality selections in $\sqrt{s_{NN}}=200$ GeV Au+Au collisions. Figure taken from [87]. Right: direct photon nuclear modification factor for minimum bias d+Au collisions at $\sqrt{s_{NN}}=200$ GeV. Figure taken from [192], the calculations are from [202].

In Fig. 13 the direct photon R_{AA} is shown for various centralities in $\sqrt{s_{NN}}=200$ GeV Au+Au collisions [87]. All R_{AA} -s are consistent with unity within uncertainties, as expected, proving that the concept of N_{coll} and the way it is calculated are sane, at least in the case when two large ions collide. Similar results were obtained at the LHC by CMS [105] (see Fig. 14), ATLAS at mid-rapidity [38] and ALICE [90]: within uncertainties R_{AA} is unity. To first order neither enhancement, nor suppression can be observed for photons, *i.e.* N_{coll} , as calculated in A+A from the Glauber model, is a meaningful quantity. Therefore, the observed large suppression of hadrons and jets is not a methodological artifact.

Moreover, the nuclear modification factor for photons *at mid-rapidity* is around unity even in very asymmetric (small-on-large nuclei) collisions, at least in minimum bias collisions, as seen on the right panel of Fig. 13 for d+Au collisions at RHIC and Fig. 15 for p+Pb at LHC³². Note that – in contrast to the Pb+Pb case – dependence on collision centrality is not shown. In fact, determination of the collision centrality in small-on-large systems became controversial since 2012³³. We will discuss this and the role of photons in eliminating possible centrality biases in Sec. IV B 3.

³⁰ While the reverse is not necessarily true, it would be a remarkable coincidence if mechanisms enhancing and depleting R_{AA} would exactly cancel each other's effect over a wide p_T range.

³¹ This explanation was supported by the observation that the exponents n at high- p_T of the power-law spectra p_T^{-n} were very similar in pp and Au+Au, therefore, the difference between the A+A and N_{coll} -scaled pp yields could be interpreted as a δp_T shift in the p_T -scale [201].

³² The deviation from unity at large rapidities may reflect a nuclear modification of the parton densities (nPDF vs free proton PDF), but there are not enough data yet to settle this issue, which quite possibly will only be resolved at a future electron-ion collider (EIC).

³³ Now often replaced by the (purely experimental) “event activity” or some other non-geometric quantity.

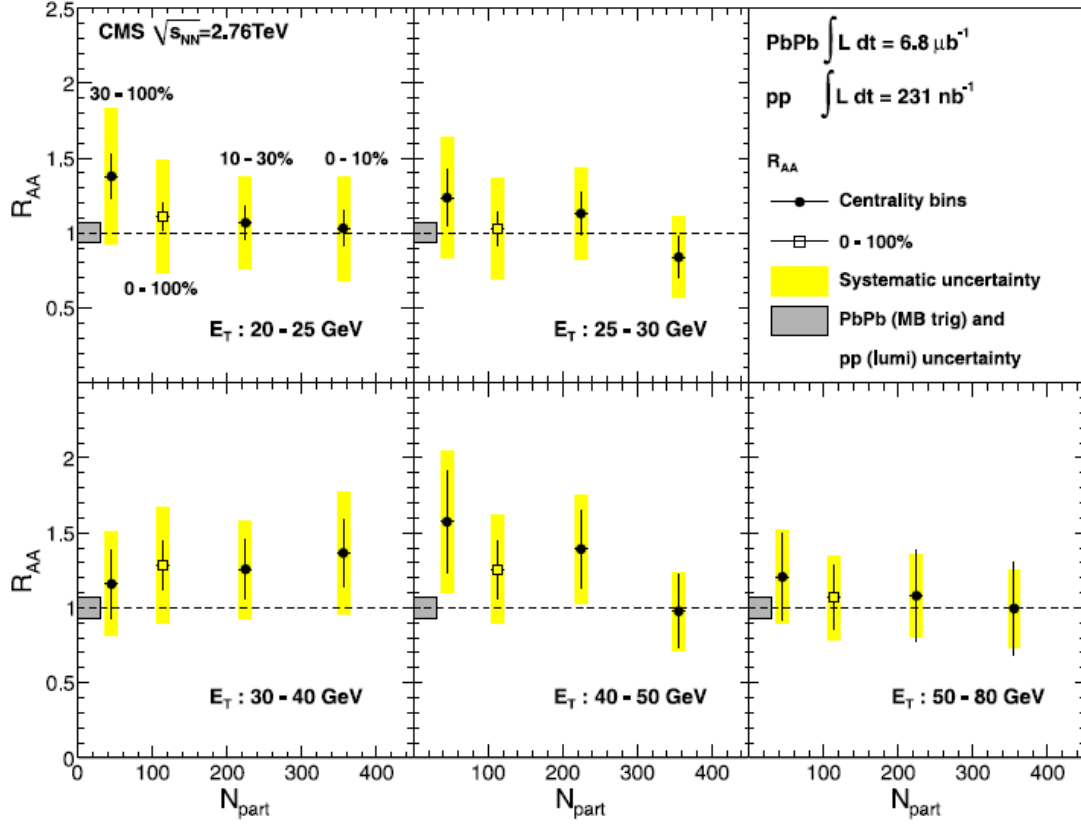


FIG. 14. The measured nuclear modification factor R_{AA} for photons as a function of N_{part} in $\sqrt{s_{NN}} = 2.76$ TeV Pb+Pb collisions. Figure taken from the CMS publication [105].

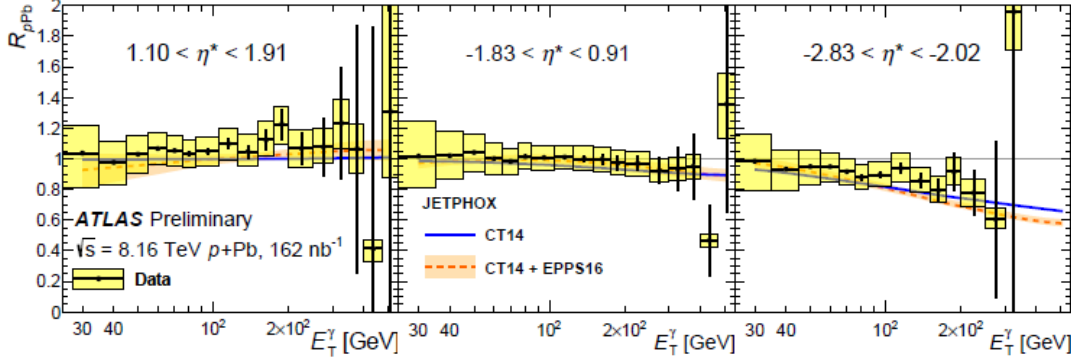


FIG. 15. Direct photon R_{pPb} in minimum bias $\sqrt{s_{NN}} = 8.16$ TeV $p+Pb$ collisions at various pseudorapidities ($\eta < 0$ means the lead-going direction). Figure taken from [194]

3. Collision centrality – photons as the standard candle

The concept of *centrality* is paramount in heavy ion collisions. Originally, in theoretical calculations, it was defined by the impact parameter b , which in case of large, spherical and identical nuclei is a well-defined quantity. Using b and the density distribution of the nucleons in the nucleus, the nuclear overlap function and the average number of participating nucleons (N_{part}), binary nucleon-nucleon collisions (N_{coll}) – or any other geometric quantity like eccentricity – can also be calculated in models [200].

Experimentally, however, b , N_{part} , N_{coll} , or any other geometric quantity, and centrality in general, can not be directly measured. Instead, events are classified based upon the distribution of some bulk observable, like transverse energy E_T or (charged) multiplicity N_{ch} , occasionally energy at zero degrees (attributed to “spectators”) or some combination thereof. Centrality is defined by percentiles of the total (minimum bias)

distribution.³⁴ These observables then are linked to the geometric quantities (b , N_{part} , N_{coll} , *etc.*) – most often by using some Monte Carlo implementation of the Glauber-model (for a comprehensive review see [200]). The typical Glauber Monte Carlo samples the distribution of nucleons in the colliding nuclei A and B, and based upon the impact parameter b calculates the overlap area/volume (T_{AB}). Next it propagates the nucleons of A and B in this volume on a straight path (*optical limit*), and using the nucleon-nucleon cross section σ_{NN} calculates the number of nucleons that participated in any interaction (N_{part}), as well as the total number of binary nucleon-nucleon interactions (N_{coll}), since a nucleon from nucleus A can interact with more than one nucleon of nucleus B and vice versa.

There are two crucial and non-trivial assumptions here: the straight path and the incoherence of the nucleon-nucleon (NN) collisions. Even if a nucleon collides n times, each interaction happens with the same σ_{NN} ³⁵. This is in line with the original Glauber-model (small momentum exchange in each interaction)³⁶.

The connection between the observed E_T or N_{ch} and the theoretical N_{part} is then made by finding a kernel distribution (usually negative binomial), which, if convolved N_{part} times for a specific b , and integrated over b reproduces the observed E_T or N_{ch} distribution. This is reasonable because the bulk observables E_T and N_{ch} are dominated by contributions from soft particles and correlated mostly with N_{part} ³⁷. On the other hand, rare hard probes (high p_T particles, jets, originating in initial, high Q^2 parton-parton scattering) are expected to scale with N_{coll} , the effective NN luminosity in heavy ion collisions. This expectation is justified as long as the individual NN collisions are incoherent and the cross section of the hard process in question is $\sigma_h \ll \sigma_{NN}$, in other words almost all NN collisions are soft, low momentum exchange, and despite the increased NN luminosity (N_{coll}) it takes hundreds or thousands of A+A collisions to have one single hard NN scattering, still accompanied by many soft NN collisions in the same event. At RHIC energies and below this condition is usually satisfied³⁸, at least for photon-producing processes³⁹, but at higher energies it may be violated in multiparton interactions (MPI) [206].

While not directly observable, N_{coll} plays a central role in the diagnostics of the hot and dense QGP formed in heavy ion collisions, as discussed above (Sec. IV B 2). But straightforward as it is, the concept of N_{coll} , and its calculated value at different centralities, hinges upon the assumptions and actual Monte Carlo implementation of the Glauber-model. Fortunately, high p_T direct photons offer a purely experimental sanity check. *To leading order*, all high p_T isolated photons are produced in initial hard scattering, like in pp , where the yields are well understood. The mean free path λ_γ of the photon in the QGP can be estimated from the equilibration time of photons in the plasma [41]

$$\tau_\gamma = \frac{9}{10\pi\alpha_{em}\alpha_s} \frac{E_\gamma e^{E_\gamma/T+1}}{T^2 e^{E_\gamma/T-1}} \frac{1}{\ln(3.7388E_\gamma/4\pi\alpha_s T)}.$$

With $\alpha_s=0.4$ and $T=200$ MeV $\tau_\gamma=481$ fm/c for 2 GeV/c photons and rapidly increasing with E_γ . This is to be compared with the $O(10)$ fm/c lifetime of the plasma. Therefore, photons from hard scattering leave the collision volume unaltered. The rate of hard scattering photons in A+A is N_{coll} times the rate in pp , so the nuclear modification factor R_{AA} of photons will be unity if and only if the Glauber calculation provides the proper N_{coll} for the given (experimental) event centrality class. High p_T direct photons should then be the “*standard candles*” when deriving N_{coll} , and in general, quantities related to collision geometry.

High p_T direct photons in A+A collisions prove that the mapping between collision geometry and bulk experimental observables via the Glauber-model works without any obvious problems. The reason is that “in heavy ion collisions, we manipulate the fact that the majority of the initial-state nucleon-nucleon collisions will be analogous to MB p+p collisions, with a small perturbation from much rarer hard interactions” [200]. The cautious phrasing is warranted, because, to quote Glauber’s original lecture “...*the approximate wave function (74) is only adequate for the treatment of small-angle scattering. It does not contain, in general, a correct estimate of the Fourier amplitudes corresponding to large momentum transfer.*” [198]. In other words in A+A the original Glauber model works, because in any particular collision, even if a few nucleons suffer hard scattering (violating the basic assumptions above), there are many more nucleons in both nuclei that collide softly and behave like the average minimum bias pp . These “normal” collisions then produce sufficient number of soft particles to make the centrality determination *essentially correct*, the more so, because the *fluctuations* of soft production in individual nucleon-nucleon collisions⁴⁰ are quite large. The only case when this logic brakes down are extremely peripheral collisions in which only a few nucleons from both nuclei interact at all⁴¹.

When very asymmetric systems collide (like $p+\text{Au}$) and a hard scattering happens, the sole projectile nucleon is necessarily part of it, suffering large momentum transfer, degrading its ability to produce soft

³⁴ Counterintuitively, the most central - smallest b - 10% is called 0-10%, the most peripheral 90-100%.

³⁵ In the last few years, in light of high precision RHIC and LHC data from very asymmetric collisions, like $p+\text{A}$, $d+\text{A}$, these assumptions have been questioned, see below.

³⁶ Recently the original assumptions have been relaxed in order to explain unexpected results in small-on-large collisions [203].

³⁷ Based on simultaneous studies of pp , $d+\text{Au}$ and $\text{Au}+\text{Au}$ collisions it has been suggested recently that the proper degree of freedom is the number of constituent-quark participants N_{qp} [204].

³⁸ Maybe with the exception of specially selected “extreme” event classes, like the top 0-1% centrality in [205].

³⁹ Remember, their cross section is suppressed by a factor of α_{em}/α_s .

⁴⁰ Negative binomial distributions, or NBDs.

particles, and there are not dozens of other projectile nucleons around that would “make up” with their average collisions for the missing multiplicity (or any other global observable used to determine centrality). The basic conditions of applicability of the Glauber-model in its original form are violated for the (only) projectile nucleon. The result is a potentially serious bias in the experimental determination of centrality in $p(d)+\text{Au}$ (or other very small on large) collisions when a hard scattering occurred in the event [207, 208]. The reduced multiplicity means that the event tends to be classified as less central than it should be based on collision geometry, potentially leading to mistaken claims of suppression of high p_T hadrons in “central” and/or their enhancement in “peripheral” $p(d)+\text{Au}$ collisions. Moreover, if there is indeed such a bias, it can increase with the p_T of the most energetic particle or jet observed: R_{AB} in “peripheral” events will increase with p_T monotonically, and continuously decrease with p_T in “central” events. Such trends were clearly seen in early results on leading hadron or jet R_{AB} when the experiments applied the traditional Glauber-model to determine centrality in very asymmetric collisions.

One way to circumvent the bias is to categorize events according to the experimentally measured “event activity” rather than the model-calculated “centrality” (this path has been adopted by the ALICE experiment, see for instance [209, 210]). This is not just a question of semantics. “Centrality” implies that all events in the class are in the same impact parameter range, similar in collision geometry, governed by similar physics and therefore directly comparable. “Event activity”, on the other hand, is a neutral, purely empirical classifier, allowing the members of the class to occasionally reflect quite different physics processes.

Another way to eliminate the bias is to assume that the direct photon R_{AB} at sufficiently high p_T is *always* unity⁴², and any deviation should be treated as a (p_T dependent) bias on how N_{coll} is calculated, *i.e.* on the centrality determination, and the centrality redefined accordingly [211]. While feasible, this is a non-trivial task. A practical workaround that leaves the centrality itself biased, but allows to decouple and study purely final state effects (like jet or leading hadron suppression) is to use the double ratio $R_{AB}^{\text{jet,hadron}}/R_{AB}^{\text{photon}}$, or, in general, the double ratio formed with electroweak bosons [212].

In any case, we would like to emphasize that – particularly in very asymmetric collisions – high p_T direct photon production should always be the standard candle with which other high p_T observables are calibrated to avoid premature or outright false physics conclusions.

4. Expected deviations of the photon R_{AA} from unity

The argument that the photon R_{AA} proves the validity of the Glauber-type calculations in heavy ion collisions hinges upon the assumption that all high p_T isolated photons are produced in initial hard scattering. One should also keep in mind that when deriving direct photon R_{AA} , all experiments (and many calculations) use the direct photon spectra in pp . Strictly speaking this is not correct: there are some minor issues, second order effects to consider. First, in A+A the binary (nucleon-nucleon) collisions are not only pp , but pn and nn as well. While irrelevant for strong interactions, this is important in electromagnetic processes⁴³, since the cross sections are proportional to the squared sum of quark charges ($\sum e_q^2$, see Eq. 1), and the fraction of u quarks is higher in pp than in any heavy ion collision⁴⁴. Therefore, if hard scattering is indeed the only source of high p_T photons, the difference between pp , pn and nn collisions decreases the direct photon R_{AA} (*isospin effect* [213], see also Fig. 13, right panel with calculations from [202]).

Another source of high p_T (nearly) isolated photons is the interaction of the hard scattered, fast quark with the (thermalized) QGP medium (*jet-photon conversion* [34]). Setting the parton masses to zero in Eqs. 1 and 2 we get for annihilation

$$d\sigma/dt = 8\pi\alpha_{em}\alpha_s e_q^2 (u/t + t/u)/9s^2$$

and the contribution is largest when $t \rightarrow 0$ ($p_q \approx p_\gamma$) or $u \rightarrow 0$ ($p_{\bar{q}} \approx p_\gamma$). For the Compton process

$$d\sigma/dt = -\pi\alpha_{em}\alpha_s e_q^2 (u/s + s/u)/3s^2$$

and the largest contribution comes again from $t \rightarrow 0$ ($p_q \approx p_\gamma$). In all cases the photon is mostly collinear with the original q, \bar{q} and provides a direct measurement of the quark momentum. In [34] the authors predicted that at RHIC energies jet conversion photons will be the dominant source of photons up to $p_T = 8 \text{ GeV}/c$, “outshining” prompt photons from initial hard scattering, but this appears to be an overestimate. If it were true, there should be a significant (factor of 2 or more) enhancement of the photon R_{AA} up to $8 \text{ GeV}/c$, but it is not observed in the data (see Fig. 13). A more detailed calculation that includes realistic parton energy

⁴² Apart of the well understood effects discussed in Sec. IV B 4.

⁴³ Colliding deuteron on deuteron at RHIC would offer clearly tagged and separated pp , pn and, most interesting, high energy nn collisions – a unique opportunity to study isospin effects (and lack thereof in strong interactions) at high \sqrt{s} . While no new physics is expected, it would serve as a powerful confirmation of some QCD and QED fundamentals, and if some unexpected results were found, they would obviously be of utmost interest. Unfortunately dd collisions didn’t happen so far, despite repeated suggestions since 2005, including those by the author.

⁴⁴ Remember, p is uud , n is udd , and the electric charge of u is $2/3$, while n is $-1/3$.

loss⁴⁵ before jet-photon conversion [71] finds a 30% reduction of the photon R_{AA} at 8 GeV/c [73]⁴⁶. Also, since the probability of jet-photon conversion increases with the pathlength of the quark in the medium, such photons should exhibit a quite unique azimuthal asymmetry. While the initial prompt photons are produced uniformly in azimuth, jet-photon conversions should be enhanced in the direction orthogonal to the reaction plane, resulting in a quite unusual *negative* v_2 of those high p_T photons. Unfortunately the effect is small [72] and so far not observed in the data [82, 214, 215], nor have jet-photon conversion photon yields been measured yet. More sophisticated analysis techniques might help in the future⁴⁷.

5. Photon - hadron/jet correlations: energy loss in the medium

Energy loss of hard scattered partons, traversing the medium formed in heavy-ion collisions, was established early on as the cause of jet quenching, but the nature of energy loss remained disputed. The simplest, single-particle observable, the nuclear modification factor R_{AA} “integrates” too many possible effects (surface bias, relative role of collisional and radiative energy loss, providing little if any “tomographic” information [216]). It does not have good discriminative power among models with widely different assumptions and mechanisms⁴⁸. Measuring R_{AA} vs the reaction plane [218] provides some more constraint on models, as do dihadron-correlations [219]. For instance, in [220] the in-plane and out-of-plane R_{AA} for high p_T π^0 is compared to four model calculations (see Fig. 16, left plot). The first three models are pQCD-based and exhibit an L^2 -dependence of the energy loss on the pathlength in the medium, while the ASW-AdS/CFT model has an energy loss proportional to L^3 , which appears to be favored over the other three scenarios. Nevertheless, the energy of the parent parton is still ill-constrained.

This can be remedied by studying back-to-back photon-hadron (or photon-jet) correlations, since the high p_T trigger photon, being a penetrating probe, calibrates the initial energy of the recoil parton before it could lose energy in the medium or start to fragment. The direct photon sets the scale of the initial hard scattering. The power of the method is illustrated in Fig. 16, right plot, from [171], where (associated) away-side charged hadron yields are measured as a function of $z_T = p_T^{assoc}/p_T^{trig}$ in pp and Au+Au with high p_T direct photon and π^0 triggers. The measured $D(z_T)$ fragmentation functions for photon and π^0 triggers are very similar in pp , but quite different in Au+Au, where the trigger π^0 now comes from a parton which already lost energy in the medium. By forming the ratio of the conditional yields (having a trigger photon/ π^0 of a given p_T)

$$I_{AA} = \frac{D(z_T)^{AuAu}}{D(z_T)^{pp}}$$

and, in particular, comparing the high- and low-end of the z_T distributions in principle one can discriminate between a picture where the medium substantially modifies the parton shower (modified FF) and one where mostly a single parton carries the energy through the medium and the lost energy shows up only at extremely low energies and angles [171].

⁴⁵ It is hard to over-emphasize the importance of treating π^0 (hadrons) and photons simultaneously.

⁴⁶ Note that this model has been challenged in [35], which claims a much reduced jet-photon conversion cross section.

⁴⁷ Jet-conversion photons are isolated or nearly isolated (*i.e.* there is no fully evolved jet), and have a negative v_2 . The only other process producing isolated photons is initial hard scattering with $v_2 = 0$ and calculable rates. Studying v_2 of isolated, medium p_T photons could in principle reveal the fraction (and thus the spectrum) of jet-conversion photons.

⁴⁸ The interested reader can find a short but excellent summary of the situation, and many references in the introduction of [217].

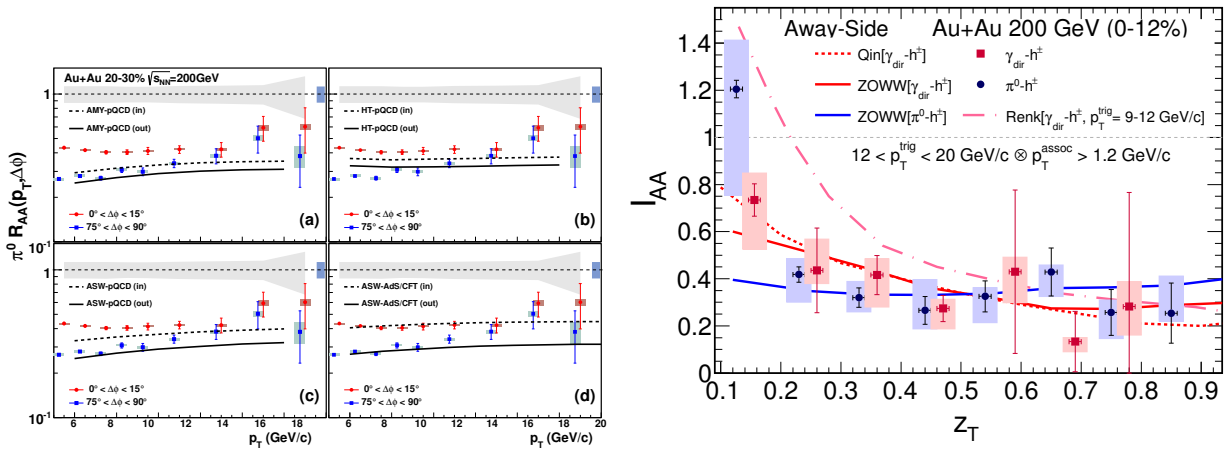


FIG. 16. (Left) $R_{AA}(\Delta\phi)$ as a function of p_T in 20-30% Au+Au collisions for in-plane (red circles) and out-of-plane (blue triangles) compared to four model calculations: (a) AMY [221, 222], (b) HT [223], (c) ASW [224] and ASW-AdS/CFT [225]. (Figure taken from [220].) (Right) STAR measurements [171] of $I_{AA}^{\gamma_{dir}}$ and $I_{AA}^{\pi^0}$, the ratio of the per-trigger conditional yield in central Au+Au and pp collisions, as a function of z_T . The points for $I_{AA}^{\gamma_{dir}}$ are shifted by 0.03 in z_T for visibility. The curves represent theoretical model predictions [216, 217, 226, 227]. (Figure taken from [171].)

Analyzing the azimuthal distribution of the back-to-back photon-jet pair in Pb+Pb CMS concluded [174] that while there is no indication of in-medium deflection of partons, there is strong parton energy loss in the medium (jet quenching), that depends on centrality and photon p_T . While this observation is not new, photon-jet correlation data provide strong constraints to in-medium energy loss models in A+A collisions. PHENIX and ATLAS also published photon-hadron and photon-jet measurements (see Table III). A recent publication by ATLAS [228] on photon-jet p_T correlations in 5.02 TeV Pb+Pb includes many comparisons to model calculations, none of them being completely satisfactory.

6. Nuclear PDFs and fragmentation function modification

As pointed out in Sec. IIB, the cross-section for hard scattering processes *factorizes* into short distance (parton-parton scattering) and long distance effects (the incoming state, *i.e.* the parton distribution functions and the fragmentation functions of the scattered partons into colorless final particles). Deep inelastic lepton-nucleus scattering [229, 230] revealed that the PDF of nucleons bound in a nucleus is different from the ones of free nucleons. In terms of Bjorken- x the nuclear effects are [231]:

- depletion at $x < 0.1$ (shadowing)
- excess at $0.1 < x < 0.3$ (anti-shadowing)
- depletion at $0.3 < x < 0.7$ (EMC-effect)
- excess towards $x \rightarrow 1$ (Fermi motion)

The nuclear PDFs $f_i^{p/A}(x, Q^2)$ for parton species i are defined relative to the free-proton PDF $f_i^p(x, Q^2)$ as

$$f_i^{p/A}(x, Q^2) = R_i^A(x, Q^2) f_i^p(x, Q^2)$$

and usually the modification $R_i^A(x, Q^2)$ is shown. Ideally, the free proton and nuclear PDFs should be fitted within the same analysis to reduce uncertainties [232], but this hasn't been done so far. – Various sets of nuclear PDFs, including impact-parameter dependent ones are available and updated from time to time [233–236]. The uncertainties are particularly large for the gluon nPDF at low x (shadowing region) [104]. As we have seen, photons are sensitive to the gluon distribution, and the low x region is experimentally accessible with prompt photon measurements at high rapidity in pA or dA collisions⁴⁹. While there are ongoing efforts at RHIC and a detector upgrade plan at LHC [237], data on prompt photon production at high rapidity are not available yet. However, inclusive photon multiplicity measurements at high rapidity, pioneered by

⁴⁹ Selecting a small “projectile” p, d and a large “target” A and measuring prompt photons at high rapidity in the projectile-going direction ensures that the parton in the target will have small x . Also, the overall multiplicity will be small, making the measurement technically feasible, while it would be virtually impossible in an AA collision.

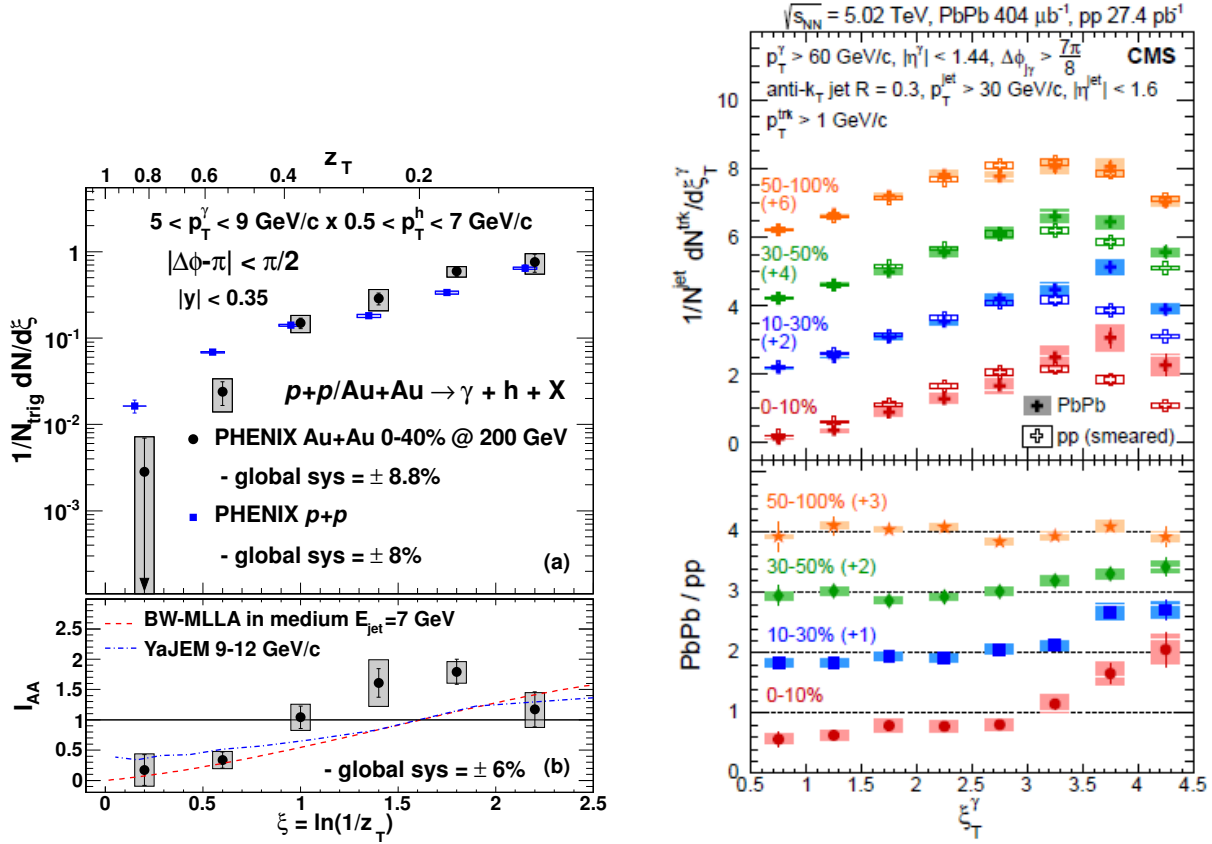


FIG. 17. Left: panel (a) shows the charged hadron yield per photon trigger as a function of $\xi = \ln(1/z_T)$ for pp and Au+Au collisions (I_{AA}). On the top the usual z_T scale is also indicated. Panel (b) shows the ratio of the Au+Au over pp fragmentation functions. (Figure taken from [170].) Right top: the centrality dependence of ξ_T^γ for jets associated with an isolated photon for Pb+Pb and pp collisions. Right bottom: the ratio of Pb+Pb over pp distributions, the experimental measure of fragmentation function modification. (Figure taken from [240].)

WA93 [100] at CERN SPS have been performed by STAR [238] at RHIC and ALICE [239] at the LHC, which provide some loose constraints on PDFs.

Fragmentation functions in hadron-hadron collisions have been discussed in Sec. II B as the probability of a parton to produce a particular final state particle at a given momentum fraction z of the original parton momentum. The high z part of the FF characterizes the *leading particle* of the jet. As we have seen, in back-to-back isolated photon-hadron correlations the photon served as the measure of the original parton momentum, setting the jet energy scale when calculating the (transverse) momentum fraction $z_T = p_T h/p_T^\gamma$ of an observed final state hadron. This picture implies that fragmentation occurs fully in the vacuum. In heavy ion collisions the situation is somewhat less clear, because the parent parton usually loses energy in the medium, for instance by radiating gluons or photons. The opposing isolated photon still measures the initial momentum of the parton, but the experimentally observed “fragmentation function” is now depleted at high z_T due to the parton energy loss before fragmentation. The low z_T behavior is less trivial: the lost energy can go into very soft and diffuse modes (no appreciable enhancement at low z_T in the jet cone), or it can still be spatially strongly correlated with the jet, in which case it is interpreted as an in-medium modification of the parton shower [241]. It turns out that such enhancement is manifest both at RHIC [170, 171] and at the LHC [240], as seen in Fig. 17, where the results are shown as a function of $\xi = \ln(1/z_T)$ in order to emphasize the soft part (large ξ). As pointed out in [242], the turn-over at the largest ξ values is due to experimental cutoff, below which particles are not counted as parts of the jet. We should also mention that the picture in which the parton shower is modified, but hadronization still occurs in the vacuum is not unique: for instance in [243] an alternate model with (colorless) prehadrons produced both inside and outside the medium is proposed.

7. A collateral benefit: photon-photon scattering

In classical electrodynamics the Maxwell-equations prohibit photon-photon interactions. Inspired by Dirac’s positron theory in 1936 Heisenberg published a seminal paper [5] describing the process of photon-

photon scattering (“Streuung von Licht an Licht”), enabled by a fundamentally new property of quantum electrodynamics (“grundsätzlich neuen Zügen der Quantenelektrodynamik”), the polarization of the vacuum. One of the related phenomena, elastic scattering of a photon in the Coulomb field of a nucleus via virtual e^+e^- scattering (Delbrück scattering) has actually been observed [4] *before* the Heisenberg paper and turned out to play an important role in the study of nuclear structure (for a review see [244]), but observation of other consequences, like photon splitting in a strong magnetic field [245] or $\gamma\gamma \rightarrow l^+l^-$ and $\gamma\gamma \rightarrow \gamma\gamma$ scattering remained elusive for a long time.

Addressing a completely different problem, excitation of an atom by a charged particle passing nearby, in 1925 Fermi realized that the Fourier-transform of the fast moving electric field is equivalent to a continuous distribution of photons (“Se noi, con un integrale di Fourier, decomponiamo questo campo nelle sue componenti armoniche riscontriamo che esso è eguale al campo elettrico che vi sarebbe in quel punto se esso fosse colpito da della luce con una conveniente distribuzione continua di frequenze.”), *de facto* laying the foundation of the equivalent photon approximation (EPA) by Weizsäcker [246] and Williams [247]. With the advent of accelerators intensive photon sources became in principle available, but the much coveted photon-photon scattering has not been observed for many more decades. In 1967 in a feasibility study of such experiments [248] the author, after enumerating other methods, even mentions the possibility of two synchronized underground nuclear explosions producing instantaneous radiation of $5 \times 10^{24}\gamma$ for about 70 ns (with the instantaneous neutrons arriving only after $1\mu\text{s}$, leaving time to collect and transmit the data), and the shock waves arriving even later. Luckily the author himself cautions wisely in a footnote: “The practice of performing this experiment, in conventional laboratories, should be discouraged because of the detrimental effect it may have on the personnel, equipment and general appearance of the neighbourhood.”

The pursuit of colliding heavy ions at relativistic energies had little if anything to do with the quest for photon-photon scattering experiments – but as a “collateral benefit” it made them possible. The electromagnetic fields of the highly accelerated charges can be treated in the EPA as photon beams [249, 250] of small virtuality ($-Q^2 < 1/R^2$ where R is the charge radius), with an E_γ^{-1} fall-off up to $\omega_{max} \approx \sqrt{s_{NN}}/(2MR)$ with M being the mass of the particle or ion [251]. While the collision rate and the photon spectrum are harder in pp , the $\gamma\gamma$ luminosities increase as Z^4 , strongly favoring heavy ion beams. Study of so-called *ultraperipheral collisions*⁵⁰ or UPCs quickly became an important topic both at RHIC and LHC, like photonuclear production of J/Ψ in ultraperipheral Au+Au collisions in PHENIX [252], or Pb+Pb collisions in ALICE [253]. STAR studied for instance the photonuclear production of $\pi^+\pi^-\pi^+\pi^-$ in Au+Au collisions [254]. As for pure photon-photon collisions CMS studied for instance the $\gamma\gamma \rightarrow \mu^+\mu^-$ [255] and $\gamma\gamma \rightarrow e^+e^-$ [256] as well as $\gamma\gamma \rightarrow W^+W^-$ [257]. Similar dilepton measurements by ATLAS have been published in [258], and the W results in [259]. The interested reader can find recent results and references in the presentations of the Photon 2017 conference [260]. As for the early developments, a very thorough historic overview has been published recently [261] with the first reference dating from 1871!

V. “THERMAL” RADIATION (LOW P_T REGION)

A. SPS, FNAL and AGS

The fixed target heavy ion program at CERN SPS started in 1986 and soon the search for thermal radiation from the system formed in nucleus-nucleus collisions was underway. The first results on inclusive photon production and its comparison to the expected hadron decay yield in p+A and A+A collisions were published by the HELIOS/NA34 collaboration [262]. Protons, ^{16}O and ^{32}S beams were used on W and Pt targets, and photons were measured with the (external) conversion technique (Sec. III B). The ratio of inclusive photons to those expected from hadron decays remained unity within uncertainties in the entire measured p_T range ($0.1 < p_T < 1.5\text{ GeV}/c$), indicating no extra (“thermal”) source. Independently, the p_T -integrated yields of inclusive photons were compared to the expected decay photon yields as a function of $\langle E_T \rangle$ (a proxy for charged multiplicity N_{ch} or collision centrality). The argument was that while decay photons should be proportional to N_{ch} (\propto number of final state particles), thermal radiation may have a quadratic dependence on N_{ch} [263]. Such excess has not been observed, the inclusive/decay photon ratio was constant within uncertainties for all colliding systems and $\langle E_T \rangle$, moreover, the absolute value of the ratio agreed remarkably well with the expected value if hadronic decays are the only source [262].

Just one year later another CERN SPS experiment, WA80 published an upper limit for thermal direct photon production using 60 and 200 AGeV proton and ^{16}O projectiles on C and Au nuclei. Technically, this measurement was complementary to HELIOS/NA34, because it measured real photons in a calorimeter with a charged particle veto detector in front of it (rather than measuring photons converted to a dielectron pair)⁵¹.

⁵⁰ Ultraperipheral collisions are defined by the impact parameter larger than the sum of radii of the two ions. The interaction can involve either one photon and a nucleus, or two photons only.

⁵¹ Observing the same signal independently and with a completely different technique obviously promotes credibility of the result – a lesson we don’t always seem to take seriously enough.

Different from HELIOS, π^0 spectra have been measured explicitly in the same setup. These were then used to estimate (via m_T scaling) the yields of η , η' , ω when simulating the expected hadron decay photons. The results were presented both as invariant yields and γ/π^0 ratios (see Sec. III D). For p+A collisions the inclusive photon spectra were completely consistent with the expected decay photon spectra (no direct photons); for $^{16}\text{O}+\text{A}$ collisions there was a hint but no clear excess either within stated uncertainties: the publication claimed a 15% upper limit on the signal for all systems.

The WA80 experiment went through a significant upgrade meant to greatly reduce systematic uncertainties, and took data with ^{32}S beam at 200 AGeV in 1990. The double ratios (see middle panel in Fig. 10) indicated no clear excess within the (reduced) uncertainties, and made it possible to set a 15% upper limit at 90% confidence level on the invariant excess photon yield for the most central collisions [116], providing a useful constraint on theoretical models.

Using the same 200 AGeV ^{32}S beam on a (segmented) Au target the CERES/NA45 experiment at CERN SPS found almost exactly the same upper limit (14%) for the emission of direct photons in central S+Au collisions [117]. CERES measured photons via external conversion, using two ring imaging Cherenkov detectors (RICH) to identify electrons with high efficiency. The shape and the absolute yield of inclusive photon p_T distributions for minimum bias collisions was well described within systematic uncertainties by known hadronic sources. Collision centrality dependence was also studied (see right panel in Fig. 10). The ratio of inclusive photons to charged hadrons, as a function of charged particle multiplicity, has been fitted with $C(1 + \alpha dN_{ch}/d\eta)$. Within systematic uncertainties the slope α was consistent with zero ($\alpha = (+0.5 \pm 1.4_{\text{stat.}}^{+4.5}_{-1.5} \text{ syst.})10^{-4}$), meaning that the number of inclusive photons is proportional to N_{ch} at all centralities, as expected if hadron decays are the sole source of photons. That means that for beams as heavy as ^{32}S none of the CERN SPS experiments found direct photons (“thermal” radiation), the more surprising because at the same time the same experiments found clear evidence of enhanced dilepton production⁵² (e^+e^- or $\mu^+\mu^-$) in the same collisions [264].

In contrast to the vigorous photon/dilepton program at CERN SPS only one experiment was dedicated to (low p_T) photon search at BNL AGS, where E855 was looking for soft photons with an 18 GeV/c p beam hitting Be and W targets [189]. The data were taken in 1990, and photons were detected in two small, movable electromagnetic calorimeters, both consisting of 19 hexagonal BaF₂ scintillating crystals, each $9.5X_0$ long. In their various data taking positions the two detectors ultimately covered a wide rapidity range, $-2.4 < y_{NN} < +0.5$. The inclusive photon spectra were measured up to 1 GeV/c in p_T , in eight bins of rapidity, and compared to the photon spectra expected from hadron decay. While the fitted slopes changed significantly with rapidity, no significant excess was found at any of the rapidities. – Due to the high energy resolution of the BaF₂ array, E855 could also study the very low p_T limit ($p_T < 100$ MeV) and found no excess beyond the expected decay yields and Bremsstrahlung from charged hadrons [189]. The result is consistent with what the HELIOS collaboration found in 450 GeV/c $p+\text{Be}$ collisions [265].

The first positive observation of direct photons in ultrarelativistic heavy ion collisions was reported by the CERN WA98 experiment using 158 AGeV ^{208}Pb beams on a Pb target [69]. Photons were measured in the LEDA PbGl calorimeter supplemented with a charged particle veto in front of it. In addition to inclusive photons, WA98 measured simultaneously π^0 and η , which reduces systematic uncertainties from decay photon subtraction. The p_T range covered was the largest so far ($0.3 < p_T < 4.0$ GeV/c, almost 6 orders of magnitude in invariant yield). It was found that the ratio of inclusive photons to the expected decay background exceeded unity at the level of $\approx 2\sigma$ in the $2.0 < p_T < 3.5$ GeV/c range in the 10% most central collisions, while no such excess was seen in the 20% most peripheral collisions (see Fig. 18, left panel). The excess ratio was used to derive the invariant direct photon yield in central collisions (see Fig. 18, right panel). The data were compared to the scaled pp yields from three earlier experiments⁵³, FNAL E629 [185], using 200 GeV/c p beam on a C target, FNAL E704 [155], using 200 GeV/c p beam on a p target, and CERN NA3 [186] also using 200 GeV/c p beam on a C target. The pp , p+A data were divided by the pp inelastic cross section (30 mb) and the mass number of the target to get the direct photon yield per nucleon-nucleon collisions, then rescaled for the difference in \sqrt{s} , finally multiplied by the calculated average number of nucleon-nucleon collisions in central Pb+Pb events (660). WA98 concluded that the shape of the direct photon spectra in Pb+Pb is similar to that expected from proton-induced reactions, but the yield is enhanced [69].

The same 158 AGeV $^{208}\text{Pb} + ^{208}\text{Pb}$ data were re-analyzed by WA98 for two particle correlations of direct photons in central collisions [107]. In the 0.2-0.3 GeV/c p_T region the direct photon interferometric radii were quite similar to the pion radii, indicating that in this p_T region photons are emitted in the late stage of the collision. A lower limit on direct photon production in the same p_T region has been given using the method described in Sec. III C; the yield exceeded predicted yields from the hadron gas.

⁵² Triggering the question by the author “if virtual photons are really there, how come real photons are virtually absent”?

⁵³ In essence this was the first attempt to establish the nuclear modification factor R_{AA} for photons (see Sec. IV B).

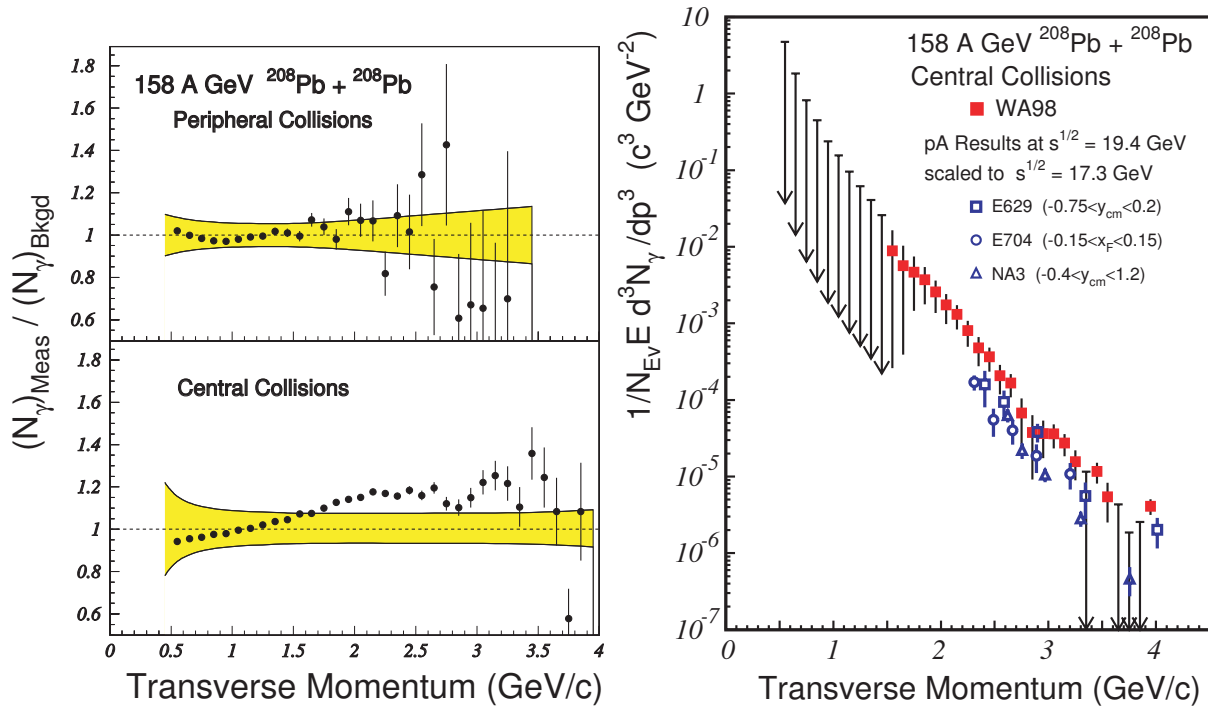


FIG. 18. Direct photon result from the WA98 experiment, 158 A GeV $^{208}\text{Pb} + ^{208}\text{Pb}$ collisions [69]. (Left panel) The ratio of measured inclusive photons to calculated decay photons as a function of p_T for peripheral (a) and central (b) collisions. Error bars on the data are statistical only, the p_T -dependent systematic uncertainties are shown as shaded bands. (Right panel) The invariant direct photon yield for central collisions. Error bars indicate combined statistical and systematic uncertainties. Data points with downward arrows indicate 90% C.L. upper limits ($\gamma_{\text{excess}} + 1.28\sigma_{\text{upper}}$). The data are compared to expected, N_{coll} -scaled pp yields from three earlier experiments (see explanation in the text). (Figures taken from [69].)

B. RHIC and LHC

The Relativistic Heavy Ion Collider (RHIC) became operational in 2000 colliding Au+Au at $\sqrt{s_{NN}} = 130$ GeV. Almost immediately two fundamental observations have been made and published that ultimately⁵⁴ became cornerstones to the claim of discovering the Quark-Gluon Plasma: the suppression of high p_T hadrons [18] and elliptic flow of charged hadrons [272]. In contrast results on photons, particularly low p_T , “thermal” photons, while shown at conferences as preliminaries starting 2005 and motivating many model calculations, were first published in a peer-reviewed journal in 2010⁵⁵.

1. “Thermal” photon yields and effective temperatures

The first published results [92, 96] were obtained with the internal conversion method (see Sec IIIB) by the PHENIX experiment at RHIC, and are reproduced in Fig. 19. Notably, the paper presented results for 200 GeV pp and Au+Au collisions simultaneously. In pp the direct photon fraction $r_\gamma = r_{\text{direct}}/r_{\text{inclusive}}$ (see Sec. IIID) was consistent with the NLO pQCD calculation⁵⁶, but for minimum bias Au+Au a clear excess over primordial photons has been found. The absolute yields for various centralities are shown in the right panel of Fig. 19, with higher p_T points added from [191]. A fit to the pp spectrum of the form $A_{pp}(1 + p_T^2/b)^{-n}$ and the same fit scaled by the nuclear overlap function T_{AA} of the respective Au+Au centrality bin is superimposed on the data. For $p_T > 4$ GeV/c the yields are consistent with T_{AA} -scaled pp , allowing little if any additional photon sources due to the medium. On the other hand, below $p_T < 4$ GeV/c there is a clear excess, and the shape of the distributions also changes from power-law (p_T^{-n} , characteristic to high p_T , hard scattering sources) to exponential. The Au+Au yields in the entire p_T -range are reproduced

⁵⁴ After being confirmed many times by measurements at different energies, systems, and ever high statistics.

⁵⁵ The influential 2005 paper [191] has shown the high p_T direct photon yields in A+A collisions and their consistency with N_{coll} independent nucleon-nucleon collisions (see Sec. IV B), but it provided only upper limits in the “thermal” region due to the limitations of the calorimetric measurement.

⁵⁶ Note that below 2 GeV/c the validity of NLO pQCD is questionable, primarily due to the poorly constrained yield of fragmentation photons, although they are predicted to exceed the prompt photon yield by a factor of 2-3 [33].

| Experiment | $\sqrt{s_{NN}}$ | method | η | p_T | Publications | Comment |
|------------------|-------------------------|--------|------------------------|----------------|--------------|--------------------------|
| UA1 / CERN SPS | $p\bar{p}$ 546, 630 GeV | calor. | $ \eta < 3.0$ | 12-30 GeV/c | [88] (1988) | di- γ , k_T |
| WA70 / CERN SPS | $\pi^- p$ 280 GeV | calor. | | 0-3.5 GeV/c | [180] (1990) | di- γ , k_T |
| CDF / FNAL | $p\bar{p}$ 1.8 TeV | calor. | $ \eta < 0.9$ | 10-35 GeV/c | [181] (1993) | di- γ , k_T |
| WA93 / CERN SPS | S+Au 200 AGeV | PMD | $2.8 < \eta < 5.2$ | | [100] (1998) | γ mult. |
| WA98 / CERN SPS | Pb+Pb 158 AGeV | PMD | $3.25 < \eta < 3.75$ | | [266] (2005) | γv_2 |
| PHENIX / RHIC | pp 200 GeV | calor. | $ \eta < 0.35$ | 5-15 GeV/c | [106] (2010) | γ -jet k_T |
| PHENIX / RHIC | Au+Au 200 GeV | calor. | $ \eta < 0.35$ | 1-12 GeV/c | [82] (2012) | γv_2 |
| ALICE / LHC | Pb+Pb 2.76 TeV | conv. | $ \eta < 0.8$ | 1-5 GeV/c | [267] (2012) | γv_2 |
| ATLAS / CERN LHC | pp 7 TeV | calor. | $ \eta < 2.37$ | 0-200 GeV/c | [182] (2012) | di- γ |
| PHENIX / RHIC | Au+Au 200 GeV | calor. | $ \eta < 0.35$ | 5-9 GeV/c | [170] (2013) | γ - hadron |
| ATLAS / CERN LHC | pp 7 TeV | calor. | $ \eta < 2.37$ | 50-300 GeV/c | [172] (2013) | γ jet |
| CMS / LHC | pp 7 TeV | calor. | $ \eta < 2.5$ | 40-300 GeV/c | [268] (2014) | γ - jet |
| ALICE / LHC | pp 0.9-7 TeV | PMD | $2.3 < \eta < 3.9$ | | [239] (2015) | γ mult |
| STAR / RHIC | Au+Au 200 GeV | comb. | $-3.7 < \eta < -2.8$ | | [238] (2015) | γ mult |
| STAR / RHIC | pp , Au+Au 200 GeV | comb. | $ \eta^\gamma < 0.9$ | 8-20 GeV/c | [171] (2016) | γ - jet |
| PHENIX / RHIC | Au+Au 200 GeV | comb. | $ \eta < 0.35$ | 1-4 GeV/c | [269] (2016) | $\gamma v_2 v_3$ |
| PHENIX / RHIC | pp 510 GeV | calor. | $ \eta < 0.35$ | 7-15 GeV/c | [177] (2017) | γ -h $\Delta\Phi$ |
| ATLAS / CERN LHC | pp 13 TeV | calor. | $ \eta < 3.2$ | 125-1500 GeV/c | [173] (2018) | γ - jet |
| CMS / CERN LHC | Pb+Pb 5.02 TeV | calor. | $ \eta^\gamma < 1.44$ | >60 GeV/c | [240] (2018) | γ - jet |
| PHENIX / RHIC | AA 39-2760 GeV | | | 1-15 GeV/c | [270] (2018) | γ scaling |
| ALICE / CERN LHC | Pb+Pb 2.76 TeV | mixed | $ \eta^\gamma < 0.9$ | 0.9-6.2 GeV/c | [214] (2018) | γv_2 |
| ATLAS / CERN LHC | pp Pb+Pb 5.02 TeV | calor. | $ \eta^\gamma < 2.37$ | 63-200 GeV/c | [228] (2018) | γ - jet |
| ATLAS / CERN LHC | $p + Pb$ 8.16 TeV | calor. | $-2.83 < \eta < 1.90$ | 20-550 GeV/c | [271] (2019) | R_{pPb} |

TABLE III. Selected measurements of photon-related observables (other than yields)

within uncertainties by the two-component fit

$$Ae^{-p_T/T} + T_{AA} \times A_{pp}(1 + p_T^2/b)^{-n}$$

where the only free parameters are A and the inverse slope T of the exponential term, which is $T = 221 \pm 19^{stat} \pm 19^{sys}$ MeV for the most central (0-20%) collisions [96]. However, the simple picture suggested by the formula above is quite misleading: there is no reason to equate T with some well-defined “temperature” of the system.

Even if we assume that the dominant source of excess photons in the $1 < p_T < 4$ GeV/c range is thermal production from the QGP and/or the hadronic gas⁵⁷, due to the “penetrating probe” nature of photons the resulting spectrum is a convolution of the *entire* space-time history of the collision and the respective instantaneous rates. In other words, T reflects some average of radiations from different temperatures, subject in addition to varying Doppler-shift from the (time-dependent) radial boost of the system. The problem is well demonstrated in Fig. 20 in the framework of one particular hydrodynamic model calculation [27], where the horizontal axes are the true instantaneous temperatures, the vertical axes are the observable inverse slopes and the size of the markers reflects the magnitude of the instantaneous rate. Different models give different correlations between the inverse slope and the true instantaneous T (see for instance Fig. 6 in [26]), but it is clear that the experimentally measured single inverse slope (often called “effective” temperature or T_{eff}) in itself provides little constraint on the evolution of the system.

This point is well illustrated in Fig. 21 (left panel) where various hydro model calculations are overlayed on the 0-20% centrality direct photon data by PHENIX [92]. By varying the “initial time” τ_0 (the time when the QGP is formed and system can be considered locally thermalized) and the initial temperature T_0 at τ_0 most calculations come reasonably close to the data. Note that T_0 and τ_0 are anti-correlated: a conservative, late formation time ($\tau_0=0.6$ fm/c) implies $T_0=300$ MeV, while the extreme fast formation ($\tau_0=0.15$ fm/c) would imply $T_0=600$ MeV. While the data could not rule out any of these scenarios, in [92] it has been argued that even the lowest T_0 is well above the $T_c \approx 170$ MeV cross-over transition temperature from the hadronic phase to the QGP, predicted by lattice QCD calculations [284–286].

The first direct photon measurement at the LHC was performed by the ALICE experiment in $\sqrt{s_{NN}} = 2.76$ TeV Pb+Pb collisions and first shown as preliminary for the $1 < p_T < 14$ GeV/c range in the 0-40% centrality bin in 2012. This analysis has been done with the external conversion technique (see Sec. III B), and a clear, exponential excess over the NLO pQCD expectation was seen below 4 GeV/c p_T , with an inverse slope of 304 ± 51 MeV. For the final publication [90] the analysis has been extended to three centrality bins (0-20%, 20-40% and 40-80%), and, more important, a second, independent measurement with the high

⁵⁷ An assumption seriously questioned by some recent models, e.g. [274–276].

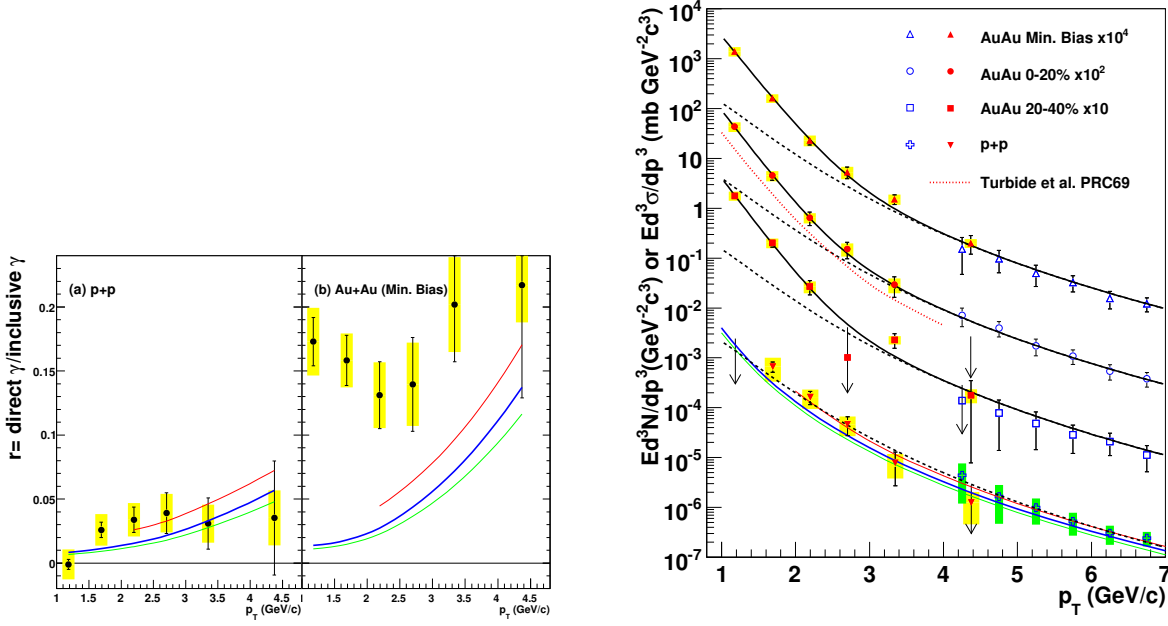


FIG. 19. (Left) The fraction r of the direct photon component over inclusive photons as a function of p_T in pp and minimum bias Au+Au collisions. The curves are NLO pQCD calculations [131]. (Right) Invariant cross-section (pp) and invariant yield (Au+Au) of direct photons as a function of p_T . The solid markers are from [96] while the open points from [136, 191]. The three curves on the pp data represent NLO pQCD calculations; the dashed curves show a modified power-law fit to the pp data, and the same scaled by T_{AA} . The solid black curves are the sum of an exponential plus the T_{AA} scaled pp fit. The red dotted curve is a prediction from [70]. (Figure taken from [96]).

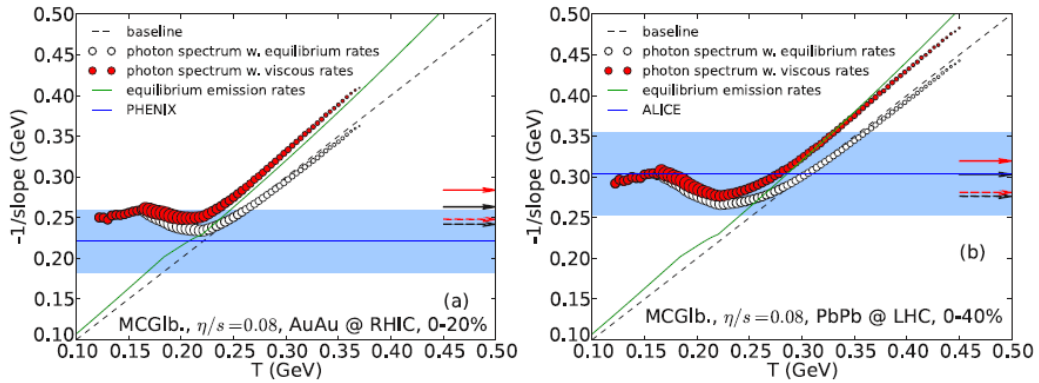


FIG. 20. Inverse photon slope parameter $T_{eff} = -1/\text{slope}$ as a function of the local fluid cell temperature, from the equilibrium thermal emission rates (solid green lines) and from hydrodynamic simulations (open and solid circles), compared with the experimental values for (a) Au+Au collisions at RHIC (PHENIX [96]) and (b) Pb+Pb collisions at the LHC (ALICE [273]). (Figure taken from [27]).

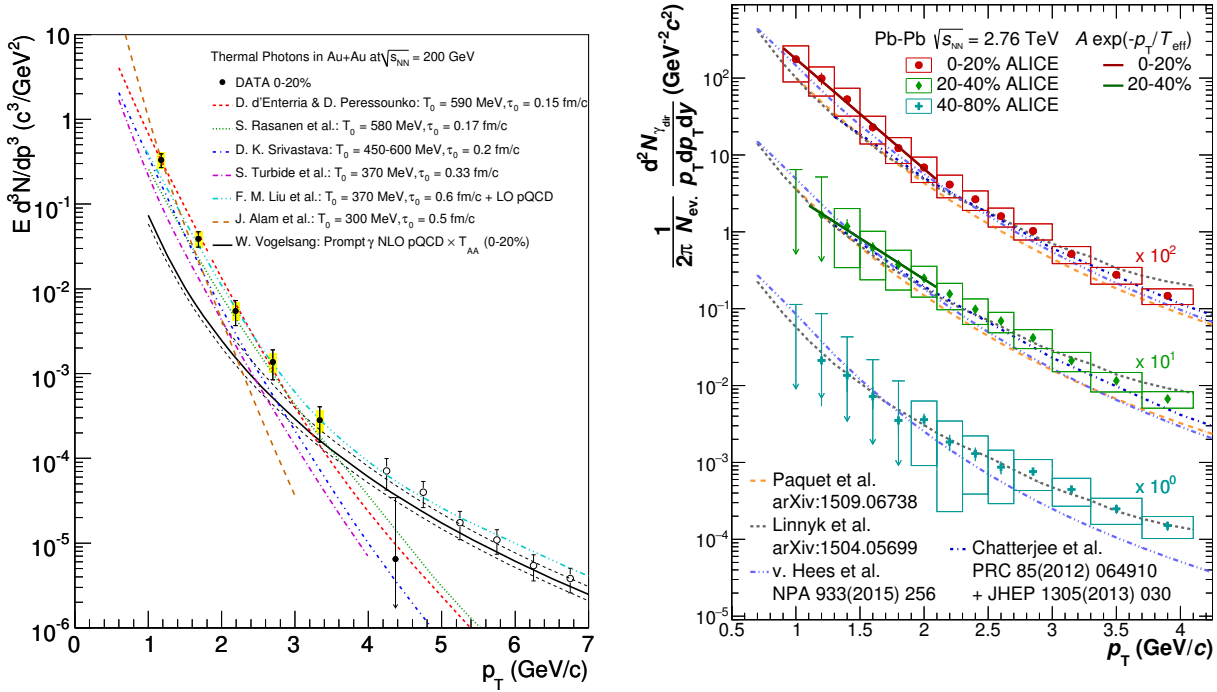


FIG. 21. (Left) Theoretical calculations of thermal photon emission are compared to direct photon data in central 0-20% Au+Au collisions by d’Enterria and Peressounko [277], Rasanen *et al* (based on [278]), Srivastava and Sinha (based on [279]), Turbide *et al* [70], Liu *et al* [280] (this calculation includes pQCD contributions), and Alam *et al* [281]. The solid and dotted black lines are pQCD calculations [131] varying μ from $0.5p_T$ to $2p_T$, and scaled by T_{AA} . (Figure taken from [92].) (Right) Direct photon spectra in Pb+Pb collisions at $\sqrt{s_{NN}} = 2.76$ TeV measured by the ALICE experiment. Invariant yields for three different centrality classes are shown and compared to model calculations [57, 74, 282, 283]. (Figure taken from [90].)

resolution, high granularity PHOS calorimeter has been added. The agreement of the inclusive photon spectra between the two methods (external conversion and calorimetry) was within 1.2 standard deviations, while the double ratios agreed within 0.4 standard deviation. The published results are the error-weighted average of the two independent measurements.

The final ALICE direct photon spectra at low p_T are shown in Fig. 21 (right panel) and compared to various model calculations. In the most central collisions there is a signal down to $p_T = 1$ GeV/c. The low p_T region $0.9 < p_T < 2.1$ is fitted with an exponential two different ways. First, the pQCD photons, as calculated in [57] are subtracted. In that case the inverse slope for 0-20% centrality is $T_{eff} = 297 \pm 12^{stat} \pm 41^{sys}$, close to the preliminary value obtained for 0-40%, but in the next centrality bin (20-40%) T_{eff} is much higher, albeit with very large uncertainties ($T_{eff} = 410 \pm 84^{stat} \pm 140^{sys}$). The role of pQCD photons is negligible up to a few GeV/c: the inverse slopes without subtraction are $T_{eff} = 304 \pm 11^{stat} \pm 40^{sys}$ and $T_{eff} = 407 \pm 61^{stat} \pm 96^{sys}$ for 0-20% and 20-40%, respectively. Finally, in peripheral collisions (40-80%) only upper limits could be established up to 2 GeV/c. Also, the spectra in Fig. 21 (right panel) are clearly ill-described by a single exponential in the $0.9 < p_T < 4.0$ GeV/c range.

Although radically different, the listed models⁵⁸ all describe the data within uncertainties. Van Hees *et al.* [282] uses an updated version of their thermal fireball model [287] based on ideal hydrodynamics with initial flow (prior to thermalization). The initial time is $\tau_0 = 0.2$ fm/c with $T_0 = 682$ MeV and $T_0 = 641$ MeV for the 0-20% and 20-40% event classes, respectively. Chatterjee *et al.* [283, 288] use an event-by-event (2+1D) longitudinally boost invariant ideal hydrodynamic model with fluctuating initial conditions. The initial time is $\tau_0 = 0.14$ fm/c with $T_0 = 740$ MeV and $T_0 = 680$ MeV for the 0-20% and 20-40% event classes, respectively. Paquet *et al.* [57] use (2+1D) longitudinally boost-invariant viscous hydrodynamics [289] with fluctuating, impact-parameter dependent glasma (IP-Glasma) initial conditions [290]. The hydro evolution starts at

⁵⁸ For a more detailed discussion of the models see Sec. VI.

$\tau_0=0.4$ fm/c with $T_0=385$ MeV and $T_0=350$ MeV for the 0-20% and 20-40% event classes, respectively. For a given τ_0 the initial temperatures are somewhat higher than for the RHIC data. In the PHSD model by Linnyk *et al.* [74] the full evolution of the system is described microscopically in an off-shell transport approach, rather than by hydrodynamics. Given the experimental uncertainties, the data in Fig. 21 (right panel) can not discriminate between the models. This is a common problem so far in the low p_T direct photon measurements.

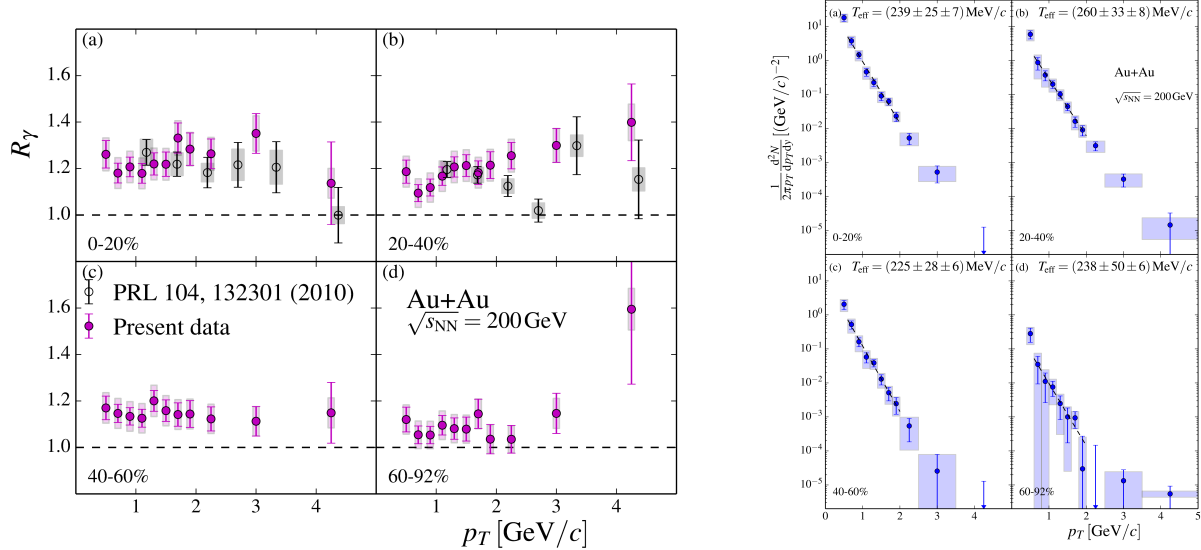


FIG. 22. (Left panels) Inclusive over decay photon ratio R_γ in the low p_T region for all centralities from the 2007 and 2010 $\sqrt{s_{NN}} = 200$ GeV Au+Au datasets, analyzed with the external conversion method (“Present data”). For comparison, the same quantity obtained earlier with the internal conversion method [96] is also shown. (Right panels) Direct photon p_T spectra after subtraction of the N_{coll} -scaled pp contribution for all centralities, along with an exponential fit in the $0.6 < p_T < 2.0$ GeV/c region. (PHENIX data, figure taken from [89].)

About the same time the PHENIX experiment repeated the measurement of low p_T direct photons on a much larger $\sqrt{s_{NN}} = 200$ GeV Au+Au dataset (taken 2007 and 2010) with the external conversion technique [89]. The results for all centralities are shown in Fig. 22. The R_γ ratios (inclusive over decay photons) in the two most central bins are compared to the corresponding ratios obtained earlier with the internal conversion method [96], and found to be consistent within stated uncertainties, although a $\sim 15\%$ difference, as predicted in [95] could not be excluded. The direct photon yield can then be obtained from the hadron decay photon yield using

$$\gamma^{direct} = (R_\gamma - 1)\gamma^{hadron}.$$

Finally, the N_{coll} -scaled pp contributions⁵⁹ are subtracted, and the resulting spectra shown in Fig. 22 (right panel) along with exponential fits in the $0.6 < p_T < 2.0$ GeV/c region. Remarkably, all inverse slopes are consistent with ~ 240 MeV, independent of centrality. The PHSD model⁶⁰ actually predicts such behavior [291] and the effective temperature in the same $0.6 < p_T < 2.0$ GeV/c region is $T_{eff} \sim 260 \pm 20$ MeV, very close to the experimental result. On the other hand, a viscous hydrodynamic calculation [27] using the VISH2+1 code [292] for system evolution predicts a weakly centrality-dependent T_{eff} , which is 267 MeV for 0-20%, dropping monotonically to 225 MeV for 60-92% centrality.

In 2017 the STAR Collaboration at RHIC published a new measurement of direct virtual photon production in $\sqrt{s_{NN}} = 200$ GeV Au+Au collisions [97] and the derived direct (real) photon invariant yields as a function of centrality in the $1 < p_T < 10$ GeV/c range, with a gap between 3 and 5 GeV/c (see Fig. 23, left plot). The basic technique used (internal conversion) is identical to the one in the PHENIX publications [92, 96], but the detectors, and consequently details of the analyses are rather different. Unfortunately the low p_T results obtained by STAR and PHENIX are incompatible, as shown in the right plot of Fig. 23, where the integrated yields in the low p_T region are compared. The small difference in the regions of integration does not explain the discrepancies. Interestingly, the centrality dependence is similar, *i.e.* the slope α of the $dN_\gamma/d\eta$ vs $dN_{ch}/d\eta$ fit to the STAR data is (within uncertainties) compatible with the PHENIX slopes [293], raising

⁵⁹ Measured at and above $p_T = 1.5$ GeV/c and extrapolated below.

⁶⁰ Which is a transport code so it does not have temperature evolution *per se*, but of course an exponential can always be fitted to the spectra.

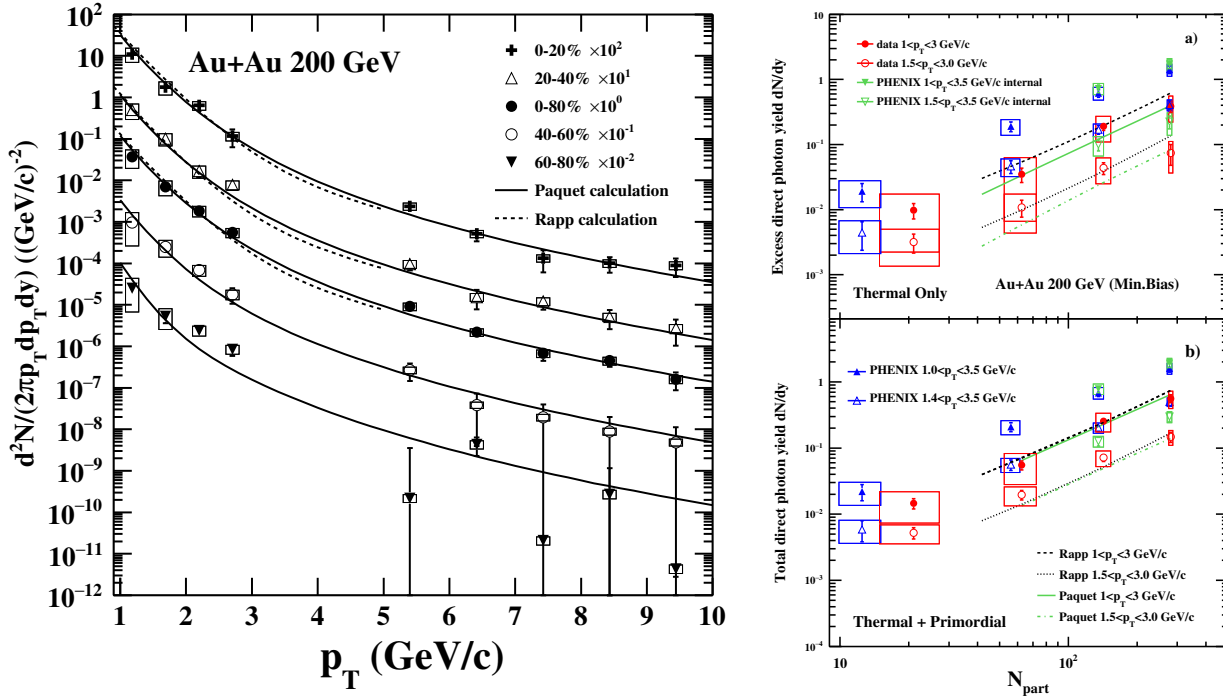


FIG. 23. (Left) Direct photon invariant yields as a function of p_T in Au+Au collisions at $\sqrt{s_{NN}} = 200$ GeV by STAR [97]. Results are compared to model calculations by van Hees *et al.* [282, 287] and Paquet *et al.* [57]. (Right) The excess [panel (a)] and total [panel (b)] direct photon yields in different p_T ranges as a function of N_{part} from STAR (circles) and PHENIX (triangles) in Au+Au collisions at $\sqrt{s_{NN}} = 200$ GeV. The down-pointing triangles represent results from the internal conversion method [96] while the up-pointing triangles represent the results from [89]. Model predictions from Rapp *et al.* [282, 287] and Paquet *et al.* [57] are also shown for the excess (a) and total (b) direct photon yields. Statistical and systematic uncertainties are shown by bars and boxes, respectively. (Figures taken from [97].)

the possibility that one of the experiments made a mistake in overall normalization⁶¹. Extrapolation of the η spectrum to low p_T (where it is not measured but is an important source of background) is done differently in STAR and PHENIX. Unfortunately, if STAR adopts the PHENIX extrapolation (everything else unchanged) the discrepancy *increases*. Despite a joint effort by the two experiments *the issue of the discrepancy is so far unresolved*. Unwelcome as they are, such situations happen, as they did in the past (and with time found a resolution). Ongoing analysis of the 2014 200 GeV Au+Au dataset by PHENIX, larger than all previous datasets combined, and with yet another method (external conversion) might help to put an end to the controversy.

The PHENIX experiment also measured low p_T direct photons with the internal conversion technique in $\sqrt{s_{NN}} = 200$ GeV Cu+Cu collisions [195], and via external conversion in $\sqrt{s_{NN}} = 62.4$ GeV and $\sqrt{s_{NN}} = 39$ GeV Au+Au collisions [270]. Preliminary results have been shown at the Quark Matter 2017 conference and reported in [294]. The inverse slope for minimum bias Cu+Cu data was $T_{eff} = 288 \pm 49(stat) \pm 50(syst)$ MeV (note the large uncertainties), while for the 62.4 and 39 GeV minimum bias data $T_{eff} = 211 \pm 24(stat) \pm 44(syst)$ MeV and $T_{eff} = 177 \pm 31(stat) \pm 68(syst)$ MeV, respectively. It should be noted that for the 62.4 and 39 GeV Au+Au data the pp contribution has not been subtracted. With the inclusion of the $\sqrt{s_{NN}} = 2.76$ TeV ALICE data large colliding systems from Cu+Cu to Pb+Pb and almost two orders of magnitude in collision energy are now covered.

While the inverse slopes in Fig 22 do not show a clear centrality-dependence, the yields certainly do. As discussed in Sec. II, the emission of hadrons, originating from a medium (QGP or hadron gas) and characterized by $dN_{ch}/d\eta$ should roughly be proportional to the number of constituents⁶², or a small power thereof, due to rescattering [295, 296], while photons, coming from binary collisions of the constituents, should be produced at a higher power AN_{part}^α . Naively one would expect $\alpha \sim 2$, but the power is substantially decreased by the rapid cooling and expansion/dilution of the system. Alternately, instead of comparing the

⁶¹ It should be noted that the high p_T part in STAR agrees with the T_{AA} -scaled pQCD calculation, just as in PHENIX [87] – see the argument about and significance of the finding that at high p_T the direct photon R_{AA} is unity in Sec. IV. On the other hand the high p_T measurement in PHENIX was done with a different technique (calorimetry), while in STAR both the low and high p_T regions were measured with the same method (internal conversion).

⁶² The appropriate degree of freedom can be N_{part} participating nucleons or N_{qp} participating constituent quarks, as pointed out in [204].

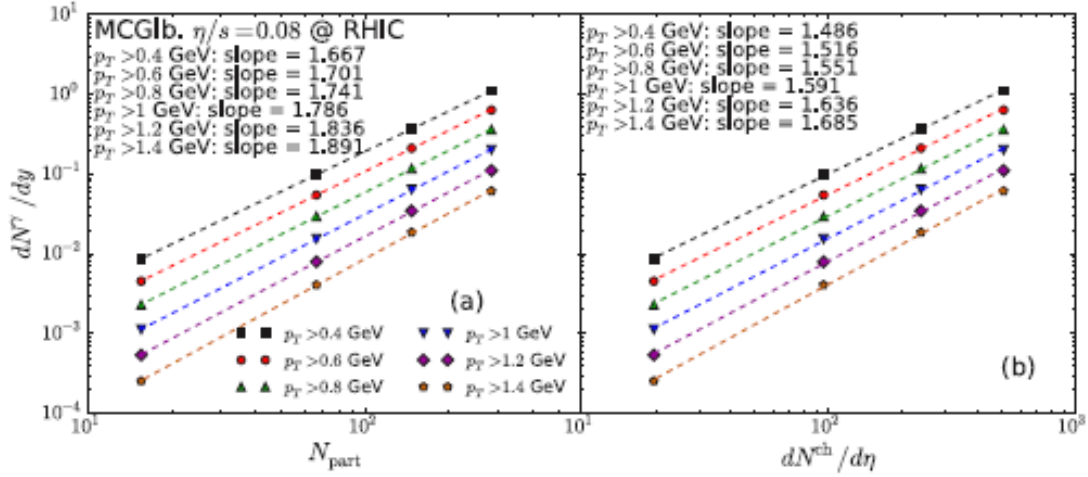


FIG. 24. Model calculation (viscous hydrodynamics [27]) of the centrality dependence of the photon yield for $\sqrt{s_{NN}} = 200$ GeV Au+Au collisions at RHIC. Centrality is expressed both in terms of (a) N_{part} and (b) $dN^{\text{ch}}/d\eta$. (Figure taken from [27].)

(integrated) photon yields to N_{part} or N_{qp} (not directly measured) one can compare them to the observed charged particle density $dN^{\text{ch}}/d\eta$, essentially the number of final state charged hadrons. In the viscous hydro model cited above [27] the dependence of the integrated photon yields on both N_{part} and $dN^{\text{ch}}/d\eta$ are calculated; also, for both sets the lower integration limit is varied from $p_T = 0.4$ GeV/c to 1.4 GeV/c. The results, including the non-negligible variation of the slopes with the lower integration limit, are shown in Fig. 24, and reflect the fact that the ratio of yields coming from the QGP and the hadron gas (HG) changes with p_T . In fact, the authors point out that taking only the HG yields for $p_T > 0.4$ GeV/c they would scale as a function of N_{part} with power 1.46 and as a function of $dN^{\text{ch}}/d\eta$ with power 1.23; the corresponding powers for the QGP are much larger, 2.05 and 1.83.

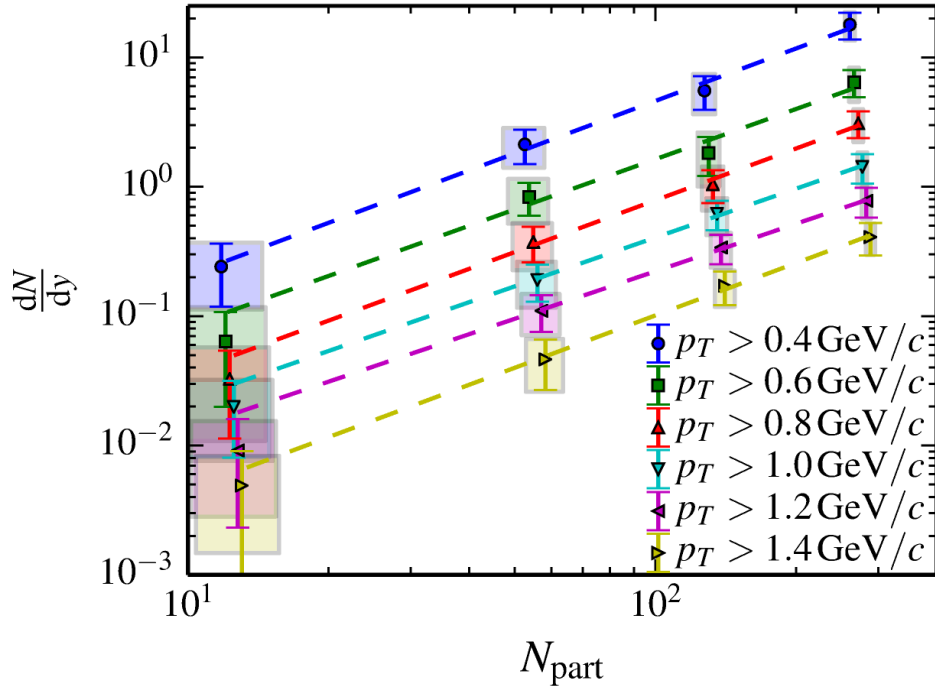


FIG. 25. Integrated "thermal" photon yields in $\sqrt{s_{NN}} = 200$ GeV Au+Au collisions measured by the PHENIX experiment as a function of N_{part} for different lower p_T integration limits. The points at a given N_{part} are slightly shifted for better visibility. The dashed lines are independent fits to a power law N_{part}^α . (Figure taken from [89].)

The first experimental results are shown in Fig. 25. Contrary to the prediction in [27], the slopes α in $dN_\gamma/dy = AN_{\text{part}}^\alpha$ did not change significantly with the p_T integration limit, and the average value is $\alpha = 1.38 \pm 0.03(\text{stat}) \pm 0.07(\text{syst})$, even somewhat lower than the purely HG slope in [27]. This constancy

of the slope was quite unexpected. The spectra are steeply falling, so the integral is mostly determined by how the spectrum looks like near the lower integration limit. If one neglects non-conventional sources and thinks only in terms of the “radiation comes either from the QGP or the HG” dichotomy, yields with the lowest p_T integration limit would clearly be overwhelmed by HG production, while yields integrated from the highest, $p_T = 1.4 \text{ GeV}/c$ limit should have some (substantial?) QGP contribution, which in turn should have a steeper centrality (N_{part}) dependence. This is reflected in other models, too. In the PHSD transport model [291] $\alpha \sim 1.5$; the scaling power from the QGP contribution alone would be higher ($\alpha \sim 1.75$), but the ratio of photons from the QGP and the hadron phase is quite small, only about 10% in the most peripheral, and 30% in the most central collisions. Also, it is strongly dependent on p_T in the low p_T region (up to $p_T = 1 \text{ GeV}/c$, see Fig. 6 in [291]). – A simple (and admittedly incomplete) model of photon production in the Glasma [297] puts the scaling power in the range $1.47 \leq \alpha \leq 2.2$, but the shape and the centrality dependence of the spectra are well described, once the normalization is fixed for one centrality and “geometric scaling” is applied. – The model claiming enhanced photon emission due to strong initial magnetic fields [298] predicts *less* enhancement in central collisions, since the magnetic field decreases with decreasing impact parameter, disfavored by the data. – It is interesting to note that recent models tend to *deprecate* QGP radiation: they assume that the bulk of the “thermal” yield is produced either before QGP is formed, or at the transition from QGP to HG and later. We will discuss these models and their implications in more detail in the context of the “direct photon puzzle”, see Sec VI.

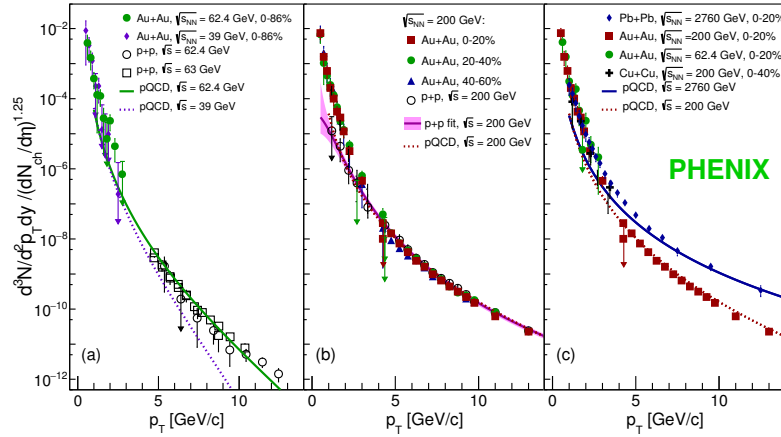


FIG. 26. Direct photon spectra normalized by $(dN_{\text{ch}}/d\eta)^{1.25}$ for Au+Au at $\sqrt{s_{NN}}$ 39 and 62.4 GeV (panel (a)) and 200 GeV (panel (b)). Panel (c) compares spectra for different $A + A$ systems at different $\sqrt{s_{NN}}$. (Figure taken from [270].)

2. Scaling of direct photon yields with $dN_{\text{ch}}/d\eta$

The integrated yield *vs* N_{part} provides good insight in the centrality dependence in a particular A+A system at a specific $\sqrt{s_{NN}}$ collision energy, but N_{part} is ill-suited for comparisons between systems and energies (also, it is not a direct experimental observable). When investigating the system size and energy dependence of photon production, the (pseudo)rapidity density of produced, final state charged particles, $dN_{\text{ch}}/d\eta$ is a more natural choice – and it is a measured, model-independent quantity.

In a recent publication [270] by PHENIX it has been pointed out that if the direct photon yields at mid-

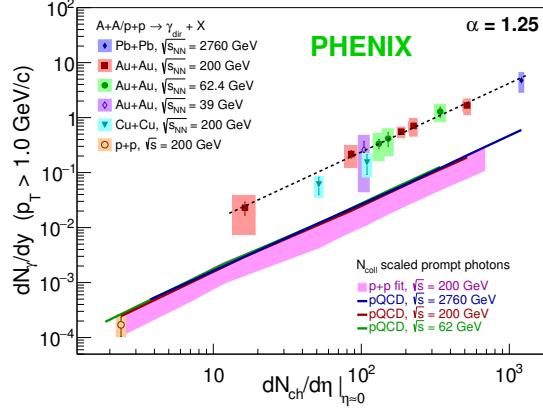


FIG. 27. Direct photon yields integrated for $p_T > 1.0 \text{ GeV}/c$ vs $dN_{\text{ch}}/d\eta$ for various colliding systems and energies. The Pb+Pb data are from ALICE, all other data are from PHENIX. (Figure taken from [270].)

rapidity are normalized by the corresponding $(dN_{\text{ch}}/d\eta)^{1.25}$ then the “thermal” photon yields are similar for a wide range of colliding nuclei⁶³, collision centralities and collision energies (see Fig. 26). Alternately, the photon yields integrated above $p_T > 1.0 \text{ GeV}/c$ as a function of $dN_{\text{ch}}/d\eta$ scale with a power $\alpha = 1.25$ for the same wide range of systems and energies and centralities (see Fig. 27). It is important to note that $N_{\text{coll}} \sim (dN_{\text{ch}}/d\eta)^{1.25} \sim N_{\text{qp}}^{1.25}$ where N_{qp} is the number of quark participants [204]⁶⁴. The origins of that scaling are unclear, but, at least qualitatively, it would fit a picture where most photons are produced in space-time near the QGP→HG transition, which in turn would be largely independent of the initial conditions (as long as QGP is formed). While highly speculative at the moment, it is an avenue worth exploring, among others by filling the $dN_{\text{ch}}/d\eta$ gap between the pp and the most peripheral A+A points in Fig. 27. This can be done two different ways. The cleaner one is to continue exploring large-on-large ion collisions (where the scaling has been observed) but decrease $\sqrt{s_{NN}}$ further, and also to analyze very peripheral data in smaller and smaller centrality bins, which in light of the increasing A+A datasets should be possible. The other possibility is to look at p+A and d+Au data – an ongoing effort – and maybe at very high multiplicity pp events. However, one has to be careful with the conclusions. As recent results from other observables indicate, initial state effects play much bigger role in very asymmetric collisions (p+A, d+Au) than in A+A, and comparing very high multiplicity, *i.e.* extremely rare pp events to average A+A collisions may also be misleading. Unfortunately telling apart new physics from experimental bias is not always trivial.

⁶³ As long as the nuclei are both sufficiently large; as of now it is still unclear what happens in very asymmetric collisions, like p+Au or d+Au.

⁶⁴ In other words, direct photon production apparently scales with N_{coll} , which is fully expected at high p_T , but quite surprising in the “thermal” region.

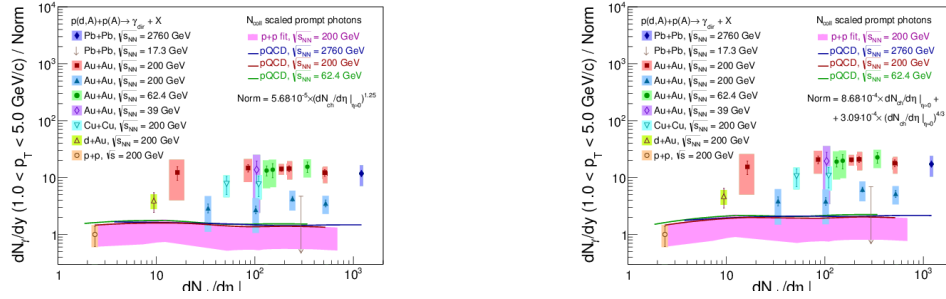


FIG. 28. Low p_T integrated direct photon yield for various colliding systems and energies, divided by fits with two different functions, $A(dN_{ch}/d\eta)^\alpha$ and $A(dN_{ch}/d\eta) + B(dN_{ch}/d\eta)^{4/3}$. The fits are normalized to the 200 GeV pp point. In addition to the data shown in Fig. 27 the PHENIX $d+Au$ data [192] and the STAR virtual photon data [97] are presented, too. Both fit functions have only two free parameters, and the data/fit is virtually indistinguishable. (Figure courtesy of Vladimir Khachatryan.)

It should be pointed out (and in fact it is mentioned in [270]), that the scaling function $A(dN_{ch}/d\eta)^\alpha$ used in Fig. 27 is not unique; the integrated yields can be equally well fitted for instance with

$$\frac{dN_\gamma}{dy} = A \frac{dN_{ch}}{d\eta} + B \left(\frac{dN_{ch}}{d\eta} \right)^{4/3}$$

another function with just two free parameters, but completely different form. In order to show that the two functions provide equally good fits, in Fig. 28 the low p_T integrated yields are divided by the two different fit functions discussed above. The functions are normalized to the pp point. Fig. 28 has a few more data points than Fig. 27, including the $d+Au$ results from PHENIX [192] and the STAR virtual photon data [97] that are incompatible with the PHENIX results. Obviously the two fits describe the data equally well, although the functional form is quite different, suggesting different physics. Remarkably, the power $4/3$ is exactly that of the second, nonlinear term in Feinberg’s 1976 paper [9] where he calculates the number of photons produced in hadron-hadron collisions if “an intermediate stage of hadronic matter” exists (see Sec. I). Very suggestive, but one has to be careful before drawing any conclusions. Nevertheless, it appears that the “excitation function” of low p_T direct photon production over a wide range of colliding systems, centralities and energies can be described with just two free parameters, a tantalizing hint that there might be some *fundamental commonality in the underlying physics*.

VI. DIRECT PHOTON FLOW – THE ERA OF THE “DIRECT PHOTON PUZZLE”

A. First results on v_2 and v_3

In a 2008 review of the electromagnetic probes [16] the authors pointed out that a *coherent and quantitative* description of the sQGP – including direct photon observations – in heavy ion collisions is still missing. The measured large photon yields in the “thermal” region [96] could be explained in a hydrodynamic framework with inverse slopes T_{eff} ranging from 370 to 660 MeV (varying the initial thermalization time τ_i , see [277] and references therein). Independently, large elliptic flow v_2 , scaling with the number of quarks was found for hadrons. The usual interpretation was (and still is) that hadrons inherit the final momentum anisotropies of the sQGP which in turn build up gradually from the initial pressure anisotropies, starting at τ_i and lasting until the time of chemical freeze-out. Photons are produced predominantly early (highest temperatures), when the pressure gradients, *i.e.* acceleration is highest, but velocities are still small, while hadrons are imprinted by the large velocities at the end of sQGP expansion. Accordingly, direct photons from the QGP were expected to have very small v_2 compared to photons from the hadron phase [72, 299, 300], which itself is still smaller than v_2 of the final state hadrons, and, per extension, v_2 of the π^0 decay photons. Interestingly, the first report on direct photon flow appeared to confirm this expectation of small photon v_2 [301], albeit with important caveats.

All this changed radically at the Quark Matter 2011 conference where PHENIX presented preliminary results on direct photon v_2 in the 1-12 GeV/c p_T region and found that “for $p_T > 4$ GeV/c the anisotropy for direct photons is consistent with zero, which is as expected if the dominant source of direct photons is initial hard scattering. However, in the $p_T < 4$ GeV/c region dominated by thermal photons, we find a substantial direct-photon v_2 comparable to that of hadrons, whereas model calculations for thermal photons in this kinematic region underpredict the observed v_2 .” [82].

The results, reproduced in Fig 29, were received with significant scepticism because they meant that “thermal” photons have v_2 just as large as final state hadrons. This was simply incompatible with the

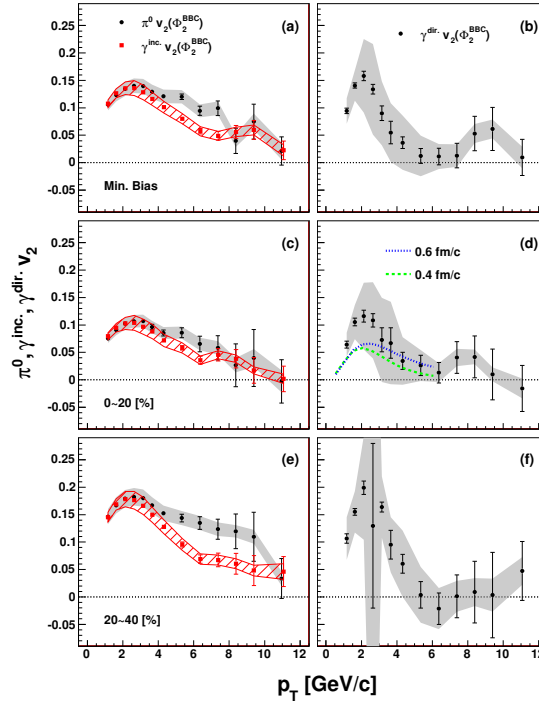


FIG. 29. (a),(c),(e) Centrality dependence of v_2 for π^0 and inclusive photons measured for minimum bias, 0-20% and 20-40% centrality Au+Au collisions at $\sqrt{s_{NN}} = 200$ GeV. (b),(d),(f) shows the direct photon v_2 , vertical bars showing statistical while shaded areas showing systematic uncertainties. Superimposed on panel (d) are calculations from [300] using two different initial times. (Figure taken from [82].)

old paradigm. The observed v_2 is a convolution of the rates (largest early on, when T is highest) and the anisotropic boost from the expansion (largest at late times, when T is in turn smallest). Hadron v_2 encodes the final, maximum velocities, but photons, being penetrating probes, are boosted only by the velocities experienced at the moment of their creation, which initially are close to zero. No theory predicted or could readily accommodate the simultaneous observation of large yields and large v_2 for “thermal” photons, and the issue quickly became dubbed the “*direct photon puzzle*”, spawning workshops [158, 302–307], impromptu collaborations of experimentalists and theorists, and a remarkable number of papers.

In 2012 the ALICE Collaboration made a similar observation at LHC energies, and has shown it as preliminary result at the Quark Matter 2012 conference [267], but in the subsequent years there was some doubt whether the observed v_2 is really significant or still consistent with zero (no flow at all). In 2016 the PHENIX Collaboration published another paper on direct photon v_2 and v_3 [269], concentrating only on the $p_T < 4$ GeV/c (“thermal”) region, measuring photons two different ways (calorimeter and conversion, see Sec. III), and confirmed the previous findings: the direct photon v_2 is large, comparable to the hadron v_2 . The new results are shown in Fig. 30. The final results by ALICE on photon v_2 in 2.76 TeV Pb+Pb collisions [214, 308] are just being published (2019) and the authors conclude that “*A comparison to RHIC data shows a similar magnitude of the measured direct-photon elliptic flow. Hydrodynamic and transport model calculations are systematically lower than the data, but are found to be compatible.*” [214] Different from the 2012 (preliminary) measurement this time (2019) ALICE applied two independent methods, conversion and calorimetry. The final data are shown in Fig. 31. Remarkably, the results are consistent with the PHENIX v_2 presented in Fig. 30. There is an ongoing effort in PHENIX to repeat the analysis with a *third* method [215] and on a dataset that is an order of magnitude larger than earlier ones; preliminary results are shown in Fig. 32. The low p_T part once again confirms earlier findings. The high p_T part should be compared to the first (2011) measurement, shown in Fig. 29. The p_T range is extended while the uncertainties are considerably smaller, and the clear message is that at high p_T the direct photon v_2 is consistent with zero, as expected, if the bulk (or all) of those photons are produced in initial hard scattering.

There is only one published direct photon v_3 measurement so far [269], and it has large uncertainties (see Fig. 30). As pointed out in [309, 310], v_3 is purely driven by initial density fluctuations, therefore, it carries information on pre-equilibrium photons, including what, if any role the initial magnetic field plays. Also, the ratio of photon v_2/v_3 serves as a “viscometer”. It has been argued already in [311] that shear viscosity (η) effects both the photon v_2 and T_{eff} extracted at low p_T . The idea was expanded in [309, 312] by studying higher order v_n and suggesting that v_2/v_3 of “thermal” photons is different from that of hadrons, because it is weighted toward earlier times, and viscous effects are largest at early times when the expansion rate is

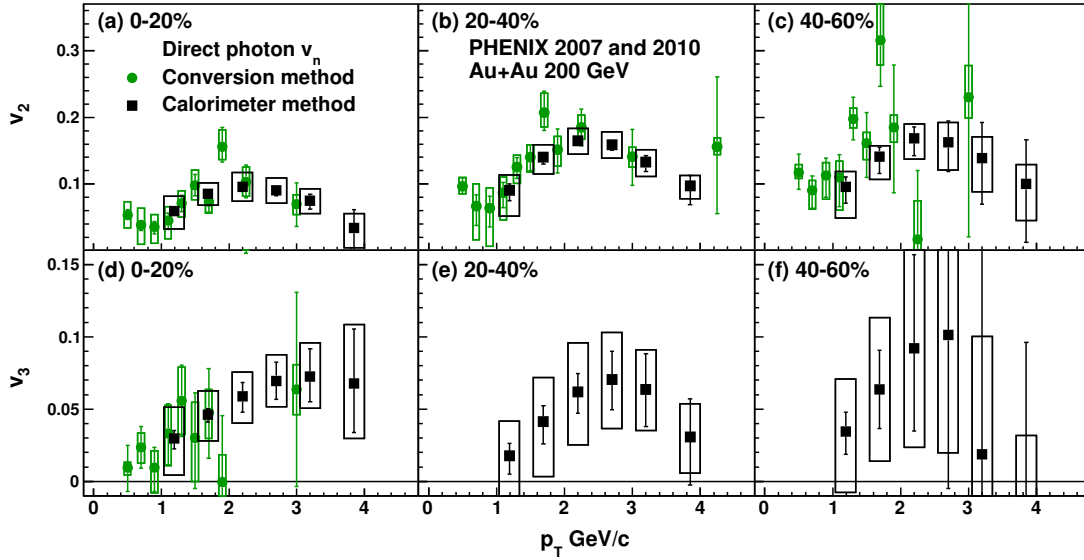


FIG. 30. Direct photon v_2 and v_3 at midrapidity ($|\eta| < 0.35$), for different centralities, measured by PHENIX with the conversion method (solid circles, green) and the calorimeter method (solid squares, black). The event plane was determined by the reaction plane detector ($1 < |\eta| < 2.8$). The error bars (boxes) around the data points are statistical (systematic) uncertainties. (Figure taken from [269].)

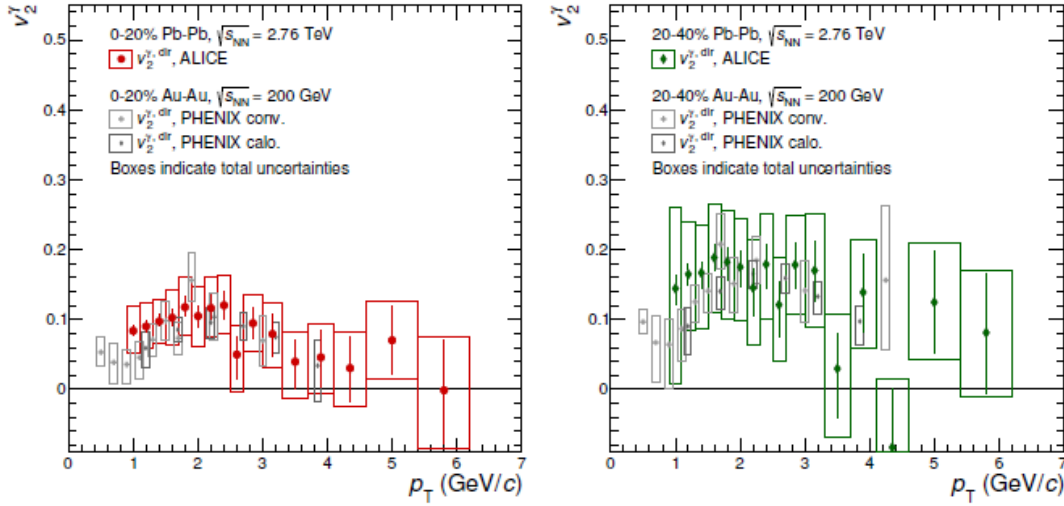


FIG. 31. Elliptic flow of direct photons in 2.76 TeV Pb+Pb collisions (ALICE) compared to PHENIX results [269] in 200 GeV Au+Au. Vertical bars are statistical, boxes are the total uncertainty. (Figure taken from [214].)

largest. The expected ratio of integrated v_2 and integrated v_3 for photons and charged hadrons is shown in Fig. 33 for two types of initial conditions (Monte-Carlo Glauber and Monte-Carlo Kharzeev-Levin-Nardi) and two values of specific shear viscosity η/s . In all settings the differences between photons and hadrons (shaded regions) are substantial, as are the predictions for the different settings (different colors), making v_2/v_3 a powerful observable to support or rule out models. Unfortunately current experimental uncertainties (see Fig. 30) are still too large to allow this, but hopefully the data will improve soon.

B. The Devil's advocate

In Sec. VID we will review the current theories, but it is fair to say that none of them is able to simultaneously describe both the observed large yields and the large v_2 . This is demonstrated for instance in Fig. 34, with more comparisons in Sec. VID. Moreover, those models that are at least partially successful tend to downplay the role of radiation from the QGP: they either emphasize pre-equilibration sources with some built-in anisotropy, or production in the hadron phase, where large v_2 comes naturally. But a *partonic*

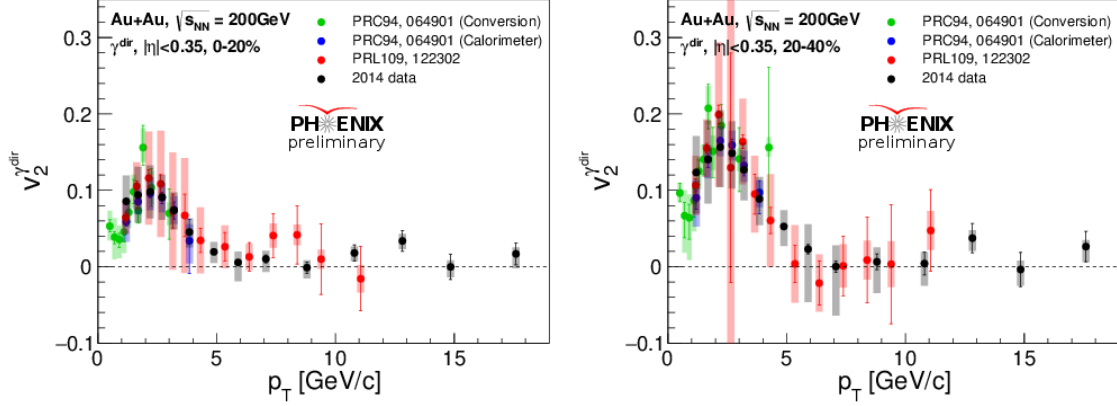


FIG. 32. Direct photon v_2 in 200 GeV Au+Au collisions, measured by PHENIX with three different techniques. The green, published data are from conversions at a known radius (HBD backplane), while the black, preliminary “2014 data” are obtained with the method that does not assume *a priori* the conversion radius (they can happen at different layers of the VTX detector). For more details see Sec. III B.

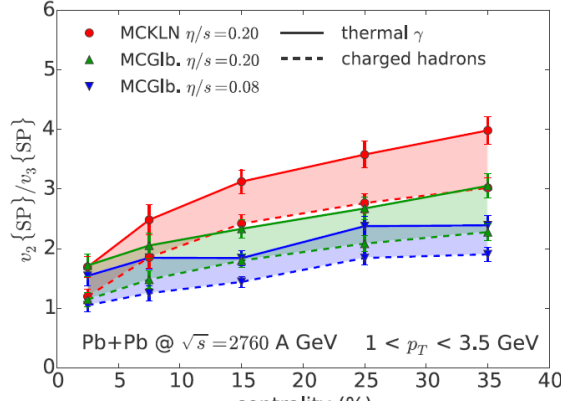


FIG. 33. The ratio of the integrated v_2 to the integrated v_3 for the LHC, for different initial conditions and η/s . The ratio is shown as a function of centrality. Solid and dashed lines show the ratio for photons and charged hadrons, respectively. (Figure taken from [309]).

medium almost without radiation would be a major paradigm change, and of course it should be proven that all other, non-electromagnetic phenomena are also consistent with it. Such unorthodox ideas would not be entirely new (see for instance [314] and references therein), but before making such leap, scientific rigor requires to pose the uncomfortable and provocative question: what if the *data* are wrong⁶⁵?

Although the substantial direct photon v_2 is now confirmed both by (semi)-independent analysis techniques and different experiments, at RHIC and the LHC⁶⁶, we shouldn’t forget that at the moment (early 2019) there are still unresolved discrepancies between the measured photon yields between PHENIX and STAR (see Fig. 23)⁶⁷, and that the yields, more precisely R_γ plays a decisive role in measuring direct photon v_2 . Moreover, a recent statistical analysis of the ALICE v_2 data (Reyers [158]) indicates that the significance of the non-zero v_2 might only be $O(1\sigma)$. Since the “direct photon puzzle” remains an unresolved issue with potentially far-reaching consequences, utmost caution is warranted, and we believe it is useful to briefly discuss the potential pitfalls of the measurements.

Looking at the formula from which n -th order direct photon flow is calculated

$$v_n^{\gamma,dir} = \frac{R_\gamma v_n^{\gamma,inc} - v_n^{\gamma,dec}}{R_\gamma - 1} \quad (7)$$

⁶⁵ After all, “*paranoia is the experimentalist’s best friend.*” Direct photon measurements are extremely difficult, and in the past decades it happened more than once that a questionable result stirred up the field for quite some time. The author, an experimentalist himself, believes such “sacrilegious” questions to us are best asked by ourselves, rather than insisting on the line “the data are what they are; if you cannot explain them, it’s your problem”.

⁶⁶ Inclusive photon v_2 has already been measured at the SPS (see for instance [266, 315]), but no attempt has been made to extract the direct photon v_2 .

⁶⁷ It would be interesting to see a direct photon v_2 measurement from STAR based on their lower yields!

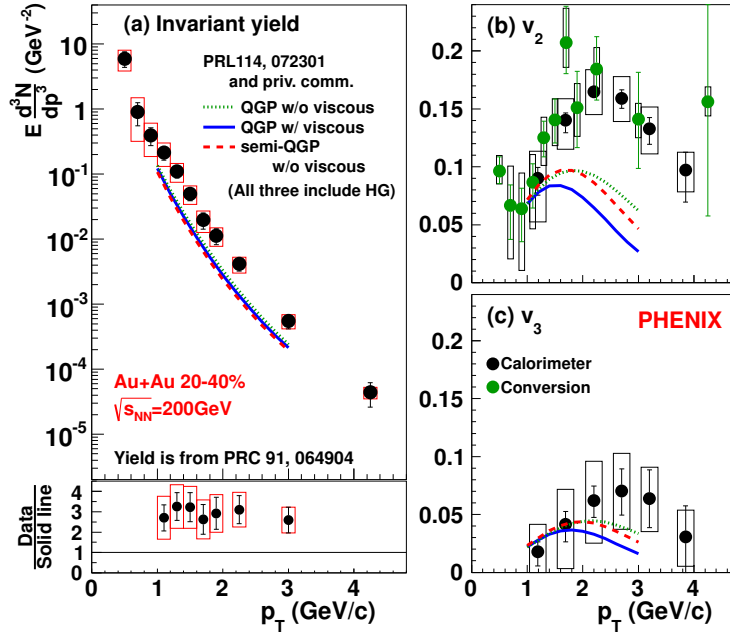


FIG. 34. Comparison of the direct photons yields and v_2 , v_3 with a hydrodynamical model [57] calculated under three different assumptions, including the “semi-QGP” scenario [313]. For more comparisons see Sec. VID. (Figure taken from [269].)

where R_γ is the excess photon ratio, $v_n^{\gamma,dir}$, $v_n^{\gamma,inc}$, $v_n^{\gamma,dec}$ are the n -th order Fourier-coefficients for direct, inclusive and decay photons, respectively, the difficulties are obvious. Since most inclusive photons come from hadron decay, $v_n^{\gamma,inc} \simeq v_n^{\gamma,dec}$ almost per definition. Moreover, R_γ , the direct photon excess is usually close to unity, often less than 2σ above it. Therefore, both the numerator and denominator in Eq. 7 are small and within uncertainties might even change sign. As pointed out originally by ALICE and discussed in detail in [269], Gaussian error propagation cannot be used⁶⁸. Instead, the probability distribution for the possible values of $v_n^{\gamma,dir}$ has to be modeled using Eq. 7 and randomizing its components with their (individually Gaussian) errors. The procedure is illustrated in Fig. 35; there the resulting uncertainty of $v_2^{\gamma,dir}$ is clearly asymmetric, and while the central values are essentially unchanged, the probability distribution would even allow $v_n^{\gamma,dir}$ to change sign. It is also obvious that the asymmetry comes from the nonlinear dependence of $v_n^{\gamma,dir}$ on R_γ , as seen in Eq. 7, so one key to better $v_n^{\gamma,dir}$ in the future is significant improvement on R_γ (or direct photon yield) measurements, which in turn starts with the cleanest possible inclusive photon sample, *i.e.* the best photon/electron identification (hadron rejection) achievable.

A recent study of the effects of hadron contamination in conversion photon (e^+e^-) measurements of v_2 [316], now the most common method in the “thermal” region, pointed out how important it is to derive $v_2^{\gamma,inc}$ from a completely clean sample. Already 1% π^\pm contamination may cause a 10-20% change in $v_2^{\gamma,inc}$, and the deviation also has a very strong p_T dependence⁶⁹.

Another serious issue is insufficient information on yields and spectra of higher mass neutral mesons, decaying in part into photons (anything above the π^0). Out of these η is by far the most important, but for instance in $\sqrt{s_{NN}}=200$ GeV Au+Au there is no measurement of the η yields or v_2 at low p_T [317, 318]. While it is firmly established that at high p_T the η/π^0 ratio is constant over a large range of colliding systems and energies [317], there is no universally accepted method to extrapolate the η spectrum to low p_T . In a recent publication of the direct virtual photon yields [97] the STAR Collaboration has shown that using two different – equally justifiable – assumptions⁷⁰ the resulting direct/inclusive photon ratio can change up to 43% in minimum bias Au+Au collisions. Note that in [97] the STAR Collaboration found that “... the excess and total yields are systematically lower than the PHENIX results in 0-20%, 20-40% and 40-60% centrality bins.” In other words, R_γ , that plays a crucial role in the v_2 measurement, is much smaller than in PHENIX. A direct photon v_n measurement by STAR with the same apparatus and on the same dataset would be very helpful step to resolve the “direct photon puzzle”.

⁶⁸ Except in the case when $v_n^{\gamma,inc} \equiv v_n^{\gamma,dec}$, meaning that either there are no “thermal” photons at all ($R_\gamma = 1$), or their $v_n^{\gamma,dir} \equiv v_n^{\gamma,dec}$.

⁶⁹ Note that in the low p_T region e/π separation is usually cleaner in experiments using Cherenkov detectors than in TPC’s if they rely only on dE/dx information, but no time-of-flight.

⁷⁰ A Tsallis blast-wave model, with the freeze-out parameters obtained by fitting other hadrons simultaneously (the standard procedure at STAR), and m_T scaling the measured π^0 spectrum (the PHENIX method), in both cases normalized to the known η/π^0 ratio at high p_T .

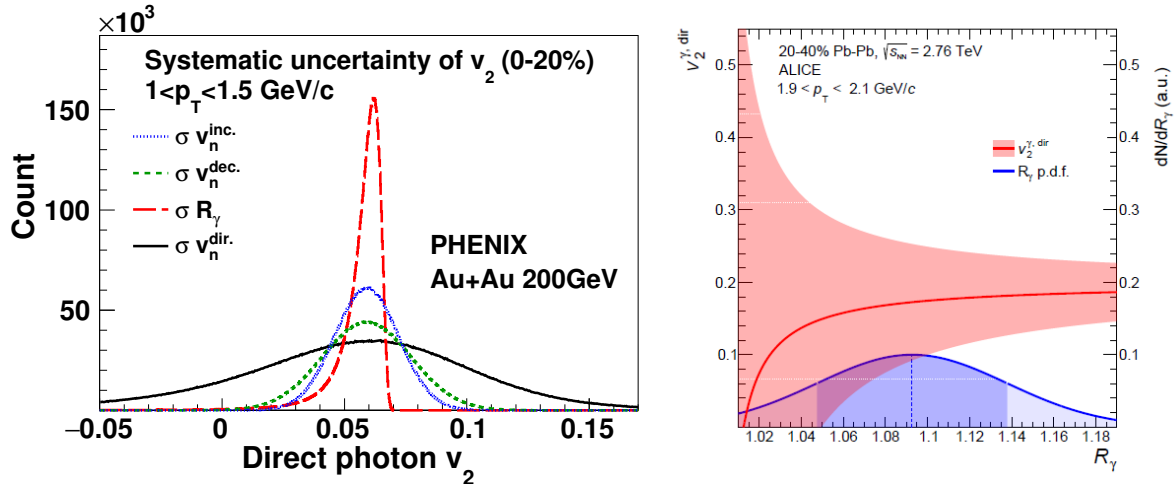


FIG. 35. (Left) An example of the direct photon v_2^{dir} measured with the calorimeter in PHENIX. Each of the various dashed curves indicate the probability distribution of v_2^{dir} result due to the variation of a single term in Eq. 7. While varying v_2^{inv} and v_2^{dec} leaves the uncertainty Gaussian, varying R_γ results in strongly asymmetric shapes. The black solid curve shows the result when all uncertainties are taken into account simultaneously. (Figure taken from [269].) (Right) Central value (solid red line) and uncertainty of the direct photon v_2 for a selected p_T interval. The upper and lower edges of the red shaded area correspond to the total uncertainty of the direct photon v_2 as obtained from linear Gaussian propagation of the uncertainties of the inclusive and decay photon v_2 . The blue Gaussian reflects the $\pm 1\sigma$ uncertainty of the measured R_γ in this p_T interval. (Figure taken from [214].)

C. Methodology: v_n with respect to what and how?

1. Event plane method

The traditional definition of v_n comes from the Fourier-expansion of the event-by-event azimuthal distribution of the emitted particles with respect to a symmetry plane Ψ characterizing the specific event. If for each order n of the expansion a separate plane Ψ_n is defined, the expansion with respect to the azimuth ϕ reduces to

$$\frac{dN(\dots)}{d\phi} = \left\langle \frac{dN(\dots)}{d\phi} \right\rangle \left(1 + \sum_n 2v_n \cos[n(\phi - \Psi_n)] \right) \quad (8)$$

where $N(\dots)$ means the number of particles (total or some subset in bins of p_T , η , etc.), Ψ_n is the azimuth of the n -th order symmetry plane in an absolute coordinate system and v_n is the amplitude of the n -th order term. A key question is how – and to what accuracy – Ψ_n is defined⁷¹.

In each heavy ion collision for a theorist there is always a clearly defined “reaction plane” (RP) spanned by the impact parameter \vec{b} and beam direction \vec{z} . For smooth initial geometry and spherical nuclei this is expected to be a mirror symmetry plane for the overlap area, against which azimuthal distributions (v_2) are calculated. If, in contrast, the continuous density distribution of nuclei is replaced by discrete, randomly placed constituents (nucleons or even partons), another symmetry plane called “participant plane” (PP) can be calculated from the constituents that actually interact [310]. The distinction is important: since $v_n(PP)$ is *defined* by the de facto interacting particles, usually it is larger than $v_n(RP)$, defined by an average of all, interacting and spectator particles (centers of gravity of the two nuclei). Note that RP and PP live both only in theory, they are not directly accessible in an experiment.

Instead, experiments reconstruct an “event plane” (EP) from the azimuthal distributions of the measured final state particles – usually charged hadrons⁷². This can lead to biases, most obviously from jets⁷³. The jet bias can be mitigated (but not fully eliminated) if the EP is determined from particles at a large (pseudo)rapidity gap from the region where the actual measurement takes place, but note that this method tacitly assumes that the n -th order symmetry angle (plane) Ψ_n is independent of pseudorapidity. There

⁷¹ Risking being pedantic we should point out that *any* azimuthal distribution can be expanded in Fourier-series, irrespective of the physical origins of the asymmetries (anisotropy) in it. An obvious example of azimuthally asymmetric events are events with jets, which will have non-zero v_n coefficients. Regrettably, v_n -s are often referred to as “ n -th order flow”, strongly suggesting collective, hydrodynamic behavior where there might be none at all.

⁷² In fixed target experiments in principle the event plane can be deduced the complementary way, from the distribution on the non-interacting “spectator” nucleons, but at colliders this is practically impossible.

⁷³ One single parton in a particular φ direction produces large final state multiplicity in a relatively narrow cone.

are other sources of bias, too, like resonance decays, Coulomb-effects, etc [319, 320]. Such correlations, unrelated to the event plane, are usually called *non-flow correlations*. Finally, it is conceivable that the EP for direct photons is not always exactly the same as for final state hadrons – from which EP is usually measured [321]. If so, this is a serious problem with no simple solution in sight: while one could in principle measure the event plane using (identified) photons instead of charged hadrons, this EP would still be essentially identical to the hadron EP, since the majority of photons come from FS hadron decays and inherit *their* event plane, rather than the – possibly decorrelated – direct photon EP.

After all these physics caveats we should mention an important practical problem with the event plane method. EP can only be measured with some finite resolution σ_{EP} ⁷⁴, which depends on multiplicity, is a strongly non-monotonic function of collision centrality, and connects the “raw” v_n^{raw} to the “true” v_n^{true} via

$$v_n^{true} = \frac{v_n^{raw}}{\sigma_{EP}}$$

Typical event plane resolutions are shown in Fig. 36. Note that the $1/\sigma_{EP}$ corrections are relatively minor for v_2 , but depend very strongly on centrality, while they can be a factor of 5 or higher for v_3 . That means that the actual modulations v_n^{raw} measured in the experiments are sometimes quite small and often similar across centralities⁷⁵. Using two or more EP detectors with different resolutions (and still getting consistent results) alleviates some of these concerns. Typical second- and third-order event plane resolutions are shown in Fig. 36.

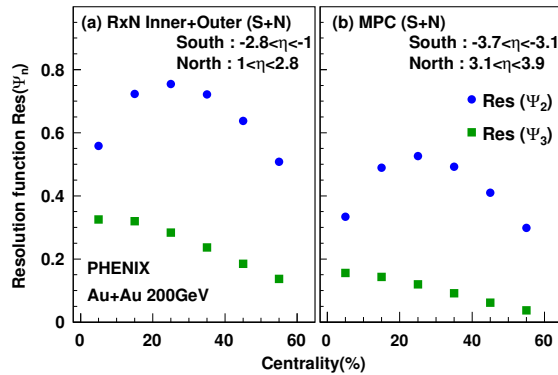


FIG. 36. Event plane resolution as a function of collision centrality for the second and third order v_n in PHENIX. The so-called Reaction Plane Detector (RxN) and the Muon Piston Calorimeter (MPC) have different granularities and cover different η ranges. (Figure taken from [269].)

Another serious issue comes from the fact that v_n can rarely be measured in a single event, instead, it is calculated from a large ensemble of events (each having its own set of Ψ_n event planes in Eq. 8). If event-by-event fluctuations of v_n were negligible, this would not be a problem, but apparently they are not. Relative fluctuations can reach 30-50% [323, 324], so the measured v_n is the mean $\langle v_n \rangle$ at best – when the event-plane resolution is high. However, if it is low, the event plane measurement yields the root-mean-square value $\sqrt{\langle v_n^2 \rangle}$, and in general the result lies somewhere between those two values [320]. This ambiguity makes comparisons between experimental results (and theory) difficult.

2. Scalar product method

Less biased methods exist to measure azimuthal asymmetries of particle distributions, notably the cumulant expansion of multiparticle correlations [325, 326] and a variant of the event plane method called “scalar product” method [319]. These “make for a superior measurement because they consistently yield the rms value of v_n , while introducing no disadvantage compared to the traditional event-plane measurements” [320]. The scalar product method is based on the n -th order flow vector of N particles defined as

$$Q_n = |Q_n| e^{in\Psi_n} = \frac{1}{N} \sum_j e^{in\phi_j}.$$

⁷⁴ The dispersion between the experimentally reconstructed Ψ_n and the true Φ_n of the underlying distribution [322].

⁷⁵ Of course from a purely mathematical point of view the procedure is correct, but the critical reader of experimental papers should be aware that the final results are small measured numbers subject to large corrections.

The flow vector Q_n of the particle in question (e.g. a photon) is then related to the flow vectors Q_{nA}, Q_{nB} of reference particles in two “subevents” A, B (in practice particles in some reaction plane detectors, separated in η from the region where v_2, v_3 are measured) and the scalar product $v_n[\text{SP}]$ is then calculated as

$$v_n[\text{SP}] = \frac{\langle Q_n Q_{nA}^* \rangle}{\sqrt{\langle Q_{nA} Q_{nB}^* \rangle}}.$$

Note that independent of multiplicity, the scalar product method always yields the root mean square v_n ($\sqrt{\langle v_n^2 \rangle}$), just as the low resolution limit in the event plane method [57, 320]

$$v_n[EP_{lowres}] = v_n[\text{SP}] = \frac{\langle v_n^\gamma v_n^h \cos(n(\Psi_n^\gamma - \Psi_n^h)) \rangle}{\sqrt{\langle (v_n^h)^2 \rangle}}$$

where the upper index h refers to the reference particles (usually hadrons).

While earlier photon flow measurements used the event plane method, in the recent direct photon elliptic flow publication by ALICE [214] the scalar product method was applied.

D. Attempts to resolve the direct photon puzzle

After stating all the caveats in the previous Section VIB for the remainder of this chapter we assume that the PHENIX results [269] are correct within stated uncertainties⁷⁶, and confront the results with various model calculations.

As discussed earlier, the essence of the direct photon puzzle is the simultaneous presence of large yields and large azimuthal asymmetries – comparable to that of hadrons – for a signal that is penetrating, produced continuously, thus integrates the entire time history of instantaneous rates and expansion velocities. The conventional line of thought was that the overwhelming part of low p_T photons is of thermal origin from the QGP and the hadron gas. It was expected that the instantaneous rates are highest early on, when temperature is highest but production is still isotropic, while large anisotropies come from photons produced late, thus inherit the maximum velocity anisotropy of their parent partons/hadrons. Plausible and not much contested *before* the observation of a photon v_2 similar to that of hadrons, but *after* the results in [82, 269] such scenario appears to be incomplete at best, completely false at worst.

Predictably, many theorists took up the challenge. Large amount of work was invested, new models, new insights were published or presented at conferences and at dedicated workshops [158, 302–307]. New ideas ranged from tuning the traditional “thermal production / hydrodynamic evolution” picture, through suggestions of new mechanisms that would give large asymmetries to the earliest photons, to the quite radical concept of suppressing photon production from the QGP phase due to slow chemical equilibration of quarks. Hydrodynamic models were upgraded from ideal to viscous, included event-by-event fluctuations of the initial geometry. Transport models (circumventing hydro) re-emerged and proved to be quite successful, as did those that re-defined the initial state based on the Color Glass Condensate (CGC) picture or the process of thermalization. Below we will discuss a few models in some detail. So far none of them provided a completely satisfactory description of the experimental observations, but they gave us a huge influx of creative new ideas at a time when they are really needed⁷⁷. The relevant literature is quite extensive, and reviewing it in its entirety would far exceed the scope of this paper. While we will present several interesting ideas that address only part of the “puzzle”, our selection gives precedence to models that attempt to explain yield and flow simultaneously.

1. Hydrodynamical models

Expanding elliptic fireball model and its extensions

The first attempt to simultaneously explain the observed high “thermal” photons yields [96] and v_2 [82] has been published 2011 in [287]. The expansion dynamics has been modeled by an elliptic blast-wave

⁷⁶ ALICE now also has yields and v_2 from the same dataset (albeit no v_3), but since the PHENIX data triggered the “direct photon puzzle” in 2011, a wider range of models have been compared to them. Note that both the PHENIX and ALICE data have been obtained by more than one analysis method involving different sets of subdetectors, which means an (almost) independent confirmation of the results within the experiments.

⁷⁷ A personal remark. A few years ago one could often hear that “we are close to being able to formulate the Standard Model of heavy ion collisions”. With the advent of surprising observations like apparent strong collectivity even in pp collisions, perplexing observations in very asymmetric collisions, loosening connection between event activity and collision geometry, hints of the critical point at very different collision energies depending on the observable, etc. – with all these new developments a comprehensive and coherent description of heavy ion collisions is not around the corner yet. Direct photons didn’t fully unveil the history encoded in them so far – some day they will, I hope. But they already did something equally important –

source, with parameters adjusted to measured spectra and v_2 of light and multi-strange hadrons. The QGP radiation is a parametrization of the complete leading order in α_s rate as given in [56], the emission in hadronic matter is based on [70]. In order to compare to data, “primordial” (prompt) photons are added two different ways: from an NLO pQCD calculation and from a fit to the measured PHENIX pp data – both scaled by the number of NN collisions. An important addition is the use of effective meson and baryon chemical potentials (rather than chemical equilibrium throughout the hadronic phase); this enhances photon production in the later hadronic stages, increasing v_2 . When the transverse acceleration of the fireball is increased from earlier $a_T=0.053c^2/\text{fm}$ to $a_T=0.12c^2/\text{fm}$, the photon spectrum is well described while v_2 is at the lower end of the systematic uncertainty band of the data⁷⁸.

The model has been updated in [282] by implementing a lattice-QCD based EOS, employing an ideal hydrodynamic model with non-vanishing initial flow, and introducing a “pseudo-critical” enhancement of the QGP and hadronic rates around $T_{pc} \approx 170$ MeV. Meson-meson Bremsstrahlung is also included. The results are compared to the PHENIX $\sqrt{s_{NN}}=200$ GeV Au+Au “thermal” photon spectra [96] and the updated v_2 and v_3 results [269] in Fig. 38. For both observables the calculations underpredict the data.

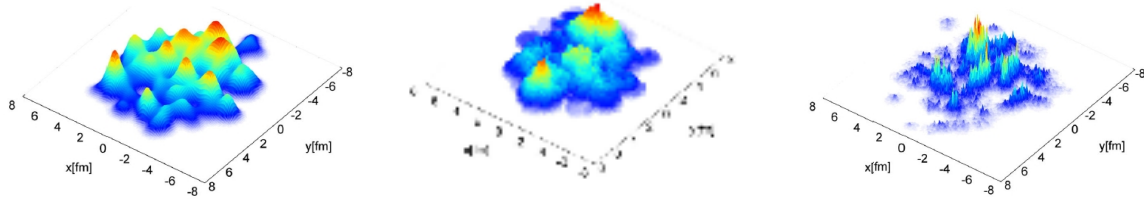


FIG. 37. Initial energy density (arbitrary units) in the transverse plane for a heavy ion collision using three different models. Left: MC Glauber. Middle: MC-KLN. Right: IP-Glasma. (Figure taken from [290].)

Ideal and viscous hydrodynamics

Elliptic flow of “thermal” photons using relativistic hydrodynamics has first been calculated in [299] assuming 0.2 fm/c thermalization time and 520 MeV initial temperature. Using the same (2+1)D hydrodynamic code in [73] the p_T range was extended by including hard processes (also in [72] it has been pointed out that at high p_T negative v_2 is expected for photons coming from jet-plasma interaction). Since no meaningful measurements of low p_T photon v_2 existed at the time, these can be considered predictions. Both calculations predicted the trend of photon v_2 first rising, then falling with p_T and essentially vanishing at high p_T , but grossly underestimated its magnitude, claiming that it will be significantly lower than the hadron v_2 .

Once it became obvious that from hadronic data estimates of η/s (shear viscosity to entropy density) ratio can be made, viscous relativistic hydro calculations became the rule. The space-time evolution of the system (and thus v_2) are obviously affected, but so are the rates, too. The effects of both shear and bulk viscosity on photon production has been studied for instance in [57, 309, 312]. Viscous corrections to the rates are small, particularly in the “thermal” region relevant here (they increase with p_T), but photon v_2 at low p_T is actually *suppressed* by 20-30%, making the “puzzle” even bigger.

Event-by-event hydrodynamics

Traditionally hydrodynamic calculations started with assuming smooth initial conditions, including geometry, a good starting point as long as the colliding ions are large, only the first few Fourier components are considered in azimuth *and* both nuclei are relatively large⁷⁹. Beyond that – and particularly for very asymmetric collisions, like $p/d+A$ – the fluctuating inner structure of the nucleus has to be taken into account on an event-by-event basis; the resulting initial density profile serves as an input to the hydro calculation. The initial configuration (density profile) can be obtained for instance with a Glauber Monte-Carlo [200]. CGC-inspired models include the early MC-KLN [327, 328], where no pre-thermal evolution of the gluons was considered, or the more recent impact-parameter dependent Glasma flux tube picture [290] (see Fig. 37). The EKRT model [329] combines the idea of gluon saturation with the dominance of few GeV jets (“mini-jets”) as principal sources of particle production [330], and also results in a “lumpy” initial state for the hydro evolution.

Assuming that thermal radiation is exponential in temperature and linear in radiating volume, initial “hotspots” from fluctuating initial conditions enhance photons at higher p_T , while the low p_T part of the

⁷⁸ An interesting consequence was the “disappearance of the QGP window”. In earlier models each of the three most important contributors to photon production – prompt radiation, thermal yields from the QGP and from the hadron phase have a characteristic p_T range where they dominate over other sources. Depending on the model, this “window” was somewhere in the 2-5 GeV/c p_T range, but in this model at maximum a_T (needed to reproduce the invariant yields) the QGP window virtually disappears.

⁷⁹ Even then, v_2 in the most central collisions is underpredicted if smooth initial conditions are chosen.

spectrum from the plasma is less effected, because it comes mostly from the volume-dominated, later plasma stage [331].

Applying event-by-event fluctuating initial conditions to Cu+Au collisions in [332] the authors argue that v_1 is more sensitive to the initial formation time of the plasma compared to v_2 , v_3 , and simultaneous measurement of v_1 , v_2 , v_3 in Cu+Au would be very helpful in clarifying the direct photon puzzle⁸⁰.

2. Initial state, (fast) thermalization

Glasma, slow chemical equilibration of quarks

Glasma is a conjectured transient state of matter between the initial state Color Glass Condensate or CGC [333] and the thermally equilibrated Quark-Gluon Plasma. In CGC most of the energy of the colliding nuclei is carried by gluons with a flat distribution up to relatively high momenta (the saturation momentum $Q_s \approx 2 \text{ GeV}/c$). Gluon splitting then provides the mechanism for early (gluon) thermalization [334], and recombination populates the high p_T gluon spectrum above $Q_s \approx 2 \text{ GeV}/c$. But to leading order quarks are needed to produce photons. Quarks are created via pair production from gluons and equilibrate later than gluons (typical times $0.8 \text{ fm}/c$ and $2 \text{ fm}/c$) [334, 335]. Photon emission from the Glasma has first been studied in [297] and shown that Glasma photon production can describe the centrality dependence of low p_T photon production (geometric scaling), and since quarks become substantial only at later stages of the Glasma, the photon v_2 also becomes higher [335], a step in the right direction, but the yields and v_2 are not adequately reproduced yet.

Bottom-up thermalization

There is little argument that the medium formed in A+A collisions becomes (locally) thermalized relatively fast⁸¹, but little is known about *how* this happens. In a 2001 paper [336] the “bottom-up” thermalization scenario was put forward to explain it. Assuming that the saturation momentum is high ($Q_s \gg \Lambda_{QCD}$) the basic idea was that early on ($\tau \approx \alpha^{-5/2} Q_s^{-1}$) emission of soft gluons dominate which quickly equilibrate and form a thermal bath, in which hard gluons lose their energy (and heat it further up) until about $\tau \approx \alpha^{-13/5} Q_s^{-1}$. Thermalization begins with the soft momentum modes. A very recent study [22] found that the “bottom-up” scenario (called BMSS) captures the correct physics of the glasma. Based on this it provides a parametric estimate of the pre-equilibrium photon production, claiming that at RHIC energies the glasma contribution is even *larger* than the thermal contribution from the QGP, particularly for more peripheral collisions (at LHC energies this is no longer true). This scenario might explain the large yields and the surprising observation that the effective temperatures barely change with collision centrality, but its effect on v_n is not studied yet.

3. Transport calculations

Parton-hadron-string dynamics (PHSD)

The parton-hadron-string dynamics (PHSD) model [274] “is an off-shell transport approach that consistently describes the full evolution of a relativistic heavy-ion collision from the initial hard scatterings and string formation through the dynamical deconfinement phase transition to the QGP as well as hadronization and the subsequent interactions in the hadronic phase.” [74]. Correspondingly, it is a skillful combination and extension of previous models describing various phases of the collision. Prompt photons (initial hard scattering) are calculated with standard pQCD. Description of the strongly interacting system out-of-equilibrium is based on the Kadanoff-Baym theory [337–339], transport description of equilibrated quarks and gluons is based on the dynamical quasiparticle model (DQPM) [340] that has nonvanishing widths of the partonic spectral functions⁸² and is tuned to match lQCD results for the QGP. For the hadronic sector the hadron-string dynamics (HSD) approach [342, 343] is used. Processes incorporated include hadron decays ($\pi^0 \rightarrow \gamma\gamma$,

⁸⁰ The prediction is that v_1 is negative at low p_T , and changes sign around $p_T = 2.5 \text{ GeV}/c$.

⁸¹ Somewhere in the range of $0.15\text{--}1 \text{ fm}/c$.

⁸² One of the consequences is that the evolution of the system closely resembles to that found in hydrodynamics with the same η/s and initial spatial eccentricity [341].

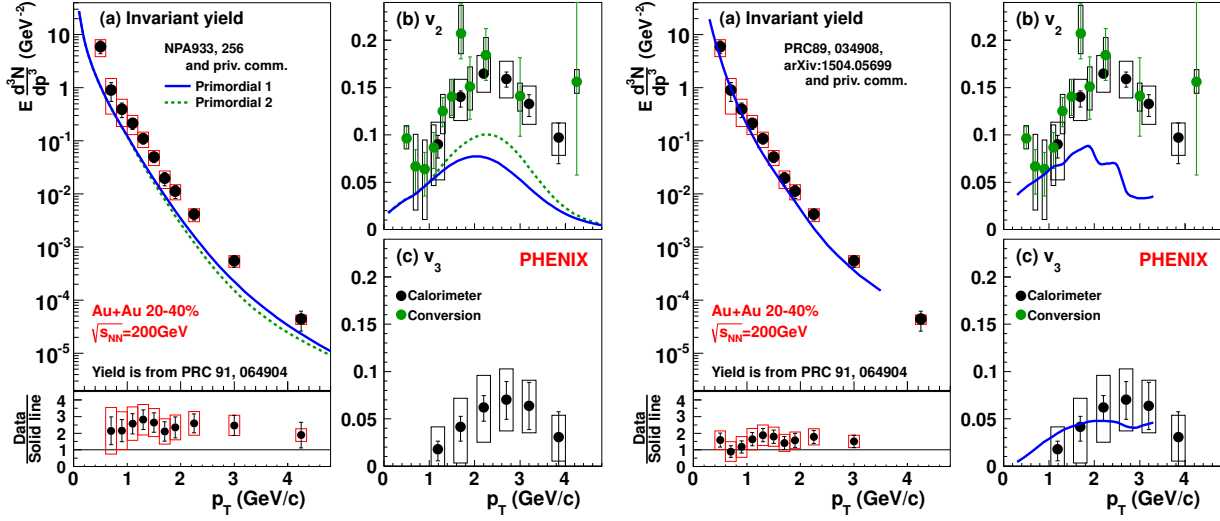


FIG. 38. (Left) Comparison of the direct photon yields [89] and the updated v_2 measurement [269] with the updated fireball model implementing pseudo-critical enhancement of thermal yields [282, 287]. The two curves for the yield and v_2 correspond to two different parametrizations of the prompt photon component as described in the text. (Figure taken from [269].) (Right) Comparison of the direct photon yields and v_2 , v_3 with the PHSD model [74, 291]. (Figure taken from [269].)

$\eta \rightarrow \gamma\gamma$, $\omega \rightarrow \pi^0 + \gamma$, $\eta' \rightarrow \pi^0 + \gamma$, $\phi \rightarrow \eta + \gamma$, $a_1 \rightarrow \pi^0 + \gamma$ ⁸³, their interactions ($\pi\pi \rightarrow \rho\gamma$, $\rho\pi \rightarrow \pi\gamma$), meson-meson and meson-baryon Bremsstrahlung ($m + m \rightarrow m + m + \gamma$, $m + B \rightarrow m + B + \gamma$), vector meson - nucleon interactions (like $V + p \rightarrow \gamma + p/n$), and the $\Delta \rightarrow N\gamma$ resonance decay. The Landau-Pomeranchuk-Migdal (LPM) effect [344], suppressing radiative photon production in dense systems due to coherence, is studied and found to influence the total yields from the QGP below 0.4 GeV, but negligible for photons from the hadronic phase. – Similarly, v_2 (v_n) is the weighted sum of the “partial flow” from the individual photon sources

$$v_n(\gamma) = \sum_i v_n(\gamma^i) w_i(p_T)$$

where the summation goes over the various processes i and $w_i(p_T)$ is the relative contribution of process i at a given p_T ($N_i(p_T)/\sum_i N_i(p_T)$). – Quantitatively, almost half of the total direct photon yield in PHSD is produced in the QGP [74]. The corresponding partial v_2 is small, and not fully compensated by the large v_2 of photons from the hadronic phase. On the other hand v_3 (“triangular flow”) is manifestly non-zero and consistent with the data at low p_T . Comparisons to PHENIX data in mid-central Au+Au collisions are shown in Fig. 38. The yield is well reproduced down to the lowest p_T , but v_2 is underpredicted except at the lowest p_T where radiation from hadrons and Bremsstrahlung is expected to dominate.

Hybrid approaches

Hybrid approaches are an excellent, pragmatic solution to the problem that various stages of the collision, like the initial stage and formation of a (thermal) medium, then the space-time evolution of this medium, and the late stages before complete kinetic freeze-out can each be most conveniently described in a different framework. The centerpiece is typically a relativistic viscous hydrodynamics code describing the evolution of the medium (for instance MUSIC [345, 346]), sufficiently modular to accept various inputs for the initial (and pre-thermal) state, instantaneous rate models, and “afterburners” for photon production by hadrons in the post-hydro era. One typical incarnation is the calculation in [289] where the initial state is determined with the IP-Glasma model, and the afterburner for hadronic rescattering is the ultrarelativistic quantum molecular dynamics (UrQMD) code. A similar scheme is applied for (“thermal”) photons in [57]; the photon emission rates used are from [70, 347, 348]. The calculations include corrections for both bulk and shear viscosity, and underestimate both the spectrum and v_2 (viscosity softens the spectra somewhat, and decreases v_2 significantly). Late stage emission (from UrQMD) on the other hand increases direct photon v_2 [57].

⁸³ The model includes *all* hadron decay photons, including those that experiments subtract, like π^0 and η ; for comparisons with measured data these obviously have to be subtracted. An advantage of calculating all photon contributions in the same framework is that when comparing to data, the exact same contributions can be discarded that have been subtracted by the particular experiment. This is true for both the yields and v_n .

Coarse graining is a method to overcome the difficulties that electromagnetic emissivities are typically calculated near thermal equilibrium, but transport formulations usually don't provide local temperatures [57]. Instead, the transport final states are divided into cells on a space-time grid (coarse grained) and local temperatures assigned using the equation of state [48, 349].

Boltzmann approach to multiparton scattering (BAMPS)

The Boltzmann approach to multiparton scattering (BAMPS) has been introduced in [350] as a 3+1 dimensional Monte Carlo cascade for on-shell partons obeying the relativistic Boltzmann equations. In a recent study [276] of nonequilibrium photon production with BAMPS finds that it is larger than that of the QGP, the spectra are harder. This is mainly due to scatterings of energetic jet-like partons with the medium⁸⁴. So far only the QGP has been studied in [276], and with a special set of initial conditions, where gluons dominate and quarks are produced by inelastic scattering, delaying their appearance. Therefore, the yields are far below what traditional hydro codes or a full transport simulation (PHSD) would give. Nevertheless there are three important partial lessons to be learned for nonequilibrium processes in the QGP proper. First, nonequilibrium spectra are harder than thermal ones. Second, $2 \rightarrow 3$ processes are important, almost on par with $2 \rightarrow 2$ processes at 2-3 GeV/c. Third, using running α_s rather than $\alpha_s = 0.3$ fixed, increases the yield by almost a factor of 2. Finally, the v_2 of these “BAMPS photons” is actually *negative*, aggravating, instead of alleviating the v_2 problem.

“No dark age” – Abelian flux tube model

The role of photons from the early stages of the collision (pre-equilibrium) is examined in [275] using the Abelian flux tube model (AFTm) to define the initial gluon fields and their evolution into the QGP. The fast decay of the fields results in quarks and gluons, which in turn scatter and produce photons very efficiently early on, before the QGP is formed. The model is somewhat similar to the “bottom-up thermalization”, but it is embedded into a relativistic transport code and follows the dynamical evolution of the system up to freeze-out. The processes implemented in the collision integral are the basic $2 \rightarrow 2$ processes as shown in Fig. 2 with cross-sections as in Eqs. 1 and 2 with $m = 0$, modified by a temperature-dependent overall factor $\Phi(T)$ to account for higher order (radiative) processes. $\Phi(T)$ is chosen such that the overall AMY production rate [56] is reproduced when the system is in the equilibrated QGP phase. The final number of quarks and gluons with this AFTm initialization is the same as with a traditional Glauber initialization for hydro (equilibrium assumed at $t_0 \approx 0.6$ fm/c), but due to early appearance of quarks the photon radiation with AFTm is about 30% higher at RHIC energies than that obtained with the Glauber model. At $p_T \approx 2$ GeV/c the contribution of early stage photons is comparable to the yields from the fully formed QGP, in other words, there is “no dark age”, the early stage is quite bright. The calculated photon spectrum from the QGP at RHIC energies is compared to other transport calculations. PHSD [74] is consistent with AFTm at higher p_T (2 GeV/c and above), but exceeds AFTm below that. BAMPS [276], in contrast, falls below AFTm in the entire $0.5 < p_T < 3$ GeV/c range due to the delayed appearance of quarks and thus reduced emission of photons. Note that currently AFTm does not address the question of direct photon v_2 , but due to the early production it would presumably underpredict the data.

4. Other ideas

“Semi-QGP”

The transition from QGP to hadron gas, now widely believed to be a cross-over, happens around a critical temperature T_c . High above T_c perturbative methods can be used, at lower temperatures hadronic models are valid, but near T_c both approaches break down. In order to understand the transition to confinement the degree of ionization of the color charge, characterized by the expectation value of the Polyakov loop is used [351, 352]. The Polyakov loop is unity (full ionization of color charge) at $T \gg T_c$, but decreases as $T \rightarrow T_c^+$, because color fields gradually evaporate and are replaced by color singlet excitations (hadrons). This intermediate state is called “semi-QGP” and its effects on “thermal” photon production and v_2 are studied in [313]. The conclusion is that the net yield from the QGP phase decreases, but at the same time the total v_2 is enhanced, since relatively more photons come from the hadronic phase, where the instantaneous v_2 is maximum. Results for yield, v_2 and v_3 calculated with this model are shown as dashed red curves in

⁸⁴ Similar to “jet-photon conversion”, discussed in Sec. IV B 4.

Fig. 34. The yield is still low, as is v_2 , and, more significantly, the maximum of v_2 is at much lower p_T than in the data. The authors themselves point out that photons from parton fragmentation should be included⁸⁵ and that the semi-QGP addresses only the $T \rightarrow T_c^+$ region, but not the possibly enhanced production in the hadronic phase, claimed for instance in [353].

Early v_2 from photons in presence of a magnetic field.

An interesting scenario has been put forward in [354] to circumvent the problem that momentum anisotropies need time to build up, therefore, early “thermal” photons will have little v_2 . The existence of a strong magnetic field in non-central heavy ion collisions has long been conjectured and its effect on both photon production and anisotropy studied for weak coupling in [298]. For a strongly coupled plasma the AdS/CFT correspondence is used in [354]. The authors find that – due to the magnetic field – photons with in-plane or out-of-plane polarization acquire different v_2 . Actually, photons with out-of-plane polarization photons will have very large positive v_2 as $p_T \rightarrow 0$, making this an unusual scenario (but also proposed in [355]) where the photon v_2 does not vanish at low p_T . However, the authors themselves warn that “the v_2 obtained in our model should be regarded as the upper bound generated solely by a magnetic field in the strongly coupled scenario” and for the full observed v_2 contributions from viscous hydrodynamics should be added. Moreover, if the strong initial magnetic field were really the principal source of large photon v_2 , then v_3 should be zero in first approximation [356], in contrast to currently available data (see Fig. 30). – A recent study [24] calculates photon production at early times from nonequilibrium gluon fusion induced by magnetic field⁸⁶ and finds that both the low p_T yields and v_2 are enhanced, mostly below 1 GeV/c, a trend not incompatible with the data in Fig. 30. However, the uncertainties on the data points are too large – a problem that ongoing analyses of much larger datasets will hopefully solve.

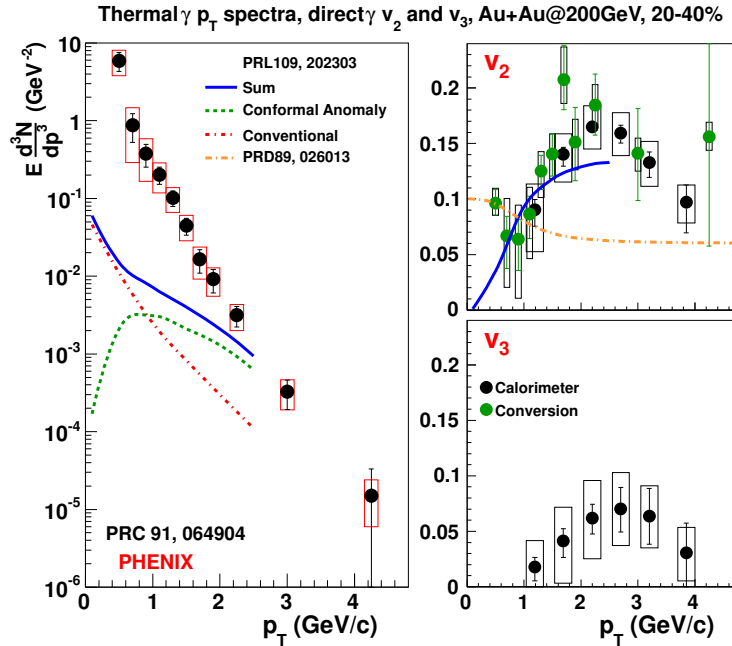


FIG. 39. Yield and anisotropy in models that include strong initial magnetic field. Calculations of the yield (conformal, conventional and sum as solid blue line) are based on [298] where the respective v_2 is also calculated. The yellow dash-dotted curve for v_2 is from [354] where yield estimates are not given. Note that for models where v_2 is due to magnetic field effects, v_3 is zero.

⁸⁵ This would enhance the yields, but not necessarily v_2 , since the jet axis does not necessarily have to coincide with the v_2 plane.

⁸⁶ A process otherwise forbidden due to charge conjugation invariance, and made possible only by the presence of the magnetic field.

VII. CONCLUDING REMARKS

Disclaimer

So far the author tried to provide a comprehensive, balanced review of the field, as free of any personal bias or preference as possible. In contrast, this last section is strictly personal; it will not necessarily reflect the consensus or even majority opinion of the field, nor is it intended to do so.

Direct photons in heavy ion collisions: promises kept, broken – and open

Let us recapitulate some major “promises” of direct photons in studying the physics of heavy ion collisions in the past decades – which expectations were fulfilled, which were not, and which are the ones where “the jury is still out”.

Validating the use of the Glauber-model in large-on-large ion collisions, proof of sanity of the concept of N_{coll} and the way it is calculated is a major success: at large p_T the direct photon R_{AA} is indeed around unity (see Sec IV B 3). Based on this there is a strong hope that photons (or other electromagnetic probes) will solve the problem of “centrality” biases in small-on-large collisions, and separate genuine new high p_T physics from experimental artifacts. (measuring $d + d$ collisions would be of additional help). In summary, *the promise to be a reliable reference for the initial geometry was kept.*

Using photons in back-to-back photon-jet measurements to set the initial (unquenched) parton energy scale is ongoing (see Sec. IV B 5), there are some early successes and no indication of problems with the method so far. *The promise to be the ultimate parton energy calibration tool was kept.*

In both cases above the probes involved are high p_T photons. For low p_T the situation is somewhat less clear.

Establishing the temperature at initial thermalization time τ_0 remained elusive; the reasons are described in Sec. V B 1 and illustrated in Figs. 20 and 21, left panel. The space-time integral of strongly varying rates smears out all information on the initial state. While dileptons may provide somewhat more differential information⁸⁷, *the promise to measure initial temperature using real photons is broken.*

Thermal radiation from the QGP was thought to be the dominant low p_T photon source up to the early 90’s, and even after that most models indicated that there is a “QGP window”, a range in the p_T spectrum where the bulk of the photons come from the QGP, *i.e.* reflect its properties. As we discussed in Sec. VI D, with the observation of large photon v_2 radiation from the QGP (at least from its “classic” form) became more and more deprecated, so it is fair to say that *the promise to study the QGP via its directly observed thermal radiation is broken.*

In [309, 312] it has been pointed out that the direct photon v_2/v_3 ratio can serve as a “viscometer” of the QGP (see Sec. VI A), particularly when compared to the corresponding ratio for charged hadrons. Current experimental uncertainties do not allow to draw conclusions yet, but significant improvements are expected in the near future, so *the promise to put constraints on the early values (and maybe the time evolution) of η/s remains open.*

The role of a large, albeit short-lived, magnetic field created in non-central collisions is actively investigated both theoretically and experimentally. As discussed in Sec. VI D 4, it may help to enhance both the photon yield and v_2 at early times, alleviating the “direct photon puzzle”. One of the scenarios even predicts large positive v_2 as $p_T \rightarrow 0$, a tantalizing possibility disfavored, but not conclusively excluded by the available data. At this point *the promise to provide independent information on the initial magnetic field is still open.*

The fine structure of the initial energy density distribution plays a decisive role in any hydrodynamic calculation. Even for collisions in the same centrality class the positions of the nucleons fluctuate event-by-event, giving rise to odd harmonics in the v_n expansion. The energy density attributed to each binary collision fluctuates, too, it is model-dependent (see Fig. 37), and its actual shape affect both the final spectra and v_n [290]. This topic will be even more important as the study of very asymmetric collisions, as well as pp , A+A collisions with extremely high or low multiplicity intensifies. Uncertainties of current published results do not allow yet to differentiate between scenarios, but *the promise to provide information on the initial state is still open.*

⁸⁷ Inverse p_T slopes *vs* pair mass can meaningfully differentiate between early and late times [16].

HBT-correlations to measure the size and shape of the system (“femtoscopy”) were immensely successful for hadronic observables, but those reflect (mostly) the status at freeze-out time. Since high p_T photons are created very early, they could provide unique information on the geometry at the initial time. This potential of high p_T photon HBT has already been pointed out in [111], but so far not attempted in any of the experiments, not the least because it requires huge statistics. Nonetheless, there are indications that at LHC it might be feasible [158], so *the promise to provide a direct view of the geometry at earliest times is still open*.

As stated repeatedly, by their penetrating nature direct photons are “historians” of the entire collision, including the dynamics of the expansion. However, decyphering their *space-time integrated* message is very model-dependent so far. As discussed in Sec. VI, none of the models describes simultaneously all real photon observables, nor embeds them into an all-encompassing “standard model” of heavy ion collisions. There is substantial progress both in microscopic transport and hydrodynamic models, as is in understanding of the role of the initial state, thanks to the copious $p/d+A$ data, but a uniform picture is still elusive. Both theorists and experimentalists have to overcome huge challenges before such picture can be drawn. Eventually we will succeed. Until then, *the journey is just as exciting and fascinating as the arrival will be*.

Quo vadis, direct photon?

There is a wide consensus in the field that direct photons, being penetrating probes, are unique tools to report on the entire history of the space-time evolution in heavy ion collisions, but also, for the very same reason they are singularly hard to interpret. In light of this, it is quite unfortunate that so far there was not a single experiment fully optimized for real photon measurements⁸⁸. While almost all current experiments have real photon capabilities, photons are only part of a much larger program, not the main (or single) focus, thus none of the detectors are without compromises from the point of view of direct photon measurements.⁸⁹ One consequence is larger systematic uncertainties than state-of-the-art technology would allow to achieve, *i.e.* less power to reject some models. A very recent proposal [358] to install a “near-massless” detector in IP2 of the LHC during Long Shutdown 4 is an important step, hopefully successful, to remedy the situation.

Another issue is that independent confirmation of certain results (by a different experiment) is often impossible. This is particularly true for low p_T (“thermal”) photons, which are the richest in information, but hardest to interpret theoretically. Also, the external (and internal) drive to constantly move to uncharted territories and discover new phenomena sometimes overshadows the need to thoroughly explore and exploit previous discoveries to their full depth and potential. Science lives on new ideas but may die on insufficiently tested old ones. *Sapienti sat*.

VIII. ACKNOWLEDGEMENTS

The author greatly acknowledges decades of fruitful cooperation, enlightening discussions and unwavering friendship of Peter Braun-Munzinger, Axel Drees, Charles Gale, Abhijit Majumder, Norbert Novitzky, agdm, Klaus Reygers, Takao Sakaguchi, Johanna Stachel and Michael J. Tannenbaum.

⁸⁸ Dileptons fared somewhat better, and it almost immediately paid off: NA60, the current standard in precision measurements quickly decided the decades-long argument on the fate of the ρ in the medium [357].

⁸⁹ This is true even if one takes into account the benefits of measuring simultaneously the hadron spectra, a huge and irreducible source of background for direct photon measurements.

-
- [1] A. S. Goldhaber and H. H. Heckman, “High-Energy Interactions of Nuclei,” *Ann. Rev. Nucl. Part. Sci.* **28**, 161–205 (1978).
 - [2] Gordon Baym, “Ultrarelativistic heavy ion collisions: the first billion seconds,” *Proceedings, 25th International Conference on Ultra-Relativistic Nucleus-Nucleus Collisions (Quark Matter 2015): Kobe, Japan, September 27-October 3, 2015*, *Nucl. Phys.* **A956**, 1–10 (2016), arXiv:1701.03972 [nucl-ex].
 - [3] Enrico Fermi, “On the theory of collisions between atoms and electrically charged particles,” *Electromagnetic probes of fundamental physics. Proceedings, Workshop, Erice, Italy, October 16-21, 2001*, *Nuovo Cim.* **2**, 143–158 (1925), [243(1925)], arXiv:hep-th/0205086 [hep-th].
 - [4] L. Meitner and H. Kosters, “Über die streuung kurzweiliger γ -strahlen.” *Z. Phys.* **84**, 137 (1933).
 - [5] W. Heisenberg, “Remarks on the Dirac theory of the positron (Folgerungen aus der Diracschen Theorie des Positrons),” (1936), [*Z. Phys.*98,714(1936)].
 - [6] F. E. Low, “Bremsstrahlung of very low-energy quanta in elementary particle collisions,” *Phys. Rev.* **110**, 974–977 (1958).
 - [7] C. O. Escobar, “Photoproduction of Large Transverse Momentum Mesons and Production of Large Transverse Momentum Photons and Leptons in Proton Proton Collisions,” *Nucl. Phys.* **B98**, 173–188 (1975).
 - [8] Glennys R. Farrar and Steven C. Frautschi, “Copious Direct Photon Production as a Possible Resolution of the Prompt Lepton Puzzle,” *Phys. Rev. Lett.* **36**, 1017 (1976).
 - [9] E. L. Feinberg, “Direct Production of Photons and Dileptons in Thermodynamical Models of Multiple Hadron Production,” *Nuovo Cim.* **A34**, 391 (1976).
 - [10] Edward V. Shuryak, “Quark-Gluon Plasma and Hadronic Production of Leptons, Photons and Psions,” *Phys. Lett.* **78B**, 150 (1978), [*Yad. Fiz.*28,796(1978)].
 - [11] T. Ferbel and W. R. Molzon, “Direct Photon Production in High-Energy Collisions,” *Rev. Mod. Phys.* **56**, 181–221 (1984).
 - [12] J. Alam, B. Sinha, and S. Raha, “Electromagnetic probes of quark gluon plasma,” *Phys. Rept.* **273**, 243–362 (1996).
 - [13] W. Cassing and E. L. Bratkovskaya, “Hadronic and electromagnetic probes of hot and dense nuclear matter,” *Phys. Rept.* **308**, 65–233 (1999).
 - [14] Thomas Peitzmann and Markus H. Thoma, “Direct photons from relativistic heavy ion collisions,” *Phys. Rept.* **364**, 175–246 (2002), arXiv:hep-ph/0111114 [hep-ph].
 - [15] P. Stankus, “Direct photon production in relativistic heavy-ion collisions,” *Ann. Rev. Nucl. Part. Sci.* **55**, 517–554 (2005).
 - [16] G. David, R. Rapp, and Z. Xu, “Electromagnetic Probes at RHIC-II,” *Phys. Rept.* **462**, 176–217 (2008), arXiv:nucl-ex/0611009 [nucl-ex].
 - [17] O. Linnyk, E. L. Bratkovskaya, and W. Cassing, “Effective QCD and transport description of dilepton and photon production in heavy-ion collisions and elementary processes,” *Prog. Part. Nucl. Phys.* **87**, 50–115 (2016), arXiv:1512.08126 [nucl-th].
 - [18] K. Adcox *et al.* (PHENIX), “Suppression of hadrons with large transverse momentum in central Au+Au collisions at $\sqrt{s_{NN}} = 130$ -GeV,” *Phys. Rev. Lett.* **88**, 022301 (2002), arXiv:nucl-ex/0109003 [nucl-ex].
 - [19] J. F. Owens, “Large Momentum Transfer Production of Direct Photons, Jets, and Particles,” *Rev. Mod. Phys.* **59**, 465 (1987).
 - [20] Edward V. Shuryak and L. Xiong, “Dilepton and photon production in the ‘hot glue’ scenario,” *Phys. Rev. Lett.* **70**, 2241–2244 (1993), arXiv:hep-ph/9301218 [hep-ph].
 - [21] Larry McLerran and Bjoern Schenke, “The Glasma, Photons and the Implications of Anisotropy,” *Nucl. Phys.* **A929**, 71–82 (2014), arXiv:1403.7462 [hep-ph].
 - [22] Jurgen Berges, Klaus Reygers, Naoto Tanji, and Raju Venugopalan, “Parametric estimate of the relative photon yields from the glasma and the quark-gluon plasma in heavy-ion collisions,” *Phys. Rev.* **C95**, 054904 (2017), arXiv:1701.05064 [nucl-th].
 - [23] Kirill Tuchin, “Photon decay in strong magnetic field in heavy-ion collisions,” *Phys. Rev.* **C83**, 017901 (2011), arXiv:1008.1604 [nucl-th].
 - [24] Alejandro Ayala, Jorge David Castano-Yepes, Cesareo A. Dominguez, Luis A. Hernandez, Saul Hernandez-Ortiz, and Maria Elena Tejeda-Yeomans, “Prompt photon yield and elliptic flow from gluon fusion induced by magnetic fields in relativistic heavy-ion collisions,” *Phys. Rev.* **D96**, 014023 (2017), [Erratum: *Phys. Rev. D*96,no.11,119901(2017)], arXiv:1704.02433 [hep-ph].
 - [25] B. G. Zakharov, “Synchrotron contribution to photon emission from quark-gluon plasma,” *JETP Lett.* **104**, 213–217 (2016), [*Pisma Zh. Eksp. Teor. Fiz.*104,no.4,215(2016)], arXiv:1607.04314 [hep-ph].
 - [26] O. Linnyk, V. P. Konchakovski, W. Cassing, and E. L. Bratkovskaya, “Photon elliptic flow in relativistic heavy-ion collisions: hadronic versus partonic sources,” *Phys. Rev.* **C88**, 034904 (2013), arXiv:1304.7030 [nucl-th].
 - [27] Chun Shen, Ulrich W Heinz, Jean-Francois Paquet, and Charles Gale, “Thermal photons as a quark-gluon plasma thermometer reexamined,” *Phys. Rev.* **C89**, 044910 (2014), arXiv:1308.2440 [nucl-th].
 - [28] Jean-Francois Paquet, “Probing the space-time evolution of heavy ion collisions with photons and dileptons,” *Proceedings, 26th International Conference on Ultra-relativistic Nucleus-Nucleus Collisions (Quark Matter 2017): Chicago, Illinois, USA, February 5-11, 2017*, *Nucl. Phys.* **A967**, 184–191 (2017), arXiv:1704.07842 [nucl-th].
 - [29] Joseph I. Kapusta, P. Lichard, and D. Seibert, “High-energy photons from quark - gluon plasma versus hot hadronic gas,” *Phys. Rev.* **D44**, 2774–2788 (1991), [Erratum: *Phys. Rev. D*47,4171(1993)].
 - [30] M. Gluck, E. Reya, and A. Vogt, “Parton fragmentation into photons beyond the leading order,” *Phys. Rev.* **D48**, 116 (1993), [Erratum: *Phys. Rev. D*51,1427(1995)].

- [31] L. Bourhis, M. Fontannaz, and J. P. Guillet, “Quarks and gluon fragmentation functions into photons,” *Eur. Phys. J.* **C2**, 529–537 (1998), arXiv:hep-ph/9704447 [hep-ph].
- [32] Patrick Aurenche, Michel Fontannaz, Jean-Philippe Guillet, Eric Pilon, and Monique Werlen, “A New critical study of photon production in hadronic collisions,” *Phys. Rev.* **D73**, 094007 (2006), arXiv:hep-ph/0602133 [hep-ph].
- [33] Michael Klasen and F. Knig, “New information on photon fragmentation functions,” *Eur. Phys. J.* **C74**, 3009 (2014), arXiv:1403.2290 [hep-ph].
- [34] Rainer J. Fries, Berndt Muller, and Dinesh K. Srivastava, “High-energy photons from passage of jets through quark gluon plasma,” *Phys. Rev. Lett.* **90**, 132301 (2003), arXiv:nucl-th/0208001 [nucl-th].
- [35] Thorsten Renk, “Photon Emission from a Medium-Modified Shower Evolution,” *Phys. Rev.* **C88**, 034902 (2013), arXiv:1304.7598 [hep-ph].
- [36] Kevin Lee Haglin, “Rate of photon production from hot hadronic matter,” *J. Phys.* **G30**, L27–L33 (2004), arXiv:hep-ph/0308084 [hep-ph].
- [37] W. Liu and R. Rapp, “Low-energy thermal photons from meson-meson bremsstrahlung,” *Nucl. Phys.* **A796**, 101–121 (2007), arXiv:nucl-th/0604031 [nucl-th].
- [38] Georges Aad *et al.* (ATLAS), “Centrality, rapidity and transverse momentum dependence of isolated prompt photon production in lead-lead collisions at $\sqrt{s_{NN}} = 2.76$ TeV measured with the ATLAS detector,” *Phys. Rev.* **C93**, 034914 (2016), arXiv:1506.08552 [hep-ex].
- [39] E. L. Bratkovskaya, S. M. Kiselev, and G. B. Sharikov, “Direct photon production from hadronic sources in high-energy heavy-ion collisions,” *Phys. Rev.* **C78**, 034905 (2008), arXiv:0806.3465 [nucl-th].
- [40] L. Xiong, Edward V. Shuryak, and G. E. Brown, “Photon production through A1 resonance in high-energy heavy ion collisions,” *Phys. Rev.* **D46**, 3798–3801 (1992), arXiv:hep-ph/9208206 [hep-ph].
- [41] C.-Y. Wong, *Introduction to High-Energy Heavy-Ion Collisions* (World Scientific, Singapore, 1994) p. 422.
- [42] Andreas Metz and Anselm Vossen, “Parton Fragmentation Functions,” *Prog. Part. Nucl. Phys.* **91**, 136–202 (2016), arXiv:1607.02521 [hep-ex].
- [43] John C. Collins, Davison E. Soper, and George F. Sterman, “Factorization of Hard Processes in QCD,” *Adv. Ser. Direct. High Energy Phys.* **5**, 1–91 (1989), arXiv:hep-ph/0409313 [hep-ph].
- [44] Raymond Brock *et al.* (CTEQ), “Handbook of perturbative QCD: Version 1.0,” *Rev. Mod. Phys.* **67**, 157–248 (1995).
- [45] P. Aurenche, A. Douiri, R. Baier, M. Fontannaz, and D. Schiff, “Prompt Photon Production at Large p(T) in QCD Beyond the Leading Order,” *Phys. Lett.* **140B**, 87–92 (1984).
- [46] P. Aurenche, R. Baier, M. Fontannaz, J. F. Owens, and M. Werlen, “The Gluon Contents of the Nucleon Probed with Real and Virtual Photons,” *Phys. Rev.* **D39**, 3275 (1989).
- [47] “Jetphox,” https://lapth.cnrs.fr/PHOX_FAMILY/jetphox.html (2009).
- [48] P. Huovinen, M. Belkacem, P. J. Ellis, and Joseph I. Kapusta, “Dileptons and photons from coarse grained microscopic dynamics and hydrodynamics compared to experimental data,” *Phys. Rev.* **C66**, 014903 (2002), arXiv:nucl-th/0203023 [nucl-th].
- [49] H. Arthur Weldon, “Simple Rules for Discontinuities in Finite Temperature Field Theory,” *Phys. Rev.* **D28**, 2007 (1983).
- [50] Larry D. McLerran and T. Toimela, “Photon and Dilepton Emission from the Quark - Gluon Plasma: Some General Considerations,” *Phys. Rev.* **D31**, 545 (1985).
- [51] Charles Gale and Joseph I. Kapusta, “Vector dominance model at finite temperature,” *Nucl. Phys.* **B357**, 65–89 (1991).
- [52] Eric Braaten and Robert D. Pisarski, “Soft Amplitudes in Hot Gauge Theories: A General Analysis,” *Nucl. Phys.* **B337**, 569–634 (1990).
- [53] P. Aurenche, F. Gelis, R. Kobes, and H. Zaraket, “Bremsstrahlung and photon production in thermal QCD,” *Phys. Rev.* **D58**, 085003 (1998), arXiv:hep-ph/9804224 [hep-ph].
- [54] P. Aurenche, F. Gelis, and H. Zaraket, “KLN theorem, magnetic mass, and thermal photon production,” *Phys. Rev.* **D61**, 116001 (2000), arXiv:hep-ph/9911367 [hep-ph].
- [55] P. Aurenche, F. Gelis, and H. Zaraket, “Landau-Pomeranchuk-Migdal effect in thermal field theory,” *Phys. Rev.* **D62**, 096012 (2000), arXiv:hep-ph/0003326 [hep-ph].
- [56] Peter Brockway Arnold, Guy D. Moore, and Laurence G. Yaffe, “Photon emission from quark gluon plasma: Complete leading order results,” *JHEP* **12**, 009 (2001), arXiv:hep-ph/0111107 [hep-ph].
- [57] Jean-Francois Paquet, Chun Shen, Gabriel S. Denicol, Matthew Luzum, Björn Schenke, Sangyong Jeon, and Charles Gale, “Production of photons in relativistic heavy-ion collisions,” *Phys. Rev.* **C93**, 044906 (2016), arXiv:1509.06738 [hep-ph].
- [58] Gokce Basar, Dmitri E. Kharzeev, Ho-Ung Yee, and Ismail Zahed, “Interplay of Reggeon and photon in pA collisions,” *Phys. Rev.* **D95**, 126005 (2017), arXiv:1703.06078 [nucl-th].
- [59] J. D. Bjorken, “Highly Relativistic Nucleus-Nucleus Collisions: The Central Rapidity Region,” *Phys. Rev.* **D27**, 140–151 (1983).
- [60] S. Z. Belenkij and L. D. Landau, “Hydrodynamic theory of multiple production of particles,” *Nuovo Cim. Suppl.* **3S10**, 15 (1956), [*Usp. Fiz. Nauk*56,309(1955)].
- [61] Enrico Fermi, “Angular Distribution of the Pions Produced in High Energy Nuclear Collisions,” *Phys. Rev.* **81**, 683–687 (1951).
- [62] R. Rapp and J. Wambach, “Chiral symmetry restoration and dileptons in relativistic heavy ion collisions,” *Adv. Nucl. Phys.* **25**, 1 (2000), arXiv:hep-ph/9909229 [hep-ph].
- [63] Chungsik Song, “Photon emission from hot hadronic matter described by an effective chiral Lagrangian,” *Phys. Rev.* **C47**, 2861–2874 (1993).

- [64] James V. Steele, Hidenaga Yamagishi, and Ismail Zahed, “Dilepton and photon emission rates from a hadronic gas,” *Phys. Lett.* **B384**, 255–262 (1996), arXiv:hep-ph/9603290 [hep-ph].
- [65] S. A. Bass and A. Dumitru, “Dynamics of hot bulk QCD matter: From the quark gluon plasma to hadronic freezeout,” *Phys. Rev.* **C61**, 064909 (2000), arXiv:nucl-th/0001033 [nucl-th].
- [66] A. Dumitru, U. Katscher, J. A. Maruhn, Horst Stoecker, W. Greiner, and D. H. Rischke, “Pion and thermal photon spectra as a possible signal for a phase transition,” *Phys. Rev.* **C51**, 2166–2170 (1995), arXiv:hep-ph/9411358 [hep-ph].
- [67] J. Cleymans, K. Redlich, and D. K. Srivastava, “Thermal particle and photon production in pb + pb collisions with transverse flow,” *Phys. Rev.* **C55**, 1431–1442 (1997), arXiv:nucl-th/9611047 [nucl-th].
- [68] K. Gallmeister, Burkhard Kampfer, and O. P. Pavlenko, “A Unique large thermal source of real and virtual photons in the reactions Pb-158-A/GeV + Pb, Au,” *Phys. Rev.* **C62**, 057901 (2000), arXiv:hep-ph/0006134 [hep-ph].
- [69] M. M. Aggarwal *et al.* (WA98), “Observation of direct photons in central 158-A-GeV Pb-208 + Pb-208 collisions,” *Phys. Rev. Lett.* **85**, 3595–3599 (2000), arXiv:nucl-ex/0006008 [nucl-ex].
- [70] Simon Turbide, Ralf Rapp, and Charles Gale, “Hadronic production of thermal photons,” *Phys. Rev.* **C69**, 014903 (2004), arXiv:hep-ph/0308085 [hep-ph].
- [71] Simon Turbide, Charles Gale, Sangyong Jeon, and Guy D. Moore, “Energy loss of leading hadrons and direct photon production in evolving quark-gluon plasma,” *Phys. Rev.* **C72**, 014906 (2005), arXiv:hep-ph/0502248 [hep-ph].
- [72] Simon Turbide, Charles Gale, and Rainer J. Fries, “Azimuthal Asymmetry of Direct Photons in High Energy Nuclear Collisions,” *Phys. Rev. Lett.* **96**, 032303 (2006), arXiv:hep-ph/0508201 [hep-ph].
- [73] Simon Turbide, Charles Gale, Evan Frodermann, and Ulrich Heinz, “Electromagnetic radiation from nuclear collisions at ultrarelativistic energies,” *Phys. Rev.* **C77**, 024909 (2008), arXiv:0712.0732 [hep-ph].
- [74] O. Linnyk, V. Konchakovski, T. Steinert, W. Cassing, and E. L. Bratkovskaya, “Hadronic and partonic sources of direct photons in relativistic heavy-ion collisions,” *Phys. Rev.* **C92**, 054914 (2015), arXiv:1504.05699 [nucl-th].
- [75] Johann Rafelski, “Melting Hadrons, Boiling Quarks,” *Eur. Phys. J.* **A51**, 114 (2015), arXiv:1508.03260 [nucl-th].
- [76] T. Matsui and H. Satz, “ J/ψ Suppression by Quark-Gluon Plasma Formation,” *Phys. Lett.* **B178**, 416–422 (1986).
- [77] K. Kajantie and H. I. Miettinen, “Temperature Measurement of Quark-Gluon Plasma Formed in High-Energy Nucleus-Nucleus Collisions,” *Z. Phys.* **C9**, 341 (1981).
- [78] F. Halzen and H. C. Liu, “Experimental Signatures of Phase Transition to Quark Matter in High-energy Collisions of Nuclei,” *Phys. Rev.* **D25**, 1842 (1982).
- [79] Frank D. Steffen and Markus H. Thoma, “Hard thermal photon production in relativistic heavy ion collisions,” *Phys. Lett.* **B510**, 98–106 (2001), [Erratum: *Phys. Lett.* B660,604(2008)], arXiv:hep-ph/0103044 [hep-ph].
- [80] Dinesh Kumar Srivastava, “Photon production in relativistic heavy ion collisions using rates with two loop calculations from quark matter,” *Eur. Phys. J.* **C10**, 487–490 (1999), [Erratum: *Eur. Phys. J.* C20,399(2001)], arXiv:nucl-th/0103023 [nucl-th].
- [81] Dinesh Kumar Srivastava and Bikash Chandra Sinha, “A Second look at single photon production in S + Au collisions at 200-A/GeV and implications for quark hadron phase transition,” *Eur. Phys. J.* **C12**, 109–112 (2000), [Erratum: *Eur. Phys. J.* C20,397(2001)], arXiv:nucl-th/9906057 [nucl-th].
- [82] A. Adare *et al.* (PHENIX), “Observation of direct-photon collective flow in $\sqrt{s_{NN}} = 200$ GeV Au+Au collisions,” *Phys. Rev. Lett.* **109**, 122302 (2012), arXiv:1105.4126 [nucl-ex].
- [83] C. W. Fabjan and T. Ludlam, “Calorimetry in High-energy Physics,” *Ann. Rev. Nucl. Part. Sci.* **32**, 335–389 (1982).
- [84] C. W. Fabjan and F. Gianotti, “Calorimetry for particle physics,” *Rev. Mod. Phys.* **75**, 1243–1286 (2003).
- [85] Richard Wigmans, *Calorimetry*, International Series of Monographs on Physics (Oxford University Press, 2017).
- [86] Richard Wigmans, “New Developments in Calorimetric Particle Detection,” (2018), arXiv:1807.03853 [physics.ins-det].
- [87] S. Afanasiev *et al.* (PHENIX), “Measurement of Direct Photons in Au+Au Collisions at $\sqrt{s_{NN}} = 200$ GeV,” *Phys. Rev. Lett.* **109**, 152302 (2012), arXiv:1205.5759 [nucl-ex].
- [88] C. Albajar *et al.* (UA1), “Direct Photon Production at the CERN Proton - anti-Proton Collider,” *Munich High Energy Physics 1988:723*, *Phys. Lett.* **B209**, 385–396 (1988).
- [89] A. Adare *et al.* (PHENIX), “Centrality dependence of low-momentum direct-photon production in Au+Au collisions at $\sqrt{s_{NN}} = 200$ GeV,” *Phys. Rev.* **C91**, 064904 (2015), arXiv:1405.3940 [nucl-ex].
- [90] Jaroslav Adam *et al.* (ALICE), “Direct photon production in Pb-Pb collisions at $\sqrt{s_{NN}} = 2.76$ TeV,” *Phys. Lett.* **B754**, 235–248 (2016), arXiv:1509.07324 [nucl-ex].
- [91] Wenqing Fan (PHENIX), “Direct Photon Production and Azimuthal Anisotropy at Low Transverse Momentum measured in PHENIX,” *Proceedings, 8th International Conference on Hard and Electromagnetic Probes of High-energy Nuclear Collisions: Hard Probes 2016 (HP2016): Wuhan, Hubei, China, September 23-27, 2016*, *Nucl. Part. Phys. Proc.* **289-290**, 153–156 (2017), arXiv:1708.08088 [nucl-ex].
- [92] A. Adare *et al.* (PHENIX), “Detailed measurement of the e^+e^- pair continuum in $p + p$ and Au+Au collisions at $\sqrt{s_{NN}} = 200$ GeV and implications for direct photon production,” *Phys. Rev.* **C81**, 034911 (2010), arXiv:0912.0244 [nucl-ex].
- [93] Norman M. Kroll and Walter Wada, “Internal pair production associated with the emission of high-energy gamma rays,” *Phys. Rev.* **98**, 1355–1359 (1955).
- [94] Peter Lichard, “Formalism for dilepton production via virtual photon bremsstrahlung in hadronic reactions,” *Phys. Rev.* **D51**, 6017–6035 (1995), arXiv:hep-ph/9812211 [hep-ph].

- [95] Kevin Dusling and Ismail Zahed, “Thermal photons from heavy ion collisions: A spectral function approach,” *Phys. Rev.* **C82**, 054909 (2010), arXiv:0911.2426 [nucl-th].
- [96] A. Adare *et al.* (PHENIX), “Enhanced production of direct photons in Au+Au collisions at $\sqrt{s_{NN}} = 200$ GeV and implications for the initial temperature,” *Phys. Rev. Lett.* **104**, 132301 (2010), arXiv:0804.4168 [nucl-ex].
- [97] L. Adamczyk *et al.* (STAR), “Direct virtual photon production in Au+Au collisions at $\sqrt{s_{NN}} = 200$ GeV,” *Phys. Lett.* **B770**, 451–458 (2017), arXiv:1607.01447 [nucl-ex].
- [98] M. M. Aggarwal *et al.*, “A preshower photon multiplicity detector for the WA93 experiment,” *Nucl. Instrum. Meth.* **A372**, 143–159 (1996).
- [99] M. M. Aggarwal *et al.*, “A Preshower photon multiplicity detector for the WA98 experiment,” *Nucl. Instrum. Meth.* **A424**, 395–413 (1999), arXiv:hep-ex/9807026 [hep-ex].
- [100] M. M. Aggarwal *et al.* (WA93), “Multiplicity and pseudorapidity distribution of photons in S + Au reaction at 200-A-GeV,” *Phys. Rev.* **C58**, 1146–1154 (1998).
- [101] A. Balanda *et al.* (HADES), “The HADES Pre-Shower detector,” *Proceedings, 5th International Workshop on Radiation Imaging Detectors (IWORID 2003): Riga, Latvia, September 7-11, 2003*, *Nucl. Instrum. Meth.* **A531**, 445–458 (2004).
- [102] M. Beddo *et al.* (STAR), “The STAR barrel electromagnetic calorimeter,” *Nucl. Instrum. Meth.* **A499**, 725–739 (2003).
- [103] Raphaelle Ichou and David d’Enterria, “Sensitivity of isolated photon production at TeV hadron colliders to the gluon distribution in the proton,” *Phys. Rev.* **D82**, 014015 (2010), arXiv:1005.4529 [hep-ph].
- [104] Francois Arleo, Kari J. Eskola, Hannu Paukkunen, and Carlos A. Salgado, “Inclusive prompt photon production in nuclear collisions at RHIC and LHC,” *JHEP* **04**, 055 (2011), arXiv:1103.1471 [hep-ph].
- [105] Serguei Chatrchyan *et al.* (CMS), “Measurement of isolated photon production in pp and PbPb collisions at $\sqrt{s_{NN}} = 2.76$ TeV,” *Phys. Lett.* **B710**, 256–277 (2012), arXiv:1201.3093 [nucl-ex].
- [106] A. Adare *et al.* (PHENIX), “High p_T direct photon and π^0 triggered azimuthal jet correlations and measurement of k_T for isolated direct photons in $p + p$ collisions at $\sqrt{s} = 200$ GeV,” *Phys. Rev.* **D82**, 072001 (2010), arXiv:1006.1347 [hep-ex].
- [107] M. M. Aggarwal *et al.* (WA98), “Interferometry of direct photons in central Pb-208+Pb-208 collisions at 158-A-GeV,” *Phys. Rev. Lett.* **93**, 022301 (2004), arXiv:nucl-ex/0310022 [nucl-ex].
- [108] R. Hanbury Brown and R. Q. Twiss, “Correlation between Photons in two Coherent Beams of Light,” *Nature* **177**, 27–29 (1956).
- [109] D. H. Boal, C. K. Gelbke, and B. K. Jennings, “Intensity interferometry in subatomic physics,” *Rev. Mod. Phys.* **62**, 553–602 (1990).
- [110] D. Peressounko, “Hanbury Brown-Twiss interferometry of direct photons in heavy ion collisions,” *Phys. Rev.* **C67**, 014905 (2003).
- [111] Steffen A. Bass, Berndt Muller, and Dinesh K. Srivastava, “Photon interferometry of Au + Au collisions at the BNL Relativistic Heavy-Ion Collider,” *Phys. Rev. Lett.* **93**, 162301 (2004), arXiv:nucl-th/0404050 [nucl-th].
- [112] Dinesh K. Srivastava and Joseph I. Kapusta, “Photon interferometry of quark gluon dynamics,” *Borlange Quark Matter 1993:0523-526*, *Phys. Lett.* **B307**, 1–6 (1993).
- [113] R. Baier, J. Engels, and B. Petersson, “Correlations with Large Transverse Momentum Photons and the Gluon Structure Function,” *11th International Symposium on Multiparticle Dynamics Bruges, Belgium, June 22-27, 1980*, *Z. Phys.* **C6**, 309–316 (1980).
- [114] R. M. Sternheimer, “Energy Distribution of gamma Rays from π^0 Decay,” *Phys. Rev.* **99**, 277–281 (1955).
- [115] T. C. Awes *et al.* (WA80), “Search for direct photon production in 200-A-GeV S + Au reactions: A Status report,” *Quark matter '95. Proceedings, 11th International Conference on Ultrarelativistic Nucleus-Nucleus Collisions, Monterey, USA, January 9-13, 1995*, *Nucl. Phys.* **A590**, 81C–91C (1995).
- [116] R. Albrecht *et al.* (WA80), “Limits on the production of direct photons in 200-A/GeV S-32 + Au collisions,” *Phys. Rev. Lett.* **76**, 3506–3509 (1996).
- [117] R. Baur *et al.* (CERES), “Search for direct photons from S - Au collisions at 200-GeV/u,” *Z. Phys.* **C71**, 571–578 (1996).
- [118] Shreyasi Acharya *et al.* (ALICE), “Direct photon production at low transverse momentum in proton-proton collisions at $\sqrt{s} = 2.76$ and 8 TeV,” (2018), arXiv:1803.09857 [nucl-ex].
- [119] M. Diakonou *et al.* (Athens-Athens-Brookhaven-CERN), “Direct Production of High p_T Single Photons at the CERN Intersecting Storage Rings,” *Phys. Lett.* **87B**, 292–296 (1979).
- [120] M. Diakonou *et al.*, “The Associated Charged Particle Multiplicity of High $p(t)$ π^0 and Single Photon Events,” *Phys. Lett.* **91B**, 301–306 (1980).
- [121] E. Anassontzis *et al.*, “High $p(t)$ Direct Photon Production in p p Collisions,” *Z. Phys.* **C13**, 277–289 (1982).
- [122] T. Akesson *et al.* (Axial Field Spectrometer), “A comparison of direct photon, π^0 , and eta production in p anti-p and pp interactions at the CERN ISR,” *Phys. Lett.* **158B**, 282–288 (1985).
- [123] J. A. Appel *et al.* (UA2), “Direct Photon Production at the CERN $\bar{p}p$ Collider,” *Berkeley High Energy Phys.1986:1119*, *Phys. Lett.* **B176**, 239 (1986).
- [124] P. Aurenche, A. Douiri, R. Baier, M. Fontannaz, and D. Schiff, “Large p_T Double Photon Production in Hadronic Collisions: Beyond Leading Logarithm QCD Calculation,” *Z. Phys.* **C29**, 459–475 (1985).
- [125] G. Sozzi *et al.* (UA6), “Direct photon production in $\bar{p}p$ and pp interactions at $\sqrt{s} = 24.3$ -GeV,” *Phys. Lett.* **B317**, 243–249 (1993).
- [126] G. Balocchi *et al.* (UA6), “Direct photon cross-sections in proton proton and anti-proton - proton interactions at $S^{*}(1/2) = 24.3$ -GeV,” *Phys. Lett.* **B436**, 222–230 (1998).
- [127] G. Balocchi *et al.* (UA6), “Determination of alpha-s and the gluon distribution using direct photon production in anti-p p and p p collisions,” *Phys. Lett.* **B317**, 250–256 (1993).

- [128] F. Abe *et al.* (CDF), “A Precision measurement of the prompt photon cross-section in $p\bar{p}$ collisions at $\sqrt{s} = 1.8$ TeV,” *Phys. Rev. Lett.* **73**, 2662–2666 (1994), [Erratum: *Phys. Rev. Lett.* 74,1891(1995)].
- [129] S. Abachi *et al.* (D0), “Isolated photon cross-section in the central and forward rapidity regions in $p\bar{p}$ collisions at $\sqrt{s} = 1.8$ TeV,” *Phys. Rev. Lett.* **77**, 5011–5015 (1996), arXiv:hep-ex/9603006 [hep-ex].
- [130] H. Baer, J. Ohnemus, and J. F. Owens, “A Next-to-leading Logarithm Calculation of Direct Photon Production,” *Phys. Rev.* **D42**, 61–71 (1990).
- [131] L. E. Gordon and W. Vogelsang, “Polarized and unpolarized prompt photon production beyond the leading order,” *Phys. Rev.* **D48**, 3136–3159 (1993).
- [132] Nikolaos Kidonakis and J. F. Owens, “Soft gluon resummation and NNLO corrections for direct photon production,” *Phys. Rev.* **D61**, 094004 (2000), arXiv:hep-ph/9912388 [hep-ph].
- [133] L. Apanasevich *et al.* (Fermilab E706), “Evidence for parton k_T effects in high p_T particle production,” *Phys. Rev. Lett.* **81**, 2642–2645 (1998), arXiv:hep-ex/9711017 [hep-ex].
- [134] L. Apanasevich *et al.* (Fermilab E706), “Measurement of direct photon production at Tevatron fixed target energies,” *Phys. Rev.* **D70**, 092009 (2004), arXiv:hep-ex/0407011 [hep-ex].
- [135] M. Bonesini *et al.* (WA70), “Production of High Transverse Momentum Prompt Photons and Neutral Pions in Proton Proton Interactions at 280-GeV/c,” *Z. Phys.* **C38**, 371 (1988).
- [136] S. S. Adler *et al.* (PHENIX), “Measurement of direct photon production in $p + p$ collisions at $s^{**}(1/2) = 200$ -GeV,” *Phys. Rev. Lett.* **98**, 012002 (2007), arXiv:hep-ex/0609031 [hep-ex].
- [137] A. Adare *et al.* (PHENIX), “Direct-Photon Production in $p + p$ Collisions at $\sqrt{s} = 200$ GeV at Midrapidity,” *Phys. Rev.* **D86**, 072008 (2012), arXiv:1205.5533 [hep-ex].
- [138] B. I. Abelev *et al.* (STAR), “Inclusive π^0 , η , and direct photon production at high transverse momentum in $p + p$ and $d + \text{Au}$ collisions at $\sqrt{s_{NN}} = 200$ GeV,” *Phys. Rev.* **C81**, 064904 (2010), arXiv:0912.3838 [hep-ex].
- [139] G. Aad *et al.* (ATLAS), “Measurement of the inclusive isolated prompt photon cross section in pp collisions at $\sqrt{s} = 7$ TeV with the ATLAS detector,” *Phys. Rev.* **D83**, 052005 (2011), arXiv:1012.4389 [hep-ex].
- [140] Vardan Khachatryan *et al.* (CMS), “Measurement of the Isolated Prompt Photon Production Cross Section in pp Collisions at $\sqrt{s} = 7$ TeV,” *Phys. Rev. Lett.* **106**, 082001 (2011), arXiv:1012.0799 [hep-ex].
- [141] Georges Aad *et al.* (ATLAS), “Measurement of the inclusive isolated prompt photon cross section in pp collisions at $\sqrt{s} = 8$ TeV with the ATLAS detector,” *JHEP* **08**, 005 (2016), arXiv:1605.03495 [hep-ex].
- [142] Morad Aaboud *et al.* (ATLAS), “Measurement of the cross section for inclusive isolated-photon production in pp collisions at $\sqrt{s} = 13$ TeV using the ATLAS detector,” *Phys. Lett.* **B770**, 473–493 (2017), arXiv:1701.06882 [hep-ex].
- [143] R. F. Cahalan, K. A. Geer, John B. Kogut, and Leonard Susskind, “Asymptotic Freedom and the Absence of Vector Gluon Exchange in Wide Angle Hadronic Collisions,” *Phys. Rev.* **D11**, 1199 (1975).
- [144] W. Vogelsang and M. R. Whalley, “A Compilation of data on single and double prompt photon production in hadron hadron interactions,” *J. Phys.* **G23**, A1–A69 (1997).
- [145] V. M. Abazov *et al.* (D0), “The ratio of the isolated photon cross sections at $\sqrt{s} = 630$ GeV and 1800 GeV,” *Lepton and photon interactions at high energies. Proceedings, 20th International Symposium, LP 2001, Rome, Italy, July 23-28, 2001*, *Phys. Rev. Lett.* **87**, 251805 (2001), arXiv:hep-ex/0106026 [hep-ex].
- [146] A. L. S. Angelis *et al.* (CMOR), “Direct Photon Production at the CERN ISR,” *Nucl. Phys.* **B327**, 541–568 (1989).
- [147] T. Akesson *et al.* (Axial Field Spectrometer), “High $p_T\gamma$ and π^0 Production, Inclusive and With a Recoil Hadronic Jet, in pp Collisions at $\sqrt{s} = 63$ -GeV,” *Sov. J. Nucl. Phys.* **51**, 836–845 (1990), [*Yad. Fiz.* 51,1314(1990)].
- [148] D. Acosta *et al.* (CDF), “Comparison of the isolated direct photon cross sections in $p\bar{p}$ collisions at $\sqrt{s} = 1.8$ -TeV and $\sqrt{s} = 0.63$ -TeV,” *Phys. Rev.* **D65**, 112003 (2002), arXiv:hep-ex/0201004 [hep-ex].
- [149] D. Acosta *et al.* (CDF), “Direct photon cross section with conversions at CDF,” *Phys. Rev.* **D70**, 074008 (2004), arXiv:hep-ex/0404022 [hep-ex].
- [150] Georges Aad *et al.* (ATLAS), “Measurement of the inclusive isolated prompt photon cross-section in pp collisions at $\sqrt{s} = 7$ TeV using 35 pb^{-1} of ATLAS data,” *Phys. Lett.* **B706**, 150–167 (2011), arXiv:1108.0253 [hep-ex].
- [151] V. M. Abazov *et al.* (D0), “Measurement of the isolated photon cross section in $p\bar{p}$ collisions at $\sqrt{s} = 1.96$ -TeV,” *Phys. Lett.* **B639**, 151–158 (2006), [Erratum: *Phys. Lett.* B658,285(2008)], arXiv:hep-ex/0511054 [hep-ex].
- [152] T. Aaltonen *et al.* (CDF), “Measurement of the Inclusive Isolated Prompt Photon Cross Section in $p\bar{p}$ Collisions at $\sqrt{s} = 1.96$ TeV using the CDF Detector,” *Phys. Rev.* **D80**, 111106 (2009), arXiv:0910.3623 [hep-ex].
- [153] J. Alitti *et al.* (UA2), “A Measurement of single and double prompt photon production at the CERN $p\bar{p}$ collider,” *Phys. Lett.* **B288**, 386–394 (1992).
- [154] A. L. S. Angelis *et al.* (CERN-Columbia-Oxford-Rockefeller, CCOR), “Search for Direct Single Photon Production at Large $p(T)$ in Proton Proton Collisions at $s^{**}(1/2) = 62.4$ -GeV,” *Phys. Lett.* **94B**, 106–112 (1980).
- [155] D. L. Adams *et al.* (E704), “Measurement of single spin asymmetry for direct photon production in $p p$ collisions at 200-GeV/c,” *Phys. Lett.* **B345**, 569–575 (1995).
- [156] C. De Marzo *et al.* (NA24), “A Measurement of Direct Photon Production at Large Transverse Momentum in $\pi^- p$, $\pi^+ p$ and pp Collisions at 300-GeV/c,” *Phys. Rev.* **D36**, 8 (1987).
- [157] David d’Enterria and Juan Rojo, “Quantitative constraints on the gluon distribution function in the proton from collider isolated-photon data,” *Nucl. Phys.* **B860**, 311–338 (2012), arXiv:1202.1762 [hep-ph].
- [158] “Electromagnetic radiation from hot and dense hadronic matter,” <https://ectstar.fbk.eu/node/4229> (2018).
- [159] P. Darriulat *et al.*, “Large Transverse Momentum Photons from High-Energy Proton Proton Collisions,” *Madison Conf.1976:0196*, *Nucl. Phys.* **B110**, 365 (1976).
- [160] E. Amaldi *et al.*, “Search for Single Photon Direct Production in $p p$ Collisions at $s^{**}(1/2) = 53.2$ -GeV,” *Phys. Lett.* **77B**, 240–244 (1978).

- [161] T. Akesson *et al.* (Axial Field Spectrometer), “High p_T Direct Photon Production at 11-degrees in pp Collisions at $\sqrt{s} = 63$ -GeV,” Phys. Lett. **123B**, 367–372 (1983).
- [162] F. Abe *et al.* (CDF), “A Prompt photon cross-section measurement in $\bar{p}p$ collisions at $\sqrt{s} = 1.8$ TeV,” Phys. Rev. **D48**, 2998–3025 (1993).
- [163] B. Abbott *et al.* (D0), “The isolated photon cross-section in $p\bar{p}$ collisions at $\sqrt{s} = 1.8$ TeV,” Phys. Rev. Lett. **84**, 2786–2791 (2000), arXiv:hep-ex/9912017 [hep-ex].
- [164] S. S. Adler *et al.* (PHENIX), “Mid-rapidity direct-photon production in p^+p collisions at $\sqrt{s} = 200$ -GeV,” Phys. Rev. **D71**, 071102 (2005), arXiv:hep-ex/0502006 [hep-ex].
- [165] Georges Aad *et al.* (ATLAS), “Measurement of the inclusive isolated prompt photons cross section in pp collisions at $\sqrt{s} = 7$ TeV with the ATLAS detector using 4.6fb^{-1} ,” Phys. Rev. **D89**, 052004 (2014), arXiv:1311.1440 [hep-ex].
- [166] Morad Aaboud *et al.* (ATLAS), “Measurement of the ratio of cross sections for inclusive isolated-photon production in pp collisions at $\sqrt{s} = 13$ and 8 TeV with the ATLAS detector,” (2019), arXiv:1901.10075 [hep-ex].
- [167] L. Cornell and J. F. Owens, “The High $p(t)$ Production of Direct Photons and Jets in Quantum Chromodynamics,” Phys. Rev. **D22**, 1609 (1980).
- [168] F. Halzen, M. Dechantsreiter, and D. M. Scott, “Structure of Direct Photon Events,” Phys. Rev. **D22**, 1617 (1980).
- [169] Michael Klasen, “Theory of hard photoproduction,” Rev. Mod. Phys. **74**, 1221–1282 (2002), arXiv:hep-ph/0206169 [hep-ph].
- [170] A. Adare *et al.* (PHENIX), “Medium modification of jet fragmentation in Au + Au collisions at $\sqrt{s_{NN}} = 200$ GeV measured in direct photon-hadron correlations,” Phys. Rev. Lett. **111**, 032301 (2013), arXiv:1212.3323 [nucl-ex].
- [171] L. Adamczyk *et al.* (STAR), “Jet-like Correlations with Direct-Photon and Neutral-Pion Triggers at $\sqrt{s_{NN}} = 200$ GeV,” Phys. Lett. **B760**, 689–696 (2016), arXiv:1604.01117 [nucl-ex].
- [172] Georges Aad *et al.* (ATLAS), “Dynamics of isolated-photon plus jet production in pp collisions at $\sqrt{s} = 7$ TeV with the ATLAS detector,” Nucl. Phys. **B875**, 483–535 (2013), arXiv:1307.6795 [hep-ex].
- [173] Morad Aaboud *et al.* (ATLAS), “Measurement of the cross section for isolated-photon plus jet production in pp collisions at $\sqrt{s} = 13$ TeV using the ATLAS detector,” Phys. Lett. **B780**, 578–602 (2018), arXiv:1801.00112 [hep-ex].
- [174] Christopher McGinn (CMS), “Photon-jet correlations in pp and PbPb collisions at 5.02 TeV with CMS,” *Proceedings, 8th International Conference on Hard and Electromagnetic Probes of High-energy Nuclear Collisions: Hard Probes 2016 (HP2016): Wuhan, Hubei, China, September 23-27, 2016*, Nucl. Part. Phys. Proc. **289-290**, 333–337 (2017).
- [175] Christine A. Aidala, Steven D. Bass, Delia Hasch, and Gerhard K. Mallot, “The Spin Structure of the Nucleon,” Rev. Mod. Phys. **85**, 655–691 (2013), arXiv:1209.2803 [hep-ph].
- [176] M. Della Negra *et al.* (CERN-College de France-Heidelberg-Karlsruhe), “Observation of Jet Structure in High p_T Events at the ISR and the Importance of Parton Transverse Momentum,” Nucl. Phys. **B127**, 1 (1977).
- [177] A. Adare *et al.* (PHENIX), “Nonperturbative-transverse-momentum effects and evolution in dihadron and direct photon-hadron angular correlations in $p+p$ collisions at $\sqrt{s}=510$ GeV,” Phys. Rev. **D95**, 072002 (2017), arXiv:1609.04769 [hep-ex].
- [178] J. D. Osborn (PHENIX), “PHENIX results on jet modification with π^0 - and photon-triggered two particle correlations in $p+p$, $p(d)+\text{Au}$, and $\text{Au}+\text{Au}$ collisions,” in *27th International Conference on Ultrarelativistic Nucleus-Nucleus Collisions (Quark Matter 2018) Venice, Italy, May 14-19, 2018* (2018) arXiv:1807.05090 [hep-ex].
- [179] J. W. Cronin, Henry J. Frisch, M. J. Shochet, J. P. Boymond, R. Mermod, P. A. Piroue, and Richard L. Sumner, “Production of hadrons with large transverse momentum at 200, 300, and 400 GeV,” *High energy physics. Proceedings, 17th International Conference, ICHEP 1974, London, England, July 01-July 10, 1974*, Phys. Rev. **D11**, 3105–3123 (1975).
- [180] E. Bonvin *et al.* (WA70), “Intrinsic Transverse Momentum in the $\pi^-p \rightarrow \gamma\gamma X$ Reaction at 280-GeV/c,” Phys. Lett. **B236**, 523–527 (1990).
- [181] F. Abe *et al.* (CDF), “Measurement of the cross-section for production of two isolated prompt photons in $\bar{p}p$ collisions at $\sqrt{s} = 1.8$ TeV,” Phys. Rev. Lett. **70**, 2232–2236 (1993).
- [182] Georges Aad *et al.* (ATLAS), “Measurement of the isolated di-photon cross-section in pp collisions at $\sqrt{s} = 7$ TeV with the ATLAS detector,” Phys. Rev. **D85**, 012003 (2012), arXiv:1107.0581 [hep-ex].
- [183] R. M. Baltrusaitis, Morris E. Binkley, B. Cox, T. Kondo, C. T. Murphy, W. Yang, L. Ettlinger, M. S. Goodman, J. A. J. Matthews, and J. Nagy, “A Search for Direct Photon Production in 200-GeV/c and 300-GeV/c Proton - Beryllium Interactions,” Phys. Lett. **88B**, 372–378 (1979).
- [184] R. Ruckl, Stanley J. Brodsky, and J. F. Gunion, “The Production of Real Photons at Large Transverse Momentum in PP Collisions,” Phys. Rev. **D18**, 2469–2483 (1978).
- [185] M. McLaughlin *et al.*, “Inclusive Production of Direct Photons in 200-GeV/c Collisions,” *11th International Symposium on Lepton and Photon Interactions at High Energies Ithaca, New York, August 4-9, 1983*, Phys. Rev. Lett. **51**, 971 (1983).
- [186] J. Badier *et al.* (NA3), “Direct Photon Production From Pions and Protons at 200-GeV/c,” Z. Phys. **C31**, 341 (1986).
- [187] J. Schukraft (HELIOS), “Recent Results From Helios (Na34) on Proton - Nucleus and Nucleus-nucleus Reactions,” *QUARK MATTER '88. PROCEEDINGS, 7TH INTERNATIONAL CONFERENCE ON ULTRARELATIVISTIC NUCLEUS-NUCLEUS COLLISIONS, LENOX, USA, SEPTEMBER 26-30, 1988*, Nucl. Phys. **A498**, 79–92 (1989).

- [188] R. Albrecht *et al.* (WA80), “Upper limit for thermal direct photon production in heavy ion collisions at 60-A/GeV and 200-A/GeV,” *Z. Phys.* **C51**, 1–10 (1991).
- [189] M. L. Tincknell *et al.*, “Low transverse momentum photon production in proton nucleus collisions at 18-GeV/c,” *Phys. Rev.* **C54**, 1918–1929 (1996).
- [190] J. Adams *et al.* (STAR), “Photon and neutral pion production in Au + Au collisions at $\sqrt{s_{NN}} = 130$ -GeV,” *Phys. Rev.* **C70**, 044902 (2004), arXiv:nucl-ex/0401008 [nucl-ex].
- [191] S. S. Adler *et al.* (PHENIX), “Centrality dependence of direct photon production in $\sqrt{s_{NN}} = 200$ -GeV Au + Au collisions,” *Phys. Rev. Lett.* **94**, 232301 (2005), arXiv:nucl-ex/0503003 [nucl-ex].
- [192] A. Adare *et al.* (PHENIX), “Direct photon production in d +Au collisions at $\sqrt{s_{NN}} = 200$ GeV,” *Phys. Rev.* **C87**, 054907 (2013), arXiv:1208.1234 [nucl-ex].
- [193] M. M. Aggarwal *et al.* (WA98), “Photon and Eta Production in p+Pb and p+C Collisions at $\sqrt{s_{NN}} = 17.4$ GeV,” *Nucl. Phys.* **A898**, 14–23 (2013), arXiv:1108.5400 [nucl-ex].
- [194] The ATLAS collaboration (ATLAS), “Prompt photon production in $\sqrt{s_{NN}} = 8.16$ TeV p +Pb collisions with ATLAS,” (2017).
- [195] A. Adare *et al.* (PHENIX), “Low-momentum direct photon measurement in Cu+Cu collisions at $\sqrt{s_{NN}} = 200$ GeV,” *Phys. Rev.* **C98**, 054902 (2018), arXiv:1805.04066 [hep-ex].
- [196] J. Pumplin, D. R. Stump, J. Huston, H. L. Lai, Pavel M. Nadolsky, and W. K. Tung, “New generation of parton distributions with uncertainties from global QCD analysis,” *JHEP* **07**, 012 (2002), arXiv:hep-ph/0201195 [hep-ph].
- [197] A. Bialas, M. Bleszynski, and W. Czyz, “Multiplicity Distributions in Nucleus-Nucleus Collisions at High-Energies,” *Nucl. Phys.* **B111**, 461–476 (1976).
- [198] R. J. Glauber, *Lectures in Theoretical Physics* (New York: Interscience, 1959) p. 315.
- [199] Roy J. Glauber, “Quantum Optics and Heavy Ion Physics,” *Proceedings, 18th International Conference on Ultra-Relativistic Nucleus-Nucleus Collisions (Quark Matter 2005): Budapest, Hungary, August 4-9, 2005*, *Nucl. Phys. A* **774**, 3–13 (2006), arXiv:nucl-th/0604021 [nucl-th].
- [200] Michael L. Miller, Klaus Reygers, Stephen J. Sanders, and Peter Steinberg, “Glauber modeling in high energy nuclear collisions,” *Ann. Rev. Nucl. Part. Sci.* **57**, 205–243 (2007), arXiv:nucl-ex/0701025 [nucl-ex].
- [201] A. Adare *et al.* (PHENIX), “Scaling properties of fractional momentum loss of high- p_T hadrons in nucleus-nucleus collisions at $\sqrt{s_{NN}}$ from 62.4 GeV to 2.76 TeV,” *Phys. Rev.* **C93**, 024911 (2016), arXiv:1509.06735 [nucl-ex].
- [202] Ivan Vitev and Ben-Wei Zhang, “A Systematic study of direct photon production in heavy ion collisions,” *Phys. Lett.* **B669**, 337–344 (2008), arXiv:0804.3805 [hep-ph].
- [203] M. Alvioli and M. Strikman, “Color fluctuation effects in proton-nucleus collisions,” *Phys. Lett.* **B722**, 347–354 (2013), arXiv:1301.0728 [hep-ph].
- [204] S. S. Adler *et al.* (PHENIX), “Transverse-energy distributions at midrapidity in p+p, d+Au, and Au+Au collisions at $\sqrt{s_{NN}} = 62.4200$ GeV and implications for particle-production models,” *Phys. Rev.* **C89**, 044905 (2014), arXiv:1312.6676 [nucl-ex].
- [205] M. M. Aggarwal *et al.* (WA98), “Suppression of High- $p(T)$ Neutral Pions in Central Pb+Pb Collisions at $\sqrt{s_{NN}} = 17.3$ -GeV,” *Phys. Rev. Lett.* **100**, 242301 (2008), arXiv:0708.2630 [nucl-ex].
- [206] B. Blok and M. Strikman, “Multiparton pp and pA Collisions: From Geometry to Parton-Parton Correlations,” *Adv. Ser. Direct. High Energy Phys.* **29**, 63–99 (2018), arXiv:1709.00334 [hep-ph].
- [207] Gabor David, “Event characterization in (very) asymmetric collisions,” *Proceedings, 9th International Workshop on High- p_T Physics at LHC: Grenoble, France, September 24-28, 2013*, *J. Phys. Conf. Ser.* **589**, 012005 (2015), arXiv:1409.6788 [nucl-ex].
- [208] Michael Kordell and Abhijit Majumder, “Jets in d(p)-A Collisions: Color Transparency or Energy Conservation,” *Phys. Rev.* **C97**, 054904 (2018), arXiv:1601.02595 [nucl-th].
- [209] Jaroslav Adam *et al.* (ALICE), “Centrality dependence of particle production in p-Pb collisions at $\sqrt{s_{NN}} = 5.02$ TeV,” *Phys. Rev.* **C91**, 064905 (2015), arXiv:1412.6828 [nucl-ex].
- [210] Shreyasi Acharya *et al.* (ALICE), “Constraints on jet quenching in p-Pb collisions at $\sqrt{s_{NN}} = 5.02$ TeV measured by the event-activity dependence of semi-inclusive hadron-jet distributions,” *Phys. Lett.* **B783**, 95–113 (2018), arXiv:1712.05603 [nucl-ex].
- [211] Gabor David, “Centrality Issues In Asymmetric Collisions: Direct Photons To The Rescue?” *Proceedings, 26th International Nuclear Physics Conference (INPC2016): Adelaide, Australia, September 11-16, 2016*, *PoS INPC2016*, 345 (2017), arXiv:1702.00542 [nucl-ex].
- [212] Zvi Citron (ATLAS), “Electroweak probes of small and large systems with the ATLAS detector,” *Proceedings, 27th International Conference on Ultrarelativistic Nucleus-Nucleus Collisions (Quark Matter 2018): Venice, Italy, May 14-19, 2018*, *Nucl. Phys.* **A982**, 603–606 (2019).
- [213] Francois Arleo, “Hard pion and prompt photon at RHIC, from single to double inclusive production,” *JHEP* **09**, 015 (2006), arXiv:hep-ph/0601075 [hep-ph].
- [214] Shreyasi Acharya *et al.* (ALICE), “Direct photon elliptic flow in Pb-Pb collisions at $\sqrt{s_{NN}} = 2.76$ TeV,” *Phys. Lett.* **B789**, 308–322 (2019), arXiv:1805.04403 [nucl-ex].
- [215] (2018), pHENIX preliminary results on direct photon flow in 200 GeV Au+Au collisions up to $p_T = 18$ GeV/c, presented at the Quark Matter 2018 Conference in Venice, Italy.
- [216] Thorsten Renk, “Towards jet tomography: gamma-hadron correlations,” *Phys. Rev.* **C74**, 034906 (2006), arXiv:hep-ph/0607166 [hep-ph].
- [217] Guang-You Qin, Jorg Ruppert, Charles Gale, Sangyong Jeon, and Guy D. Moore, “Jet energy loss, photon production, and photon-hadron correlations at RHIC,” *Phys. Rev.* **C80**, 054909 (2009), arXiv:0906.3280 [hep-ph].

- [218] S. Afanasiev *et al.* (PHENIX), “High- p_T π^0 Production with Respect to the Reaction Plane in Au + Au Collisions at $\sqrt{s_{NN}}(1/2) = 200$ -GeV,” *Phys. Rev.* **C80**, 054907 (2009), arXiv:0903.4886 [nucl-ex].
- [219] C. Adler *et al.* (STAR), “Disappearance of back-to-back high p_T hadron correlations in central Au+Au collisions at $\sqrt{s_{NN}} = 200$ -GeV,” *Phys. Rev. Lett.* **90**, 082302 (2003), arXiv:nucl-ex/0210033 [nucl-ex].
- [220] A. Adare *et al.* (PHENIX), “Neutral pion production with respect to centrality and reaction plane in Au+Au collisions at $\sqrt{s_{NN}}=200$ GeV,” *Phys. Rev.* **C87**, 034911 (2013), arXiv:1208.2254 [nucl-ex].
- [221] Peter Brockway Arnold, Guy D. Moore, and Laurence G. Yaffe, “Photon emission from ultrarelativistic plasmas,” *JHEP* **11**, 057 (2001), arXiv:hep-ph/0109064 [hep-ph].
- [222] Peter Brockway Arnold, Guy D. Moore, and Laurence G. Yaffe, “Photon and gluon emission in relativistic plasmas,” *JHEP* **06**, 030 (2002), arXiv:hep-ph/0204343 [hep-ph].
- [223] Xin-Nian Wang and Xiao-feng Guo, “Multiple parton scattering in nuclei: Parton energy loss,” *Nucl. Phys.* **A696**, 788–832 (2001), arXiv:hep-ph/0102230 [hep-ph].
- [224] Carlos A. Salgado and Urs Achim Wiedemann, “Calculating quenching weights,” *Phys. Rev.* **D68**, 014008 (2003), arXiv:hep-ph/0302184 [hep-ph].
- [225] C. Marquet and T. Renk, “Jet quenching in the strongly-interacting quark-gluon plasma,” *Phys. Lett.* **B685**, 270–276 (2010), arXiv:0908.0880 [hep-ph].
- [226] Hanzhong Zhang, J. F. Owens, Enke Wang, and Xin-Nian Wang, “Tomography of high-energy nuclear collisions with photon-hadron correlations,” *Phys. Rev. Lett.* **103**, 032302 (2009), arXiv:0902.4000 [nucl-th].
- [227] Xiao-Fang Chen, Carsten Greiner, Enke Wang, Xin-Nian Wang, and Zhe Xu, “Bulk matter evolution and extraction of jet transport parameter in heavy-ion collisions at RHIC,” *Phys. Rev.* **C81**, 064908 (2010), arXiv:1002.1165 [nucl-th].
- [228] Morad Aaboud *et al.* (ATLAS), “Measurement of photonjet transverse momentum correlations in 5.02 TeV Pb + Pb and pp collisions with ATLAS,” *Phys. Lett.* **B789**, 167–190 (2019), arXiv:1809.07280 [nucl-ex].
- [229] J. J. Aubert *et al.* (European Muon), “The ratio of the nucleon structure functions F_2^n for iron and deuterium,” *Phys. Lett.* **123B**, 275–278 (1983).
- [230] M. Arneodo *et al.* (New Muon), “The Q^{*2} dependence of the structure function ratio $F_2^{\text{Sn}} / F_2^{\text{C}}$ and the difference $R^{\text{Sn}} - R^{\text{C}}$ in deep inelastic muon scattering,” *Nucl. Phys.* **B481**, 23–39 (1996).
- [231] K. J. Eskola, V. J. Kolhinen, and P. V. Ruuskanen, “Scale evolution of nuclear parton distributions,” *Nucl. Phys.* **B535**, 351–371 (1998), arXiv:hep-ph/9802350 [hep-ph].
- [232] Kari J. Eskola, Petja Paakkinen, Hannu Paukkunen, and Carlos A. Salgado, “EPPS16: Nuclear parton distributions with LHC data,” *Eur. Phys. J.* **C77**, 163 (2017), arXiv:1612.05741 [hep-ph].
- [233] K. J. Eskola, V. J. Kolhinen, and C. A. Salgado, “The Scale dependent nuclear effects in parton distributions for practical applications,” *Eur. Phys. J.* **C9**, 61–68 (1999), arXiv:hep-ph/9807297 [hep-ph].
- [234] Ilkka Helenius, Kari J. Eskola, Heli Honkanen, and Carlos A. Salgado, “Impact-Parameter Dependent Nuclear Parton Distribution Functions: EPS09s and EKS98s and Their Applications in Nuclear Hard Processes,” *JHEP* **07**, 073 (2012), arXiv:1205.5359 [hep-ph].
- [235] K. Kovarik *et al.*, “nCTEQ15 - Global analysis of nuclear parton distributions with uncertainties in the CTEQ framework,” *Phys. Rev.* **D93**, 085037 (2016), arXiv:1509.00792 [hep-ph].
- [236] A. Kusina, “Nuclear parton distributions from the nCTEQ group,” *Proceedings, 24th International Workshop on Deep-Inelastic Scattering and Related Subjects (DIS 2016): Hamburg, Germany, April 11-15, 2016*, PoS **DIS2016**, 026 (2016), arXiv:1611.01117 [hep-ph].
- [237] Mauro Rogerio Cosentino (ALICE FoCal), “Probing Nuclear PDF and Gluon Saturation At The LHC with Forward Direct Photons,” *Proceedings, 26th International Nuclear Physics Conference (INPC2016): Adelaide, Australia, September 11-16, 2016*, PoS **INPC2016**, 327 (2017), arXiv:1701.08677 [nucl-ex].
- [238] L. Adamczyk *et al.* (STAR), “Charged-to-neutral correlation at forward rapidity in Au+Au collisions at $\sqrt{s_{NN}}=200$ GeV,” *Phys. Rev.* **C91**, 034905 (2015), arXiv:1408.5017 [nucl-ex].
- [239] Betty Bezverkhnay Abelev *et al.* (ALICE), “Inclusive photon production at forward rapidities in proton-proton collisions at $\sqrt{s} = 0.9, 2.76$ and 7 TeV,” *Eur. Phys. J.* **C75**, 146 (2015), arXiv:1411.4981 [nucl-ex].
- [240] Albert M Sirunyan *et al.* (CMS), “Observation of medium induced modifications of jet fragmentation in PbPb collisions using isolated-photon-tagged jets,” (2018), arXiv:1801.04895 [hep-ex].
- [241] Thorsten Renk, “Gamma-hadron correlations as a tool to trace the flow of energy lost from hard partons in heavy-ion collisions,” *Phys. Rev.* **C80**, 014901 (2009), arXiv:0904.3806 [hep-ph].
- [242] Dmitri E. Kharzeev and Frashr Loshaj, “Jet energy loss and fragmentation in heavy ion collisions,” *Phys. Rev.* **D87**, 077501 (2013), arXiv:1212.5857 [hep-ph].
- [243] B. Z. Kopeliovich, H. J. Pirner, I. K. Potashnikova, Ivan Schmidt, A. V. Tarasov, and O. O. Voskresenskaya, “Quantum-mechanical description of in-medium fragmentation,” *Phys. Rev.* **C78**, 055204 (2008), arXiv:0809.4613 [hep-ph].
- [244] A. I. Milstein and Martin Schumacher, “Present status of Delbruck scattering,” *Phys. Rept.* **243**, 183–214 (1994).
- [245] Stephen L. Adler, “Photon splitting and photon dispersion in a strong magnetic field,” *Annals Phys.* **67**, 599–647 (1971).
- [246] C. F. von Weizsacker, “Radiation emitted in collisions of very fast electrons (Ausstrahlung bei Stossen sehr schneller Elektronen),” *Z. Phys.* **88**, 612–625 (1934).
- [247] E. J. Williams, “Nature of the high-energy particles of penetrating radiation and status of ionization and radiation formulae,” *Phys. Rev.* **45**, 729–730 (1934).
- [248] P. L. Csonka, “Are photon-photon scattering experiments feasible?” *Phys. Lett.* **24B**, 625–628 (1967).
- [249] Stanley J. Brodsky, Toichiro Kinoshita, and Hidezumi Terazawa, “Dominant colliding beam cross-sections at high-energies,” *Phys. Rev. Lett.* **25**, 972–975 (1970).

- [250] Stanley J. Brodsky, Toichiro Kinoshita, and Hidezumi Terazawa, “Two Photon Mechanism of Particle Production by High-Energy Colliding Beams,” *Phys. Rev.* **D4**, 1532–1557 (1971).
- [251] David d’Enterria and Gustavo G. da Silveira, “Observing light-by-light scattering at the Large Hadron Collider,” *Phys. Rev. Lett.* **111**, 080405 (2013), [Erratum: *Phys. Rev. Lett.* 116,no.12,129901(2016)], arXiv:1305.7142 [hep-ph].
- [252] S. Afanasiev *et al.* (PHENIX), “Photoproduction of J/ψ and of high mass $e+e-$ in ultra-peripheral Au+Au collisions at $s^{*}(1/2) = 200\text{-GeV}$,” *Phys. Lett.* **B679**, 321–329 (2009), arXiv:0903.2041 [nucl-ex].
- [253] Betty Abelev *et al.* (ALICE), “Coherent J/ψ photoproduction in ultra-peripheral Pb-Pb collisions at $\sqrt{s_{NN}} = 2.76\text{ TeV}$,” *Phys. Lett.* **B718**, 1273–1283 (2013), arXiv:1209.3715 [nucl-ex].
- [254] B. I. Abelev *et al.* (STAR), “Observation of $\pi^+ \pi^- \pi^+ \pi^-$ Photoproduction in Ultra-Peripheral Heavy Ion Collisions at STAR,” *Phys. Rev.* **C81**, 044901 (2010), arXiv:0912.0604 [nucl-ex].
- [255] Serguei Chatrchyan *et al.* (CMS), “Exclusive photon-photon production of muon pairs in proton-proton collisions at $\sqrt{s} = 7\text{ TeV}$,” *JHEP* **01**, 052 (2012), arXiv:1111.5536 [hep-ex].
- [256] Serguei Chatrchyan *et al.* (CMS), “Search for exclusive or semi-exclusive photon pair production and observation of exclusive and semi-exclusive electron pair production in pp collisions at $\sqrt{s} = 7\text{ TeV}$,” *JHEP* **11**, 080 (2012), arXiv:1209.1666 [hep-ex].
- [257] Vardan Khachatryan *et al.* (CMS), “Evidence for exclusive $\gamma\gamma \rightarrow W^+W^-$ production and constraints on anomalous quartic gauge couplings in pp collisions at $\sqrt{s} = 7$ and 8 TeV ,” *JHEP* **08**, 119 (2016), arXiv:1604.04464 [hep-ex].
- [258] Georges Aad *et al.* (ATLAS), “Measurement of exclusive $\gamma\gamma \rightarrow \ell^+ \ell^-$ production in proton-proton collisions at $\sqrt{s} = 7\text{ TeV}$ with the ATLAS detector,” *Phys. Lett.* **B749**, 242–261 (2015), arXiv:1506.07098 [hep-ex].
- [259] Morad Aaboud *et al.* (ATLAS), “Measurement of exclusive $\gamma\gamma \rightarrow W^+W^-$ production and search for exclusive Higgs boson production in pp collisions at $\sqrt{s} = 8\text{ TeV}$ using the ATLAS detector,” *Phys. Rev.* **D94**, 032011 (2016), arXiv:1607.03745 [hep-ex].
- [260] “Photon 2017: International conference on the structure and the interactions of the photon – international workshop on photon-photon collisions – international workshop on high energy photon colliders,” <https://indico.cern.ch/event/604619/> (2017).
- [261] K. Scharnhorst, “Photon-photon scattering and related phenomena. Experimental and theoretical approaches: The early period,” (2017), arXiv:1711.05194 [physics.hist-ph].
- [262] T. Akesson *et al.*, “Inclusive Photon Production in P a and A-a Collisions at $200\text{-GeV}/u$,” *Z. Phys.* **C46**, 369–376 (1990).
- [263] V. Cerny, P. Lichard, and Jan Pisut, “A Clear Cut Test of Low Mass Dilepton Production Mechanism in Hadronic Collisions,” *Z. Phys.* **C31**, 163 (1986).
- [264] Itzhak Tserruya, “Summary of low mass dilepton and direct photon results,” *Quark matter ’95. Proceedings, 11th International Conference on Ultrarelativistic Nucleus-Nucleus Collisions, Monterey, USA, January 9-13, 1995*, *Nucl. Phys.* **A590**, 127C–137C (1995).
- [265] J. Antos *et al.*, “Soft photon production in $400\text{-GeV}/c$ p - Be collisions,” *Z. Phys.* **C59**, 547–554 (1993).
- [266] M. M. Aggarwal *et al.* (WA98), “Azimuthal anisotropy of photon and charged particle emission in Pb-208 + Pb-208 collisions at $158\text{-A-GeV}/c$,” *Eur. Phys. J.* **C41**, 287–296 (2005), arXiv:nucl-ex/0406022 [nucl-ex].
- [267] Daniel Lohner (ALICE), “Measurement of Direct-Photon Elliptic Flow in Pb-Pb Collisions at $\sqrt{s_{NN}} = 2.76\text{ TeV}$,” *Proceedings, Workshop for Young Scientists on the Physics of Ultrarelativistic Nucleus-Nucleus Collisions (Hot Quarks 2012): Copamarina, Puerto Rico, October 14-20, 2012*, *J. Phys. Conf. Ser.* **446**, 012028 (2013), arXiv:1212.3995 [hep-ex].
- [268] Serguei Chatrchyan *et al.* (CMS), “Measurement of the triple-differential cross section for photon+jets production in proton-proton collisions at $\sqrt{s}=7\text{ TeV}$,” *JHEP* **06**, 009 (2014), arXiv:1311.6141 [hep-ex].
- [269] A. Adare *et al.* (PHENIX), “Azimuthally anisotropic emission of low-momentum direct photons in Au+Au collisions at $\sqrt{s_{NN}} = 200\text{ GeV}$,” *Phys. Rev.* **C94**, 064901 (2016), arXiv:1509.07758 [nucl-ex].
- [270] A. Adare *et al.* (PHENIX), “Beam-energy and centrality dependence of direct-photon emission from ultra-relativistic heavy-ion collisions,” Submitted to: *Phys. Rev. Lett.* (2018), arXiv:1805.04084 [hep-ex].
- [271] Morad Aaboud *et al.* (ATLAS), “Measurement of prompt photon production in $\sqrt{s_{NN}} = 8.16\text{ TeV}$ $p+\text{Pb}$ collisions with ATLAS,” (2019), arXiv:1903.02209 [nucl-ex].
- [272] K. H. Ackermann *et al.* (STAR), “Elliptic flow in Au + Au collisions at $(S(NN))^{*}(1/2) = 130\text{ GeV}$,” *Phys. Rev. Lett.* **86**, 402–407 (2001), arXiv:nucl-ex/0009011 [nucl-ex].
- [273] Martin Wilde (ALICE), “Measurement of Direct Photons in pp and Pb-Pb Collisions with ALICE,” *Proceedings, 23rd International Conference on Ultrarelativistic Nucleus-Nucleus Collisions : Quark Matter 2012 (QM 2012): Washington, DC, USA, August 13-18, 2012*, *Nucl. Phys.* **A904-905**, 573c–576c (2013), arXiv:1210.5958 [hep-ex].
- [274] W. Cassing and E. L. Bratkovskaya, “Parton-Hadron-String Dynamics: an off-shell transport approach for relativistic energies,” *Nucl. Phys.* **A831**, 215–242 (2009), arXiv:0907.5331 [nucl-th].
- [275] L. Oliva, M. Ruggieri, S. Plumari, F. Scardina, G. X. Peng, and V. Greco, “Photons from the Early Stages of Relativistic Heavy Ion Collisions,” *Phys. Rev.* **C96**, 014914 (2017), arXiv:1703.00116 [nucl-th].
- [276] Moritz Greif, Florian Senzel, Heiner Kremer, Kai Zhou, Carsten Greiner, and Zhe Xu, “Nonequilibrium photon production in partonic transport simulations,” *Phys. Rev.* **C95**, 054903 (2017), arXiv:1612.05811 [hep-ph].
- [277] David G. d’Enterria and Dmitri Peressounko, “Probing the QCD equation of state with thermal photons in nucleus-nucleus collisions at RHIC,” *Eur. Phys. J.* **C46**, 451–464 (2006), arXiv:nucl-th/0503054 [nucl-th].
- [278] P. Huovinen, P. V. Ruuskanen, and S. S. Rasanen, “Photon emission in heavy ion collisions at the CERN SPS,” *Phys. Lett.* **B535**, 109–116 (2002), arXiv:nucl-th/0111052 [nucl-th].

- [279] Dinesh Kumar Srivastava and Bikash Sinha, “Radiation of single photons from Pb + Pb collisions at the CERN SPS and quark hadron phase transition,” *Phys. Rev.* **C64**, 034902 (2001), arXiv:nucl-th/0006018 [nucl-th].
- [280] Fu-Ming Liu, Tetsufumi Hirano, Klaus Werner, and Yan Zhu, “Centrality-dependent direct photon p(t) spectra in Au + Au collisions at RHIC,” *Phys. Rev.* **C79**, 014905 (2009), arXiv:0807.4771 [hep-ph].
- [281] Jan-e Alam, Sourav Sarkar, T. Hatsuda, Tapan K. Nayak, and Bikash Sinha, “Photons from Pb Pb collisions at CERN SPS,” *Phys. Rev.* **C63**, 021901 (2001), arXiv:hep-ph/0008074 [hep-ph].
- [282] Hendrik van Hees, Min He, and Ralf Rapp, “Pseudo-critical enhancement of thermal photons in relativistic heavy-ion collisions?” *Nucl. Phys.* **A933**, 256–271 (2015), arXiv:1404.2846 [nucl-th].
- [283] Rupa Chatterjee, Hannu Holopainen, Thorsten Renk, and Kari J. Eskola, “Collision centrality and τ_0 dependence of the emission of thermal photons from fluctuating initial state in ideal hydrodynamic calculation,” *Phys. Rev.* **C85**, 064910 (2012), arXiv:1204.2249 [nucl-th].
- [284] Szabolcs Borsanyi, Zoltan Fodor, Christian Hoelbling, Sandor D. Katz, Stefan Krieg, Claudia Ratti, and Kalman K. Szabo (Wuppertal-Budapest), “Is there still any T_c mystery in lattice QCD? Results with physical masses in the continuum limit III,” *JHEP* **09**, 073 (2010), arXiv:1005.3508 [hep-lat].
- [285] Szabolcs Borsanyi, Zoltan Fodor, Christian Hoelbling, Sandor D. Katz, Stefan Krieg, and Kalman K. Szabo, “Full result for the QCD equation of state with 2+1 flavors,” *Phys. Lett.* **B730**, 99–104 (2014), arXiv:1309.5258 [hep-lat].
- [286] A. Bazavov, P. Petreczky, and J. H. Weber, “Equation of State in 2+1 Flavor QCD at High Temperatures,” *Phys. Rev.* **D97**, 014510 (2018), arXiv:1710.05024 [hep-lat].
- [287] Hendrik van Hees, Charles Gale, and Ralf Rapp, “Thermal Photons and Collective Flow at the Relativistic Heavy-Ion Collider,” *Phys. Rev.* **C84**, 054906 (2011), arXiv:1108.2131 [hep-ph].
- [288] Rupa Chatterjee, Hannu Holopainen, Ilkka Helenius, Thorsten Renk, and Kari J. Eskola, “Elliptic flow of thermal photons from event-by-event hydrodynamic model,” *Phys. Rev.* **C88**, 034901 (2013), arXiv:1305.6443 [hep-ph].
- [289] S. Ryu, J. F. Paquet, C. Shen, G. S. Denicol, B. Schenke, S. Jeon, and C. Gale, “Importance of the Bulk Viscosity of QCD in Ultrarelativistic Heavy-Ion Collisions,” *Phys. Rev. Lett.* **115**, 132301 (2015), arXiv:1502.01675 [nucl-th].
- [290] Bjoern Schenke, Prithwish Tribedy, and Raju Venugopalan, “Fluctuating Glasma initial conditions and flow in heavy ion collisions,” *Phys. Rev. Lett.* **108**, 252301 (2012), arXiv:1202.6646 [nucl-th].
- [291] O. Linnyk, W. Cassing, and E. L. Bratkovskaya, “Centrality dependence of the direct photon yield and elliptic flow in heavy-ion collisions at $\sqrt{s_{NN}} = 200$ GeV,” *Phys. Rev.* **C89**, 034908 (2014), arXiv:1311.0279 [nucl-th].
- [292] Huichao Song and Ulrich W. Heinz, “Causal viscous hydrodynamics in 2+1 dimensions for relativistic heavy-ion collisions,” *Phys. Rev.* **C77**, 064901 (2008), arXiv:0712.3715 [nucl-th].
- [293] (2017), lijuan Ruan, private communication.
- [294] Deepali Sharma (PHENIX), “PHENIX measurements of low momentum direct photons from large ion collisions as a function of beam energy and system size,” *Proceedings, 26th International Conference on Ultra-relativistic Nucleus-Nucleus Collisions (Quark Matter 2017): Chicago, Illinois, USA, February 5-11, 2017*, *Nucl. Phys.* **A967**, 700–703 (2017).
- [295] K. Kajantie, Joseph I. Kapusta, Larry D. McLerran, and A. Mekjian, “Dilepton Emission and the QCD Phase Transition in Ultrarelativistic Nuclear Collisions,” *Phys. Rev.* **D34**, 2746 (1986).
- [296] Dinesh Kumar Srivastava and Klaus Geiger, “Scaling of particle production with number of participants in high-energy A+A collisions in the parton cascade model,” *Quark matter '99. Proceedings, 14th International Conference on ultrarelativistic nucleus nucleus collisions, QM'99, Torino, Italy, May 10-15, 1999*, *Nucl. Phys.* **A661**, 592–595 (1999), arXiv:nucl-th/9906080 [nucl-th].
- [297] Mickey Chiu, Thomas K. Hemmick, Vladimir Khachatryan, Andrey Leonidov, Jinfeng Liao, and Larry McLerran, “Production of Photons and Dileptons in the Glasma,” *Nucl. Phys.* **A900**, 16–37 (2013), arXiv:1202.3679 [nucl-th].
- [298] Gokce Basar, Dmitri Kharzeev, Dmitri Kharzeev, and Vladimir Skokov, “Conformal anomaly as a source of soft photons in heavy ion collisions,” *Phys. Rev. Lett.* **109**, 202303 (2012), arXiv:1206.1334 [hep-ph].
- [299] Rupa Chatterjee, Evan S. Frodermann, Ulrich W. Heinz, and Dinesh K. Srivastava, “Elliptic flow of thermal photons in relativistic nuclear collisions,” *Phys. Rev. Lett.* **96**, 202302 (2006), arXiv:nucl-th/0511079 [nucl-th].
- [300] Rupa Chatterjee and Dinesh K. Srivastava, “Elliptic flow of thermal photons and formation time of quark gluon plasma at RHIC,” *Phys. Rev.* **C79**, 021901 (2009), arXiv:0809.0548 [nucl-th].
- [301] S. S. Adler *et al.* (PHENIX), “Measurement of identified π^0 and inclusive photon v(2) and implication to the direct photon production in $s(NN)^{1/2} = 200$ -GeV Au+Au collisions,” *Phys. Rev. Lett.* **96**, 032302 (2006), arXiv:nucl-ex/0508019 [nucl-ex].
- [302] “Thermal photons and dileptons,” <https://www.bnl.gov/tpd/> (2011).
- [303] “Thermal radiation workshop,” <https://www.bnl.gov/trw2012/> (2012).
- [304] “Electromagnetic probes of strongly interacting matter: Status and future of low-mass lepton-pair spectroscopy,” <http://www.ectstar.eu/node/92> (2013).
- [305] “Emmi rrtf on direct-photon flow puzzle,” <https://indico.gsi.de/conferenceDisplay.py?confId=2661> (2014).
- [306] “Thermal photons and dileptons in heavy-ion collisions,” <https://www.bnl.gov/tpd2014/> (2014).
- [307] “New perspectives on photons and dileptons in ultrarelativistic heavy-ion collisions at rhic and lhc,” <http://www.ectstar.eu/node/1232> (2015).
- [308] Mike Sas (ALICE), “Direct photon elliptic flow in Pb-Pb collisions at $\sqrt{s_{NN}} = 2.76$ TeV,” in *27th International Conference on Ultrarelativistic Nucleus-Nucleus Collisions (Quark Matter 2018) Venice, Italy, May 14-19, 2018* (2018) arXiv:1810.03861 [nucl-ex].

- [309] Chun Shen, Ulrich W. Heinz, Jean-Francois Paquet, Igor Kozlov, and Charles Gale, “Anisotropic flow of thermal photons as a quark-gluon plasma viscometer,” *Phys. Rev.* **C91**, 024908 (2015), arXiv:1308.2111 [nucl-th].
- [310] Rupa Chatterjee, Dinesh K. Srivastava, and Thorsten Renk, “Thermal photon v_3 at LHC from fluctuating initial conditions,” *Proceedings, 24th International Conference on Ultra-Relativistic Nucleus-Nucleus Collisions (Quark Matter 2014): Darmstadt, Germany, May 19-24, 2014*, *Nucl. Phys.* **A931**, 670–674 (2014), arXiv:1407.8329 [nucl-th].
- [311] Kevin Dusling, “Photons as a viscometer of heavy ion collisions,” *Nucl. Phys.* **A839**, 70–77 (2010), arXiv:0903.1764 [nucl-th].
- [312] Chun Shen, Ulrich Heinz, Jean-Francois Paquet, and Charles Gale, “Thermal photon anisotropic flow serves as a quark-gluon plasma viscometer,” *Proceedings, 6th International Conference on Hard and Electromagnetic Probes of High-Energy Nuclear Collisions (Hard Probes 2013): Cape Town, South Africa, November 4-8, 2013*, (2014), 10.1016/j.nuclphysa.2014.07.042, [*Nucl. Phys.*A932,184(2014)], arXiv:1403.7558 [nucl-th].
- [313] Charles Gale, Yoshimasa Hidaka, Sangyong Jeon, Shu Lin, Jean-Francois Paquet, Robert D. Pisarski, Daisuke Satow, Vladimir V. Skokov, and Gojko Vujanovic, “Production and Elliptic Flow of Dileptons and Photons in a Matrix Model of the Quark-Gluon Plasma,” *Phys. Rev. Lett.* **114**, 072301 (2015), arXiv:1409.4778 [hep-ph].
- [314] Edward Shuryak, “Strongly coupled quark-gluon plasma in heavy ion collisions,” *Rev. Mod. Phys.* **89**, 035001 (2017), arXiv:1412.8393 [hep-ph].
- [315] M. M. Aggarwal *et al.* (WA98), “Centrality and transverse momentum dependence of collective flow in 158-A-GeV Pb+Pb collisions measured via inclusive photons,” *Nucl. Phys.* **A762**, 129–146 (2005), arXiv:nucl-ex/0410045 [nucl-ex].
- [316] F. Bock, C. Loizides, T. Peitzmann, and M. Sas, “Impact of residual contamination on inclusive and direct photon flow,” *J. Phys.* **G44**, 025106 (2017), arXiv:1606.06077 [nucl-ex].
- [317] S. S. Adler *et al.* (PHENIX), “High transverse momentum η meson production in p^+p , d^+ Au and Au+Au collisions at $S(NN)^{(1/2)} = 200$ -GeV,” *Phys. Rev.* **C75**, 024909 (2007), arXiv:nucl-ex/0611006 [nucl-ex].
- [318] A. Adare *et al.* (PHENIX), “Azimuthal anisotropy of π^0 and η mesons in Au + Au collisions at $\sqrt{s_{NN}} = 200$ GeV,” *Phys. Rev.* **C88**, 064910 (2013), arXiv:1309.4437 [nucl-ex].
- [319] C. Adler *et al.* (STAR), “Elliptic flow from two and four particle correlations in Au+Au collisions at $s(NN)^{(1/2)} = 130$ -GeV,” *Phys. Rev.* **C66**, 034904 (2002), arXiv:nucl-ex/0206001 [nucl-ex].
- [320] Matthew Luzum and Jean-Yves Ollitrault, “Eliminating experimental bias in anisotropic-flow measurements of high-energy nuclear collisions,” *Phys. Rev.* **C87**, 044907 (2013), arXiv:1209.2323 [nucl-ex].
- [321] (2014), Jean-Francois Paquet, private communication.
- [322] Arthur M. Poskanzer and S. A. Voloshin, “Methods for analyzing anisotropic flow in relativistic nuclear collisions,” *Phys. Rev.* **C58**, 1671–1678 (1998), arXiv:nucl-ex/9805001 [nucl-ex].
- [323] B. Alver *et al.* (PHOBOS), “System size, energy, pseudorapidity, and centrality dependence of elliptic flow,” *Phys. Rev. Lett.* **98**, 242302 (2007), arXiv:nucl-ex/0610037 [nucl-ex].
- [324] B. Alver *et al.* (PHOBOS), “Elliptic flow fluctuations in $s(NN)^{(1/2)} = 200$ -GeV Au+Au collisions at RHIC,” *Proceedings, 19th International Conference on Ultra-Relativistic nucleus-nucleus collisions (Quark Matter 2006): Shanghai, P.R. China, November 14-20, 2006*, *J. Phys.* **G34**, S907–S910 (2007), arXiv:nucl-ex/0701049 [NUCL-EX].
- [325] Nicolas Borghini, Phuong Mai Dinh, and Jean-Yves Ollitrault, “A New method for measuring azimuthal distributions in nucleus-nucleus collisions,” *Phys. Rev.* **C63**, 054906 (2001), arXiv:nucl-th/0007063 [nucl-th].
- [326] Nicolas Borghini, Phuong Mai Dinh, and Jean-Yves Ollitrault, “Flow analysis from multiparticle azimuthal correlations,” *Phys. Rev.* **C64**, 054901 (2001), arXiv:nucl-th/0105040 [nucl-th].
- [327] Dmitri Kharzeev and Eugene Levin, “Manifestations of high density QCD in the first RHIC data,” *Phys. Lett.* **B523**, 79–87 (2001), arXiv:nucl-th/0108006 [nucl-th].
- [328] Dmitri Kharzeev, Eugene Levin, and Marzia Nardi, “Color glass condensate at the LHC: Hadron multiplicities in pp, pA and AA collisions,” *Nucl. Phys.* **A747**, 609–629 (2005), arXiv:hep-ph/0408050 [hep-ph].
- [329] K. J. Eskola, K. Kajantie, P. V. Ruuskanen, and Kimmo Tuominen, “Scaling of transverse energies and multiplicities with atomic number and energy in ultrarelativistic nuclear collisions,” *Nucl. Phys.* **B570**, 379–389 (2000), arXiv:hep-ph/9909456 [hep-ph].
- [330] H. Niemi, K. J. Eskola, and R. Paatelainen, “Event-by-event fluctuations in a perturbative QCD + saturation + hydrodynamics model: Determining QCD matter shear viscosity in ultrarelativistic heavy-ion collisions,” *Phys. Rev.* **C93**, 024907 (2016), arXiv:1505.02677 [hep-ph].
- [331] Rupa Chatterjee, Hannu Holopainen, Thorsten Renk, and Kari J. Eskola, “Enhancement of thermal photon production in event-by-event hydrodynamics,” *Phys. Rev.* **C83**, 054908 (2011), arXiv:1102.4706 [hep-ph].
- [332] Pingal Dasgupta, Rupa Chatterjee, and Dinesh K. Srivastava, “Directed flow of photons in Cu+Au collisions at RHIC,” (2019), arXiv:1901.04943 [nucl-th].
- [333] Larry D. McLerran and Raju Venugopalan, “Computing quark and gluon distribution functions for very large nuclei,” *Phys. Rev.* **D49**, 2233–2241 (1994), arXiv:hep-ph/9309289 [hep-ph].
- [334] Akihiko Monnai and Berndt Mller, “Collinear parton splitting in early thermalization and chemical equilibration,” (2014), arXiv:1403.7310 [hep-ph].
- [335] Akihiko Monnai, “Thermal photon v_2 with slow quark chemical equilibration,” *Phys. Rev.* **C90**, 021901 (2014), arXiv:1403.4225 [nucl-th].
- [336] R. Baier, Alfred H. Mueller, D. Schiff, and D. T. Son, “‘Bottom up’ thermalization in heavy ion collisions,” *Phys. Lett.* **B502**, 51–58 (2001), arXiv:hep-ph/0009237 [hep-ph].
- [337] Gordon Baym and Leo P. Kadanoff, “Conservation Laws and Correlation Functions,” *Phys. Rev.* **124**, 287–299 (1961).
- [338] Gordon Baym, “Selfconsistent approximation in many body systems,” *Phys. Rev.* **127**, 1391–1401 (1962).

- [339] Benoit Vanderheyden and Gordon Baym, “Selfconsistent approximations in relativistic plasmas: Quasiparticle analysis of the thermodynamic properties,” *J. Stat. Phys.* (1998), 10.1023/B:JOSS.0000033166.37520.ae, [*J. Statist. Phys.*93,843(1998)], arXiv:hep-ph/9803300 [hep-ph].
- [340] W. Cassing, “Dynamical quasiparticles properties and effective interactions in the sQGP,” *Nucl. Phys.* **A795**, 70–97 (2007), arXiv:0707.3033 [nucl-th].
- [341] W. Cassing and E. L. Bratkovskaya, “Parton transport and hadronization from the dynamical quasiparticle point of view,” *Phys. Rev.* **C78**, 034919 (2008), arXiv:0808.0022 [hep-ph].
- [342] W. Ehehalt and W. Cassing, “Relativistic transport approach for nucleus nucleus collisions from SIS to SPS energies,” *Nucl. Phys.* **A602**, 449–486 (1996).
- [343] E. L. Bratkovskaya and W. Cassing, “Dilepton production from AGS to SPS energies within a relativistic transport approach,” *Nucl. Phys.* **A619**, 413–446 (1997), arXiv:nucl-th/9611042 [nucl-th].
- [344] Joern Knoll and Robert Lenk, “Coherence effects in radiative scattering: A Study of an exactly solvable hard scattering model,” *Nucl. Phys.* **A561**, 501–524 (1993).
- [345] “Music – a (3+1)d hydrodynamic code for heavy-ion collisions,” <http://www.physics.mcgill.ca/music/> (2010).
- [346] Bjoern Schenke, Sangyong Jeon, and Charles Gale, “(3+1)D hydrodynamic simulation of relativistic heavy-ion collisions,” *Phys. Rev.* **C82**, 014903 (2010), arXiv:1004.1408 [hep-ph].
- [347] Matthew Heffernan, Paul Hohler, and Ralf Rapp, “Universal Parametrization of Thermal Photon Rates in Hadronic Matter,” *Phys. Rev.* **C91**, 027902 (2015), arXiv:1411.7012 [hep-ph].
- [348] Nathan P. M. Holt, Paul M. Hohler, and Ralf Rapp, “Thermal photon emission from the system,” *Nucl. Phys.* **A945**, 1–20 (2016), arXiv:1506.09205 [hep-ph].
- [349] Stephan Endres, Hendrik van Hees, Janus Weil, and Marcus Bleicher, “Dilepton production and reaction dynamics in heavy-ion collisions at SIS energies from coarse-grained transport simulations,” *Phys. Rev.* **C92**, 014911 (2015), arXiv:1505.06131 [nucl-th].
- [350] Zhe Xu and Carsten Greiner, “Thermalization of gluons in ultrarelativistic heavy ion collisions by including three-body interactions in a parton cascade,” *Phys. Rev.* **C71**, 064901 (2005), arXiv:hep-ph/0406278 [hep-ph].
- [351] Yoshimasa Hidaka and Robert D. Pisarski, “Suppression of the Shear Viscosity in a ”semi” Quark Gluon Plasma,” *Phys. Rev.* **D78**, 071501 (2008), arXiv:0803.0453 [hep-ph].
- [352] Kenji Fukushima and Vladimir Skokov, “Polyakov loop modeling for hot QCD,” *Prog. Part. Nucl. Phys.* **96**, 154–199 (2017), arXiv:1705.00718 [hep-ph].
- [353] Chang-Hwan Lee and Ismail Zahed, “Electromagnetic Radiation in Hot QCD Matter: Rates, Electric Conductivity, Flavor Susceptibility and Diffusion,” *Phys. Rev.* **C90**, 025204 (2014), arXiv:1403.1632 [hep-ph].
- [354] Berndt Muller, Shang-Yu Wu, and Di-Lun Yang, “Elliptic flow from thermal photons with magnetic field in holography,” *Phys. Rev.* **D89**, 026013 (2014), arXiv:1308.6568 [hep-th].
- [355] Alejandro Ayala, Jorge David Castao-Yepes, Isabel Dominguez Jimenez, Jordi Salinas San Martn, and Mara Elena Tejeda-Yeomans, “Centrality dependence of photon yield and elliptic flow from gluon fusion and splitting induced by magnetic fields in relativistic heavy-ion collisions,” (2019), arXiv:1904.02938 [hep-ph].
- [356] Adam Bzdak and Vladimir Skokov, “Anisotropy of photon production: initial eccentricity or magnetic field,” *Phys. Rev. Lett.* **110**, 192301 (2013), arXiv:1208.5502 [hep-ph].
- [357] R. Arnaldi *et al.* (NA60), “First measurement of the rho spectral function in high-energy nuclear collisions,” *Phys. Rev. Lett.* **96**, 162302 (2006), arXiv:nucl-ex/0605007 [nucl-ex].
- [358] “A next-generation lhc heavy-ion experiment,” <https://indico.cern.ch/event/779787/> (2018).